



**Design, Synthesis and Evaluation of  
Hybrid Intracellularly Targeted  
Anticancer and Antimicrobial Agents**

**KIRAN AZIZ**

**MRes**

**2023**

**Design, Synthesis and Evaluation of Hybrid Intracellularly Targeted Anticancer  
and Antimicrobial Agents**

**KIRAN AZIZ**

**Thesis submitted in partial fulfilment of the requirements of Edinburgh Napier University for the  
degree of Master of Science by Research (MRes)**

**June 2023**

## Abstract

One of the most important barriers to the success of anticancer therapy is the dysregulation of apoptotic pathways that limit effectiveness of current chemotherapy. A long-term objective seeks to exploit links between apoptosis and the functions of mitochondria to favour apoptosis and thus circumvent mechanisms of multi-drug resistance.

The specific aims of this research are the synthesis, characterisation and evaluation of a series of novel anthraquinone-based, tri-partite hybrid DCA-ciprofloxacin-TPP compounds to repurpose clinically useful antibiotics as non-genotoxic anticancer agents; and towards the design of dual anticancer and antibacterial agents.

These hybrid compounds consist of 3 components: ciprofloxacin (a broad-spectrum clinically useful 2<sup>nd</sup> generation fluoroquinolone antibiotic), dichloroacetate (DCA, a metabolic inhibitor of mitochondrial oxidation), and a triphenylphosphonium (TPP) cationic group, a hydrophobic carrier group with delocalised charge, capable of passing through mitochondrial membranes and accumulating in this organelle.

Dichloroacetate (DCA) is characterised as an apoptosis inducer in cancer cells; specifically, its clean mechanism of action to inhibit the critical mitochondrial enzyme pyruvate dehydrogenase kinase 2 (PDK2).

Four members of the series code-named Aq-Pip-DCA, Aq-Pip-Lys(TFA)-NH-TPP, Aq-Pip-Lys(Cp-TFA)-NH-TPP, and Aq-Pip-Lys(Cp-DCA)-NH-TPP hybrids showed good antibacterial activity. Ciprofloxacin (CIPRO) conjugate Aq-Pip-Lys(Cp-TFA)-NH-TPP was the most potent agent to inhibit bacterial growth in both sensitive (ATCC47055) and resistant (LIB213) strains of *Escherichia coli* (MIC 0.5 and 8 mg/L, respectively), and in *Staphylococcus aureus* both sensitive (82) and resistant (83) strains with MIC values 4 and 64 mg/L. In preliminary experiments, compounds from the series have shown cytotoxic activity against the resistant HCT15 colon carcinoma cell line at micromolar concentrations. Ciprofloxacin-TPP-DCA hybrids could provide multi-targeted leads for the design of biologically active agents with dual anticancer and antimicrobial activities.

## **Declaration**

I hereby declare that the thesis and the research work upon which it is based were conducted by the author, Kiran Aziz.

**Kiran Aziz**

## **Acknowledgement**

Most importantly, I would like to express my sincere gratitude and deepest appreciation to my supervisors, Dr David Mincher, Dr Agnes Turnbull and Dr Janis MacCallum who have supported me throughout my research project and MRes study with their motivation, patience, enthusiasm and enormous knowledge. I could not have imagined having a better advisor for my MRes study and not being possible to write this thesis without their help and support.

I would like to thank to ESPRC National Mass Spectrometry Facility, University of Swansea. Thanks, are also due to NMR facility at Heriot-watt University.

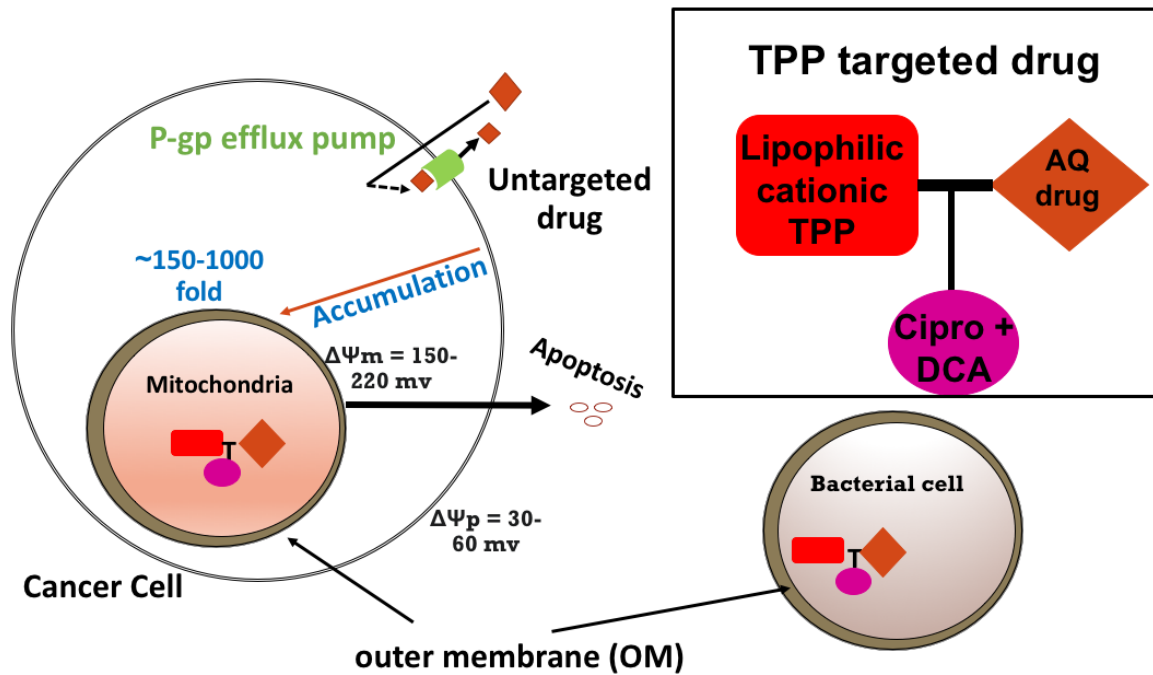
Thanks, are also due to past and present lab mates and PHD students in particular Ewoma and Omar Mohammed for the help and support during my lab and study.

I would like to thank to Dr Donald Morrison, Dr Lesley Young and the research technician team for their help and support during my time at Edinburgh Napier University.

Last but not least, I would like to thank to my family for their great support, patience and enthusiasm. My special thanks to my father and mother who gave me support during my study and I am grateful to their sacrifices they had made.

## Graphical Abstract Concept Diagram

Anthraquinone-DCA-ciprofloxacin-TPP<sup>+</sup> hybrid conjugates were designed as agents for targeted drug delivery to mitochondria of cancer cells, evading the nucleus, by exploiting their high mitochondrial membrane potential. By structural and evolutionary analogy, it was proposed that the conjugates could be targeted to bacterial cells to create anticancer or antibacterial or dual acting agents.



Design concept of intracellularly-targeted anticancer and antibacterial agents

## **Table of Contents**

<b>Chapter 1 Introduction</b> .....	1
1.1) Aim.....	1
1.2) Hypothesis.....	1
1.3) Background.....	1
1.3.1) Cancer chemotherapy and resistance.....	1
1.3.2) Cancer drug resistance.....	3
1.3.3) Bacterium-induced resistance.....	6
1.4) Mitochondria.....	8
1.4.1) Metabolism of cancer cells.....	10
1.4.2) Mitochondrial dysfunction and cancer cells.....	12
1.4.3) Bacterial infections and cancer progression.....	14
1.5) Concept of drug design and discovery.....	16
1.5.1) Ciprofloxacin (CIPRO).....	17
1.5.2) Dichloroacetic acid (DCA).....	21
1.5.3) Anthraquinones (AQ).....	24
1.5.4) Triphenylphosphonium cation (TPP <sup>+</sup> ).....	26
<b>Chapter 2 Results and Discussion</b> .....	29
2.1) Background.....	29
2.2) Rational drug design.....	29
2.2.1) Synthetic strategy.....	33
2.3) Synthesis of hybrid anthraquinone, TPP <sup>+</sup> , Ciprofloxacin and DCA Conjugates.....	37
2.3.1) Synthesis of AQ-PIP-BOC (KA1).....	37
2.3.2) Synthesis of AQ-PIP-TFA (KA2).....	40
2.3.3) Synthesis of AQ-PIP-DCA (KA3).....	42
2.3.4) Synthesis of AQ-PIP-Lys (BOC)-Fmoc (KA4).....	44
2.3.5) Synthesis of AQ-PIP-Lys (BOC) (KA5).....	47
2.3.6) Synthesis of AQ-PIP-Lys (BOC)-TPP (KA6).....	49
2.3.7) Synthesis of AQ-PIP-Lys (TFA)-TPP (KA7).....	51
2.3.8) Synthesis of CIPRO-BOC (KA8).....	53
2.3.9) Synthesis of AQ-TPP-CIPRO-BOC (KA9).....	55
2.3.10) Synthesis of AQ-TPP-CIPRO-TFA (KA10).....	58
2.3.11) Synthesis of AQ-TPP-CIPRO-DCA (KA11).....	60

2.4) <i>In-vitro</i> biological assays.....	63
2.4.1) Antibacterial activity.....	63
i) Measurement of minimum inhibitory concentrations (MIC) and minimum bactericidal concentration (MBC).....	63
2.4.2) Anticancer activity.....	64
i) MTT assay.....	64
2.5) Summary.....	70
2.6) Conclusion.....	72
<b>Chapter 3 Experimental</b> .....	<b>73</b>
3.1) General analytical techniques.....	73
3.1.1) Thin- layer chromatography (TLC).....	73
3.1.2) Silica gel column chromatography.....	73
3.1.3) Liquid-liquid extraction.....	73
3.1.4) Mass spectrometry.....	73
3.1.5) Nuclear magnetic resonance (NMR) ( <sup>1</sup> H and <sup>13</sup> C).....	74
3.2) Synthesis of anthraquinone derivative of DCA conjugate.....	74
3.2.1) Synthesis of AQ-PIP-BOC (KA1).....	74
3.2.2) Synthesis of AQ-PIP-TFA (KA2).....	75
3.2.3) Synthesis of AQ-PIP-DCA (KA3).....	75
3.3) Synthesis of anthraquinone hybrid TPP <sup>+</sup> , ciprofloxacin and DCA conjugates.....	76
3.3.1) Synthesis of AQ-PIP-Lys (BOC)-Fmoc (KA4).....	76
3.3.2) Synthesis of AQ-PIP-Lys (BOC) (KA5).....	77
3.3.3) Synthesis of AQ-PIP-Lys (BOC)-TPP (KA6).....	77
3.3.4) Synthesis of AQ-PIP-Lys (TFA)-TPP (KA7).....	78
3.3.5) Synthesis of CIPRO-BOC (KA8).....	78
3.3.6) Synthesis of AQ-TPP-CIPRO-BOC (KA9).....	79
3.3.7) Synthesis of AQ-TPP-CIPRO-TFA (KA10).....	79
3.3.8) Synthesis of AQ-TPP-CIPRO-DCA (KA11).....	80
3.4) <i>In-vitro</i> biological assays.....	80
3.4.1) Antibacterial assay .....	81
3.4.1.01) Measurement of minimum inhibitory concentrations (MIC) and minimum bactericidal concentration (MBC).....	81
i) Drugs.....	81



ii) Material for MIC and MBC.....	81
iii) Bacterial isolates.....	81
iv) MIC assay.....	81
v) Plate spreading method.....	82
vi) MBC assay.....	82
3.4.2) Antiproliferative assay.....	83
3.4.2.01) Cell culture.....	83
i) Materials of cell culture.....	83
ii) Cell culture method.....	83
iii) Growth curves.....	83
3.4.2.02) Micro-culture tetrazolium assay (MTT).....	84
i) Drugs.....	84
ii) Materials for MTT assay.....	84
iii) Pre-treatment phase (Day 1).....	84
iv) Treatment Phase (Day 2).....	84
v) MTT Phase (Day 5).....	85

## **Structure Library**

## **References**

## List of Figures

Figure 1.1: General principle of drug resistance.....	4
Figure 1.2: Chemical Structure of gemcitabine.....	4
Figure 1.3: Effect of bacteria on gemcitabine in colon cancer cells.....	5
Figure 1.4: Cancer drug resistance mechanisms .....	6
Figure 1.5: Biosynthetic and bioenergetic processes of mitochondria.....	8
Figure 1.6: Chemical structure of Chloramphenicol.....	11
Figure 1.7: Bacterial infections leading to cancer cells' development.....	15
Figure 1.8: Chemical Structure of ciprofloxacin.....	17
Figure 1.9: Chemical structures of TPP <sup>+</sup> -conjugated with ciprofloxacin through (a) an ester bond and (b) amide bond.....	18
Figure 1.10: Chemical structure of 7-((4-substitued)piperazin-1-yl) derivatives of ciprofloxacin.....	19
Figure 1.11: Chemical structure of Levofloxacin.....	19
Figure 1.12: Anticancer potential of ciprofloxacin.....	20
Figure 1.13: Chemical structure of Tetracycline.....	20
Figure 1.14: Chemical structure of Tigecycline.....	21
Figure 1.15: Chemical structure of DCA.....	21
Figure 1.16: Mechanism of action of DCA.....	22
Figure 1.17: Chemical structure of DCA derivative of ciprofloxacin.....	23
Figure 1.18: Chemical structure of Mito-DCA.....	23

Figure 1.19: Chemical structure of anthraquinone.....	24
Figure 1.20: Chemical Structure of doxorubicin analogue with TPP <sup>+</sup> -cation and DCA .....	26
Figure 1.21: Chemical Structure of (4-carboxybutyl)triphenylphosphonium bromide.....	26
Figure 1.22: Translocation of triphenyl phosphonium cation to mitochondria of cancer cells.....	27
Figure 1.23: Chemical structure of SH1.....	28
Figure 2.1: Rational design of novel dual anticancer and antibacterial hybrid Drugs.....	32
Figure 2.2: Overview of the proposed synthesis of target compound KA11.....	34
Figure 2.3: Chemical structure of piperazine ring showing the points of attachment to other groups.....	35
Figure 2.4: Nucleophilic displacement of chlorine by piperazine (an addition- elimination sequence).....	36
Figure 2.5: Anatomy of TPP <sup>+</sup> -based functional analogues of SH1.....	37
Figure 2.6: The high-resolution mass spectrum ESI (+) of KA1.....	38
Figure 2.7: Correlation between observed data and theoretical <sup>13</sup> C isotope profile of KA1.....	39
Figure 2.8: NMR assignments and peak positions in ppm for KA1 (AQ-2-pip-Boc).....	39
Figure 2.9: The high-resolution mass spectrum ESI (+) of KA2.....	41
Figure 2.10: Correlation between observed data and the theoretical <sup>13</sup> C isotope of KA2.....	41
Figure 2.11: The high-resolution mass spectrum ESI (+) of KA3.....	43
Figure 2.12: Correlation between observed data and <sup>13</sup> C theoretical isotope profile of KA3.....	44

Figure 2.13: The high-resolution mass spectrum ESI (+) of KA4.....	46
Figure 2.14: Correlation between observed data and the <sup>13</sup> C theoretical isotope model of KA4.....	46
Figure 2.15: The high-resolution mass spectrum (ESI) (+) of KA5.....	48
Figure 2.16: Correlation between observed data and <sup>13</sup> C theoretical isotope of KA5 for cation [M+H] <sup>+</sup> .....	48
Figure 2.17: The high-resolution mass spectrum (ESI) (+) of KA6.....	50
Figure 2.18: Correlation between observed data and theoretical <sup>13</sup> C isotope profile of KA6.....	51
Figure 2.19: The high-resolution mass spectrum (ESI) (+) of KA7.....	52
Figure 2.20: Correlation between observed data and theoretical isotope of KA7.....	53
Figure 2.21: The high-resolution mass spectrum (ESI) (+) of KA8.....	54
Figure 2.22: Correlation between observed data and theoretical <sup>13</sup> C isotope of KA8.....	55
Figure 2.23: The high-resolution mass spectrum (ESI) (+) of KA9.....	57
Figure 2.24: Correlation between observed data and <sup>13</sup> C theoretical isotope profile of KA9.....	57
Figure 2.25: The high-resolution mass spectrum (ESI) (+) of KA10.....	59
Figure 2.26: Correlation between observed data and <sup>13</sup> C theoretical isotope profile of KA10.....	59
Figure 2.27: The high-resolution mass spectrum (ESI) (+) of KA11.....	62

Figure 2.28: Correlation between observed data and <sup>13</sup> C theoretical isotope profile of KA11.....	62
Figure 2.29: Conversion of tetrazolium salt to formazan.....	65
Figure 2.30: Comparative Cell Viability analysis of HCT-15 cells between SH1 & KA3.....	66
Figure 2.31: Comparative Cell Viability analysis of HCT-15 cells between SH1 & KA7.....	67
Figure 2.32: Comparative Cell Viability analysis of HCT-15 cells between SH1 & KA10.....	67
Figure 2.33: Comparative Cell Viability analysis of HCT-15 cells between SH1 & KA11.....	68

## **List of Schemes**

Scheme 01: Synthesis of KA1.....	38
Scheme 02: Synthesis of KA2 (by TFA mediated deprotection of KA1).....	40
Scheme 03: Synthesis of KA3.....	43
Scheme 04: Synthesis of KA4.....	45
Scheme 05: Synthesis of KA5 (deprotection of KA4 with piperidine).....	47
Scheme 06: Synthesis of KA6.....	50
Scheme 07: Synthesis of KA7.....	52
Scheme 08: Synthesis of KA8.....	54
Scheme 09: Synthesis of KA9.....	56
Scheme 10: Synthesis of KA10.....	58
Scheme 11: Synthesis of KA11.....	61

## **List of Tables**

Table 2.1: <i>In-vitro</i> minimum inhibitory concentration (MIC) of novel compounds on <i>E. coli</i> & <i>S. aureus</i> for 24 h incubation period.....	63
Table 2.2: Determination of IC <sub>50</sub> of tested compounds against HCT-15 cell line.....	68

## **Abbreviations**

ATP	Adenosine triphosphate
ABC	ATP-binding cassette transmembrane proteins
AIF	Apoptotic inducing factors
AML	Acute Myeloid Leukemia
Apaf-1	Apoptotic protease activating factor
AQ-TPP	Anthraquinone-triphenylphosphonium
AQ	Anthraquinone
ATCC47055	Product code (47055) of strain of <i>E. coli</i> of Supplier American Type Culture Collection
BAK	BCL-2 Antagonist Killer
BAX	B-cell Leukaemia/Lymphoma 2-associated X Protein
BCL-2 family	B-cell lymphoma 2 family
BOC	<i>Tert</i> -butyloxycarbonyl protecting group
CIPRO	Ciprofloxacin
CDD	Cytidine deaminase
CRC	Colorectal Cancer
Da	Dalton
DCA	Dichloroacetic acid
DCM	dichloromethane
DIPEA	N, N-diisopropylethylamine
dFdU	2',2'-difluorodeoxyuridine
DMF	Dimethylformamide
DMSO	Dimethyl Sulfoxide
DNA	Deoxyribonucleic acid
DOX	Doxorubicin
ETC	Electron transport chain
EMT	Epithelial-mesenchymal transition
ESI	Electrospray ionization
FADH <sub>2</sub>	Flavin adenine dinucleotide
FBS	Foetal Bovine Serum



FDA	Food and drug administration
Fmoc	Fluorenylmethoxycarbonyl
Gem	Gemcitabine
HATU	Hexafluorophosphate Azabenzotriazole Tetramethyl Uronium
HCT-15	Human colon tumourigenic
HIFs	Hypoxia inducible factors
HOBT	Hydroxy benzotriazole
IC <sub>50</sub>	half maximal inhibitory concentration
IL-6, IL-1	Pro-inflammatory cytokines
LIB213	Li Black environmental isolate from clear water with a product code 213 of strain of <i>E. coli</i>
MAP Kinase	Mitogen-activated protein kinase
MCF-7	Michigan Cancer Foundation-7
MDR1 level	Multiple drug sensitivity
MHA	Muller-Hinton Agar
MHB	Muller-Hinton Broth
MM	Multiple Myeloma
$\Delta\psi_m$	Mitochondrial membrane potential
MBC	Minimum bactericidal concentration
MIC	Minimum inhibitory concentration
MRSA	Methicillin resistant <i>Staphylococcus Aureus</i>
MSSA	Methicillin sensitive <i>Staphylococcus Aureus</i>
MMP	Mitochondrial membrane permeabilization
mtDNA	Mitochondrial Deoxyribonucleic acid
MTP	Mitochondrial transition pores
MDR	Multi-drug resistance
MRP1	Multi-drug resistance-associated proteins
MTT assay	Microculture tetrazolium assay
m/z	Mass to charge ratio
NADH	Nicotinamide adenine dinucleotide
NCTC6571	National Collection of Type Culture of <i>Staphylococcus aureus</i> with product code 6571

NMR	Nuclear magnetic resonance
OD450	Optical density using 450 nm filtered microplate reader
OXPPOS	Oxidative phosphorylation
PBS	phosphate buffered saline
P-gp	P-glycoproteins
PDH	Pyruvate dehydrogenase
PDK	Pyruvate dehydrogenase kinase
PYBOP	benzotriazol-1-yloxytripyrrolidinophosphonium hexafluorophosphate
R <sub>f</sub>	Retention factor
RMS	Root mean square
RNA	Ribonucleic acid
RPMI-1640	Roswell Park Memorial Institute-1640 medium
RT-PCR	Reverse transcriptase polymerase chain reaction
ROS	Reactive Oxygen Species
SAR	Structure Activity Relationship
TCA cycle	Tricarboxylic acid cycle
TFA	Trifluoroacetic acid
THF: H <sub>2</sub> O	Tetrahydrofuran: water
TLC	Thin layer chromatography
TLR	Toll-like receptors
TPP <sup>+</sup>	Triphenyl phosphonium cations
WHO	World Health Organization

## Chapter 1

### Introduction

#### 1.1) Aim

To synthesize, characterize and evaluate a series of novel hybrid anthraquinone-dichloroacetic acid (DCA)-ciprofloxacin-triphenylphosphonium (TPP<sup>+</sup>) compounds as potential dual anticancer and antibacterial agents.

#### 1.2) Hypothesis

Novel anthraquinone-triphenylphosphonium conjugates will be transferred directly into the mitochondria of cancer cells, avoiding the nucleus to afford non-genotoxic agents with the potential to circumvent multi-drug resistance (MDR). Further, it is hypothesized that such conjugates, incorporating triphenylphosphonium cations (TPP<sup>+</sup>) could be targeted (especially) to Gram-negative pathogens, given the evolutionary relationship and structural similarity between their double membranes and those of mitochondria. Anthraquinone-TPP hybrids incorporating ciprofloxacin also have potential as new antibacterial agents or as modulators of anticancer drug efficacy.

#### 1.3) Background

##### 1.3.1) Cancer chemotherapy and resistance

Chemotherapy is one of the most common methods of cancer treatment (Schmidt *et al.*, 2008) which is clinically effective at the beginning to control tumour growth (Li *et al.*, 2008) yet cancer cells in vivo re-proliferate over time and fail to respond to treatment. Pre-existence of resistance-mediating factors in tumours makes the chemotherapy ineffective, and results in high proportions of cancer cells after the treatment. Multi-drug resistance (MDR) is a main obstacle to the success of chemotherapy (Filipa, Antonio and Isabel, 2011) in which trans-membrane glycoproteins, notably P-glycoprotein, behave as so-called efflux pumps capable of removing exogenous substances including anticancer drugs and metal compounds from cancer cells.

A high degree of molecular heterogeneity of tumours plays a significant role in the incidence of multi-drug resistance which is associated with lethal side-effects and increased recurrence rates. Resistance can also develop due to mutations during treatment of tumours as well as through other adaptive processes, such as activation of alternative compensatory signaling pathways to inactivate the drug through structural modification and increased expression of biological targets (Jones, Matsui and Smith, 2004).

These problems are exacerbated after the transfer of acquired resistance from one drug into another anticancer treatment regimen despite having mechanistic and structural differences among used agents. This phenomenon is generally characterised as multidrug resistance (MDR). MDR is one of the extensive forms of drug resistance (Schmidt *et al.*, 2008) which is caused by the overexpression of P-glycoproteins (P-gp), and multi-drug resistance-associated proteins (MRP1) (Grant and Blackmore, 1994) and similarly, antimicrobial resistance (Nicolas *et al.*, 2019). In general, drug resistance presents as a major barrier to successful management of chemotherapy.

This hypothesis that the pattern of gene expressions of residual tumour cells after treatment is different from initial tumour cells leads to a unified explanation of success and failure of chemotherapy that the majority of cancer cells would be damaged by chemotherapy, yet a small population of chemotherapy-resistant cancer cells would be spared by tumour regrowth. Despite continuous efforts to develop effective clinical outcomes, there is still a need for a fully satisfactory clinical outcome to overcome the increasing complications of chemo-resistance.

Chemo-resistance is not merely a matter of some drug-resistant factors, rather it is a complex, dynamic and elusive system (Hu and Xuan, 2008). A wide range of molecular mechanisms has been associated with chemo-resistance (Stein, 1967). Efflux of anticancer agents through P-glycoproteins (P-gp) is a major contributing factor which can be solely responsible for chemo-resistance that limits the approach of cancer therapy directly to targeting cells (Sutendra *et al.*, 2011).

Including these, the presence of bacteria in cancer cells can also lead to resistance of chemotherapeutics (Zhang *et al.*, 2021). Bacterial infections have also been recognized as one of major barriers impeding the successful management of chemotherapy in cancer patients leading to antimicrobial resistance. Antimicrobial resistance which is also called as multi-drug resistant bacteria (MDR bacteria) is the greatest threat for cancer patients due to the use and misuse of multiple antimicrobials (Nicolas *et al.*, 2019). Infections caused by MDR bacterial strains such as *Staphylococcus aureus*, *E. coli* are harder to treat as they play a key role to resist the transfer of antimicrobial agents through drug resistant mechanisms (Zhang *et al.*, 2018).

Therefore, dual-active compounds having both antibiotic and antitumour properties could be a better choice to inhibit the growth of malignant cells effectively to overcome the barriers to successful management of chemotherapy (Zhang *et al.*, 2021).

### **1.3.2) Cancer drug resistance**

The process of development of cancer drug resistance is complex and elusive due to the dynamic progression of interaction between drugs and cancer cells. Resistance of cancer cells against anticancer drugs has never been exposed unless effectiveness of chemotherapy deteriorates. The principle of drug resistant cancer is associated with a combination of different factors. There are dominant cellular factors which are solely responsible for drug-resistance in cancer cells such as increasing rates of drug efflux (Vogelstein and Kinzler, 2004) and decreasing rates of anticancer drug influx (**Figure 1.1**).

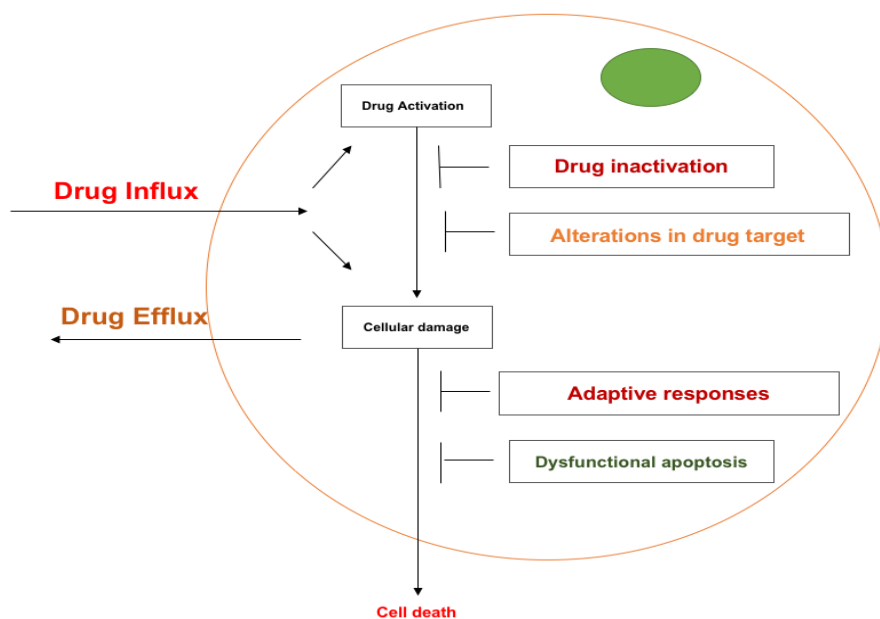


**Figure 1.1:** Cellular factors responsible for drug resistance

Drug efflux is mediated by the ATP-binding cassette (ABC) transmembrane proteins such as P-glycoproteins (P-gp) which is the primary cause of chemo-resistance and affects normal cellular functions such as signal transduction, uptake of extracellular materials, secretions of hormones and proteins, prevention of harmful xenobiotic. P-glycoproteins (P-gp) (Triller *et al.*, 2006) and multidrug resistant-associated proteins (MRP1) (Baldi *et al.*, 2004) function as unilateral “pumps” that can recognize multiple substrates and block the entrance of anticancer drugs to cancer cells (Nicolas *et al.*, 2019). Intra-tumoural bacterial populations contribute to cancer drug resistance by altering the cancer drug’s structure and metabolism to render it ineffective. For instance, Gemcitabine (**Figure 1.2**), a common first line treatment in some chemotherapies, could be metabolised into its inactive form by *E. coli* leading to cancer drug resistance (Rudin *et al.*, 2011).

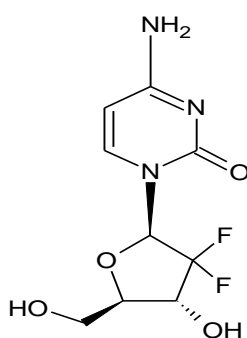


**Figure 1.2:** Chemical Structure of gemcitabine

Bacteria are able to transform exogenous substances or organic molecules such as pollutants, nutrients and toxins through endogenous enzymes (Arora and Jain, 2012) which has increased the potential interaction between bacteria and systematically or orally administered drugs (Lehouritis, *et al.*, 2015). Gemcitabine (2', 2'-difluorodeoxycytidine, Gem) is a nucleoside analogue which is phosphorylated by deoxycytidine kinase to its active metabolites. However, bacteria transform gemcitabine into its inactive form (2', 2'-difluorodeoxyuridine, dFdU) due to the presence of long isoform of the enzyme cytidine deaminase (CDD) which results in resistance to gemcitabine (**Figure 1.3**) (Xi *et al.*, 2022).

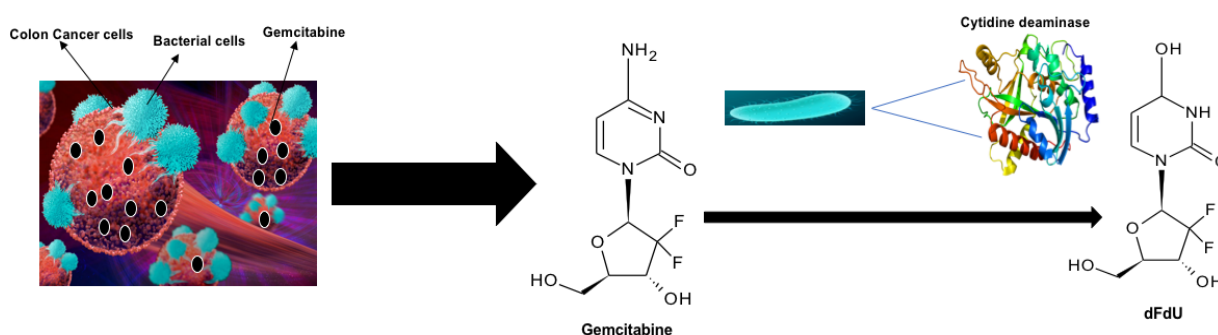


**Figure 1.3:** Effect of bacteria on gemcitabine in colon cancer cells (adapted from Xi *et al.*, 2022)

Bacterial resistance is an ongoing concern through multiple mechanisms such as the targeted protein is modified by drug-efflux or drug-influx pumps as bacteria are more vulnerable to evolutionary change and variation than other organisms (Croix, 1996). There are multiple targets approaching cancer drug resistance which depend upon two fundamental bases. At the upstream base, many of the anticancer agents induce the release of P-gp, and MRP1 to block the entry of anticancer drugs to prevent them from reaching their target. At the downstream base, anticancer agents induce apoptosis in cancer cells, while malignancy is genetically predisposed to apoptotic resistance which impedes the apoptotic action of anticancer drugs (Gewirtz, 1999).

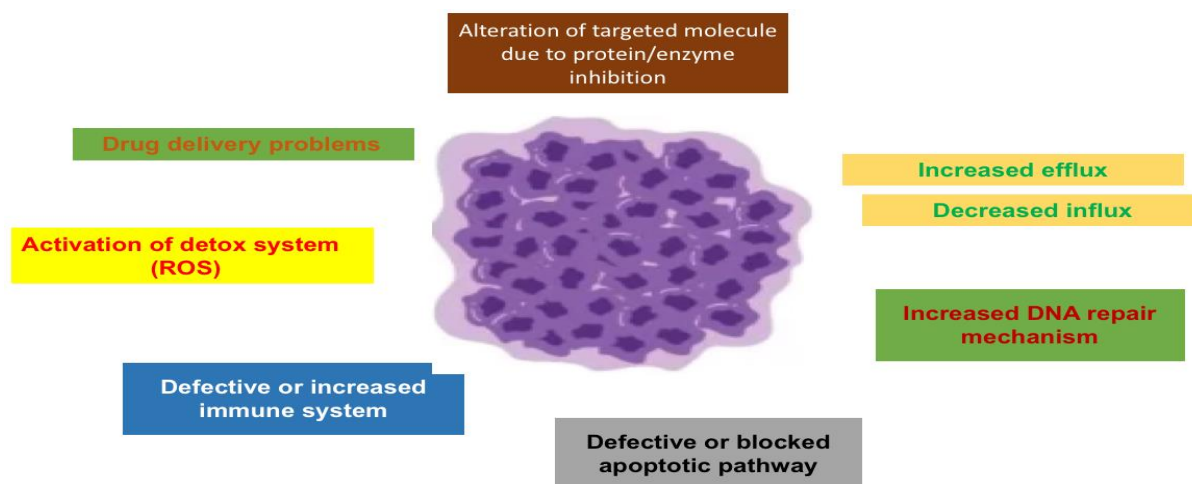


**Figure 1.4:** Anti-cancer drug resistance mechanisms

Mechanism of resistance of anticancer drugs (**Figure 1.4**) can also be articulated with the complications in drug delivery, activation of detox system (ROS homeostasis) of cancer cells deactivate the detox mechanism of cancer drug therapy, defective immune system (Pluen *et al.*, 2001), activation of DNA repair system and blocking of apoptosis (Stein, 1967).

It is therefore clear that introduction of chemotherapy to cancer patients will be effective at the beginning, yet normal cellular factors could impede the development of chemotherapy and increase the need of a successful approach to target basic mechanisms of tumors' growth.

### 1.3.3) Bacterium-induced resistance

Microbes and malignancy both exhibit a symbiotic relationship which is regarded as a double-edged sword. However, on the one hand bacteria can act as an emerging cancer therapy approach (Park *et al.*, 2017) by using multifunctional bacteria-driven 'microswimmers' as targeted drug delivery systems with significantly enhanced drug transfer to tumours, when compared with free drug (doxorubicin) or the passive drug-loaded microparticles alone.

On the other hand, microbial infections can cause major complications for cancer patients leading to granulocytopenia due to myelosuppressive chemotherapy (Schimpff *et al.*, 1971). Microbes can trigger cancer cells' progression through



several mechanisms: promotion of epithelial-mesenchymal transition (EMT), modulation of immune system and induction of chronic inflammation (Geng *et al.*, 2020; Li *et al.*, 2019) through direct translocation which affect the metabolism of host cells and cause genotoxicity.

Immunosuppression can also be caused by myelosuppressive cytotoxic chemotherapy that led to increased risk of infections. Induced immunosuppression by chemotherapy practices or the breakdown of mucosal barriers make the cancer patients susceptible to microbial infections (Holland, Fowler, and Shelburne, 2014).

The emergence of multi-drug resistant bacteria many of which, according to the World Health Organization (WHO) list, are Gram-negative pathogens, has been described as 'the silent pandemic of antimicrobial resistance'. *E. coli* has been recognized as a causal factor in infections in cancer patients, particularly those with hematological malignancies with neutropenia, B-cell-mediated immunity or splenic function dysfunction (Safdar and Armstrong, 2011).

Colorectal Cancer (CRC) is the second leading cause of mortality in men and women worldwide. Insights of microbial involvement in the gut environment have contributed to our understanding of the mechanism of CRC initiation and strains of *E. coli* have been causally associated with the development of CRC due to the incidence of colitis (Arthur *et al.*, 2013).

*Methicillin resistant Staphylococcus aureus (MRSA)* has been accounted for microbial infections in cancer cells and accounted for one of the leading causes of invasive bacterial resistance in cancer patients (Mikulska *et al.*, 2014).

There is no clear mechanism of multi-drug resistance (MDR) in cancer cells. The World Health Organization (WHO) considers it a serious challenge of the twenty-first century (Morrison and Zembower, 2020; Patel *et al.*, 2021). Oncologists have observed that resistance to cancer cells has never been detected until it is exposed to cancer therapy. Despite the availability of several clinically effective anticancer regimens, work is still in progress to develop a targeted approach with impressive cytotoxic activity against resistant mechanisms (Perez, Adachi and Bonomo, 2014).

## 1.4) Mitochondria

Mitochondria are a major compartment of human cells which are bound by double membrane, characterized as a bio-energetic and biosynthetic organelle that utilize the substrates of the cytoplasm to drive the mechanistic pathway of fatty acids, electron transport chain (ETC), TCA cycle (Sullivan and Chandel, 2013), respiratory chain to synthesize fatty acids, nucleotides, amino acids, lipids, iron clusters and antioxidants (NADPH) as well (Morais *et al.*, 1994).

Mitochondria have evolved some billion years ago from  $\alpha$ -proteobacteria and became endosymbionts later in eukaryotic cells, as per the theory proposed originally by Lynn Sagan in 1967 (Sagan, 1967). The evolution of complex cellular systems of mitochondria has made it independent of host cells due to the presence of their own genomic material (Yang *et al.*, 1985). Mitochondrial biological activities exhibit similar characteristics to bacterial ancestors of mitochondria such as double membrane, energy production and existence of their own DNA (Sullivan and Chandel, 2013).

Mitochondria have long been recognized as a powerhouse of eukaryotic cells that leads to the production of energy (ATP) through oxidative phosphorylation (OXPHOS) and the respiratory chain (Eisenberg-Bord and Schuldiner, 2017). Mitochondria are more than a central core of energy for cell homeostasis and are involved in all aspects of cellular metabolism. Their structure, function and pathology are intermittently connected to each other and that has made it relatively easy to study all aspects of mitochondria.

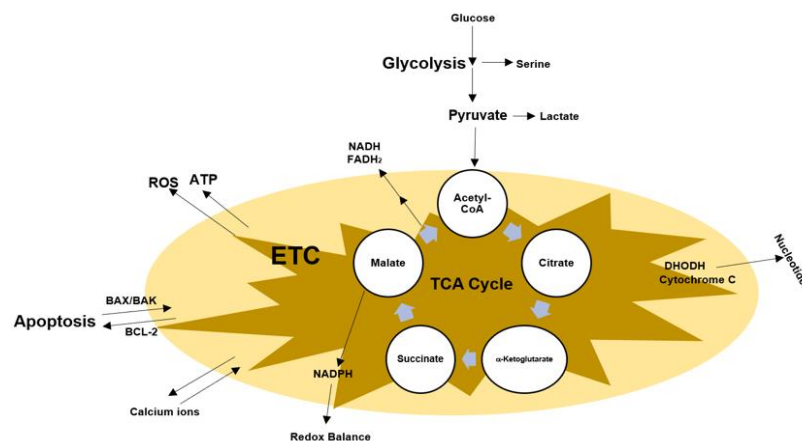


**Figure 1.5:** Biosynthetic and bioenergetic processes of mitochondria

Glycolysis is a universal pathway of normal cells that utilizes one molecule of glucose to convert it into two molecules of pyruvic acid and the released energy is restored in the form of ATP and reducing equivalent NADH. The main aim of glycolysis is to provide energy (ATP) to all metabolic pathways of a normal cell through electron transport system (ETC). The substrates of glycolysis, anabolic and catabolic reactions of fatty acids and amino acids are processed through TCA cycle to generate high energy electrons (NADH and FADH<sub>2</sub>) to power electron transport chain (ETC) (Khutornenko *et al.*, 2010) and to generate reactive oxygen species (ROS) which can stimulate the activation of signaling transduction pathways such as MAP kinase and HIFs which are essential for the regulation of cell homeostasis (Sullivan and Chandel, 2013). ETC is an essential requirement which is processed through OXPHOS and is also associated with the generation of ROS (**Figure 1.5**) (Anderson *et al.*, 1981).

Mitochondria also play a critical role to programmed cell death due to the emergence of BCL-2 family proteins, cytochrome-c, and apoptotic inducing factors (AIF) which comprise of proteins released to induce apoptosis. Pro-apoptotic proteins activate the release of BAX and BAK which induce pore formation and deactivate anti-apoptotic factors to alter membrane potential. Then, cytochrome-c stimulates the release of apoptotic inducing factors (AIF) from the pores of mitochondrial membrane (Lant and Derry, 2013). Mitochondrial pores stimulate the release of cytochrome-c which forms a complex for apoptosis by the addition of apoptotic protease activating factor (Apaf-1) to accelerate apoptosis (Valero *et al.*, 2005). The mitochondrial membrane potential is an electrochemical gradient and play a critical role in the stability of mitochondrial processes such as apoptosis, release of ROS and also activate nuclear encoded proteins to translate through mitochondrial membranes (Heerdt, Houston & Augenlicht, 2005).

Mitochondria regulate through critical cell processes from ATP production to apoptosis and measuring their function could be an imperative way to target cancer cells through different aspects of cellular metabolism (Frezza, Cipolat and Scorrano, 2007).

### 1.4.1) Metabolism of cancer cells

Abnormal cell metabolism is a hallmark of cancer cells' growth, yet its regulation is not completely understood (Yu *et al.*, 2017). Cancer cells regulate through multiple metabolic pathways to complete the supply of energy production and biosynthetic metabolites depending upon the requirements of cellular dysfunction (Pavlova and Thompson, 2016). Cancer cells' progression and resistance to therapies depend upon the suppression of apoptosis.

Mitochondria which are regarded as powerhouse of cells play an important role in the progression of cancer cells as an energy source through the generation of reactive substrates (Mashayekhi *et al.*, 2014). Cancer cells exhibit various degrees of mitochondrial dysfunction through metabolism, mitochondrial membrane potential ( $\Delta\psi_m$ ) or the generation of ROS which could provide a general possibility to target cancer cells and improve therapeutic efficacy of chemotherapeutics (Hara *et al.*, 2011a).

Mitochondrial DNA (mtDNA) plays a key role in the metabolic regulation of replication system of cancer cells (Wen, Zhu, and Huang, 2013). There are several approaches that have been developed to target cancer cells' progression through mitochondrial metabolism which is associated with multiple changes in cellular functioning (Trachootham *et al.*, 2008).

Mitochondrial Membrane Potential ( $\Delta\psi_m$ ) is an important factor of mitochondria and changes response to apoptotic signals, microenvironment and localization of an individual cell during growth (Heerdt, Houston and Augenlicht, 2005). The most noticeable difference between healthy and cancer cells is the mitochondrial membrane potential ( $\Delta\psi_m$ ) (Constance and Lim, 2012) as mitochondria produce relatively high transmembrane electric potential of -180mV in cancer cells as compared to plasma membrane which produces potential of -60mV in healthy cells (Jean, *et al.*, 2014).

In the similar way, initiation and development of cancer cells is influenced by bacterial infections leading to genomic stability and integrity to cause DNA damage

(Geng *et al.*, 2020). Bacterial infections are one of the most important inflammatory factors leading to DNA damage and increasingly recognized as a risk factor for cancer cells' progression (Moergel *et al.*, 2013). The mechanism of development of cancer cells is hard to determine due to diverse interaction between microbes and host cells. Microbial infections have been reported for cancer-inducing factors by damaging host cells' DNA, induction of inflammation, suppression of immune system, promotion of epithelial-mesenchymal transition (EMT), hormone secretion and lymph proliferation (Geng *et al.*, 2020; Li *et al.*, 2020). Bacteria can translocate to cause genotoxicity which affect the metabolism of host cell's environment (Zhou *et al.*, 2020). Microbial susceptibility could be a practical therapeutic approach into tumour to colonize hypoxic environment of cancer cells without suppressing the immune system (Zhang *et al.*, 2018).

There are certain antibiotics including chloramphenicol that have been characterized to target mitochondrial biogenesis. Chloramphenicol can inhibit both bacterial and mitochondrial protein synthesis, causing mitochondrial stress and decreased ATP biosynthesis. The adverse effect of suppressing mitochondrial protein synthesis in the treatment of infections has reduced its use as an antibiotic (Schwarz and Firkin, 1976). Overuse and abuse of antibiotics can increase the risk of cancer. Chloramphenicol has been shown to promote cancer progression, which may be more related to its 70S ribosomal inhibitory action and should be avoided in patients undergoing chemotherapy (Li *et al.*, 2010).

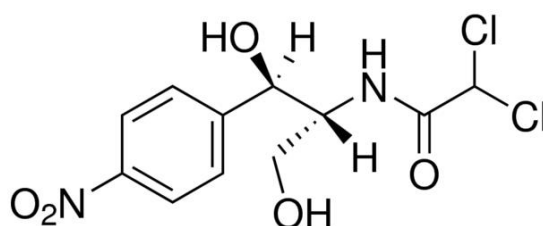


**Figure 1.6:** Chemical structure of Chloramphenicol

#### 1.4.2) Mitochondrial dysfunction and cancer cells

Cells proliferate through multiple metabolic and biosynthetic pathways for energy production depending upon the availability of metabolites and cellular functions. In normal conditions, mitochondria (double-membrane organelle) play an essential role not only as a powerhouse of cell but also as a reservoir to promote apoptotic proteins essential for induction of apoptosis (Pavlova, and Thompson, 2016) and utilize glucose, fatty acids, amino acids for energy production through several biochemical pathways such as OXPHOS, electron transport chain (ETC) and the generation of ROS.

The process of tumorigenesis exhibits several degrees of dysfunction in mitochondria such as higher mitochondrial membrane potential ( $\Delta\psi_m$ ), shift of energy metabolism, blocked apoptosis, and elevated level of ROS (Lu, Ogasawara, and Huang, 2008). These alternative pathways could provide a therapeutic approach to target mitochondria of cancer cells and improve the selectivity of chemotherapy in oncology (Hara *et al.*, 2011b).

Mitochondrial dysfunction is manifested by a switch of energy metabolism from (OXPHOS) to glycolysis and release of ROS leading to development of cancer cells (Wen, Zhu and Huang, 2013). Transport of electrons through mitochondrial respiratory chain is associated with the generation of ROS, which are formed by the reaction of leaked electrons from respiratory chain with oxygen to release superoxide, in the process of OXPHOS. Mitochondrial oxidative damage leads to a change at the level of ATP and ROS balance affect upon the cell viability and proliferation (Hara *et al.*, 2011b).

Glycolysis is generally regarded as the dominant metabolic pathways of cancer cells' proliferation. Cancer cells have a high dependence on glycolysis which is quite unlikely in normal conditions of cells. Mitochondria play a vital role in the survival and death of cells and the feature of an outer membrane and an inner mitochondrial membrane is unique for organelles and due to the presence of highly dense and abundant phospholipids with a high protein to lipid ratio (Chen *et al.*, 2010). Clearly,

these features point to its exploitation as a biological intracellular target for therapeutic intervention.

Aerobic glycolysis is an aggressive metabolic phenotype to produce energy (ATP) in the presence of excessive oxygen which is also the premise underpinning the Warburg effect (Warburg, 1956). ATP production at a high rate can lead to the generation of biomass of fatty and amino acids which are essential targets for rapid cell proliferation (Hsu and Sabatini, 2008). In general, cancer cells take up glucose as a glycolytic flux to produce lactate instead of oxygen as an intermediate to fulfill the metabolic demand of cancer cell proliferation (Bock *et al.*, 2013).

In addition to those, mitochondrial outer and inner membranes are the major barriers to passive diffusion of small molecules such as xenobiotics due to high mitochondrial membrane potential ( $\Delta\psi_m$ ) in cancer cells.  $\Delta\psi_m$  decreases the opening of mitochondrial transition pores (MTP) which is a mega-channel involved in mitochondrial membrane permeabilization (MMP) and release of pro-apoptotic factors to induce mitochondrial apoptosis.

Including the heterogeneity of genetics and histology of tumour cells, malignancy is also associated with an induction of common pathways to support the proliferation of cancer cells through catabolism, anabolism, and redox cycle (Li *et al.*, 2012). Hence, mitochondrial dysfunction of cancer cells could be an attractive therapeutic approach to cause apoptosis of cancer cells.

Considerable attention has been devoted to mitochondrial stresses because they can stimulate both beneficial and pathogenic adaptive responses, and there is growing evidence that retrograde signalling (mitochondria to nuclear messaging) can affect pathways that include regulation of cell proliferation, cell migration and invasion, apoptosis-resistance and chemo-resistance (Sullivan and Chandel, 2014; Guha *et al.*, 2017).

Retrograde signalling could provide mechanisms by which altered mitochondrial function leads to changes in nuclear gene expression and metabolism mediated by specific transcription factors in favour of enhanced tumour initiation and invasion.

Furthermore, the connections between mitochondrial retrograde signalling and metabolic alterations in the tumour microenvironment are the focus of a recent review (Yang and Kim, 2019).

Consequently, agents that can prevent the tumour-promoting effects that may arise from retrograde signalling would be of therapeutic importance and strengthens the motivation in this study to design molecules that can be delivered selectively to this organelle in cancer.

### **1.4.3) Bacterial infections and cancer progression**

Bacterial infection is a common and continuous problem in cancer patients. Direct and indirect effect of cancer on immune system increases the susceptibility of infections in cancer patients (Hugonnet *et al.*, 2004). There are more than a million bacterial species present in a human body. Different bacterial species are found to initiate cancer development through different mechanisms at different sites. For example, Fusobacterial species can cause colon and oral carcinoma (Geng *et al.*, 2020).

Inflammation is a natural response of immune system to protect the regulation of host cells. Persistence to chronic inflammation could lead to cancer cell progression but it is not specific to bacterial species (Liu *et al.*, 2015) (**Figure 1.7a**). The longer persistence of bacterial species in host epithelial cells stimulates the secretion of pro-inflammatory cytokines (IL-6, IL-1) leading to severe inflammation (Sugimoto, Ohno, Graham, and Yamaoka, 2011) which is further associated with DNA damage (Habib, Moinuddin and Ali, 2005), aberrant cell differentiation, mutation, and cancer cells' metastasis (Irrazabal *et al.*, 2020). The amplified inflammation by bacterial infection results in enhanced cell division leading to metastasis of cancer cells (**Figure 1.7b**) (Korniluk *et al.*, 2017).

Bacterial infections are tumour stimulating and carcinogenic to cause genomic instability which produces toxins to hamper the regular stability of signals associated with cancer cells' proliferation (Tegos *et al.*, 2008). Genomic stability is a key factor to maintain the integrity of cells by protecting cells from oxidative stress, DNA



replication errors and several exogenous carcinogens causing DNA damage (**Figure 1.7c**). Genomic instability process tumorigenesis through spontaneous mutation leading to metastasis (Dixon *et al.*, 2015). Not all bacterial strains are carcinogenic, yet Gram-negative bacteria favour genomic instability and oncogenic transformation to induce DNA damage (Weyler *et al.*, 2014).

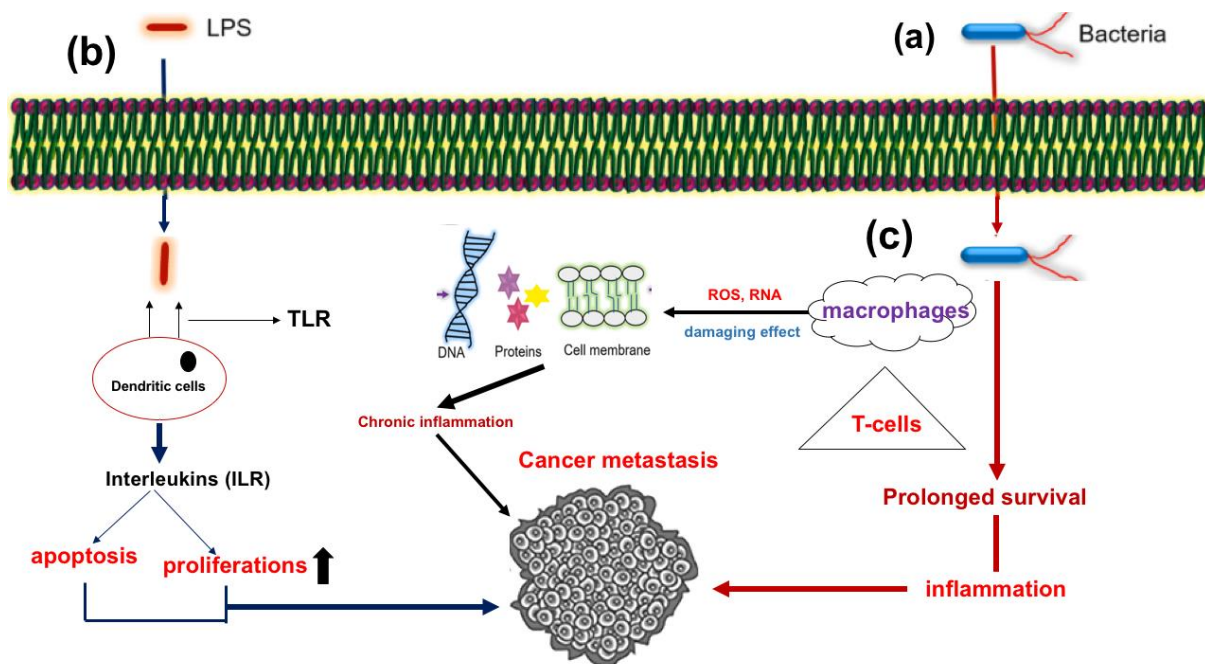


**Figure 1.7:** Bacterial infections leading to cancer cells' development

It was also reported that a baseline of cancer development is the immune cell hyper-activation/evasion by bacteria. Bacterial outer surface has complex antigenic moieties (Sivagnanam, Zhu and Schlichter, 2010), and lipopolysaccharides rich capsule which bind with specific toll-like receptors (TLR) which signals the regulatory pathway of cell proliferation and apoptosis. Hyper-activation of TLR and escaping of immune recognition can cause cancer cell development (Bergenhengouwen *et al.*, 2016) (**Figure 1.7b**). For example, *E. coli* caused uncontrolled metastasis in non-small cell lung cancer by the hyper-activation of TLR4 and TLR9 which is related with lipid synthesis (Ye *et al.*, 2016).

Historically, no connection was known between bacterial infections and cancer, however, two different mechanisms are considered to be amongst the major causes of cancer. One of these is chronic inflammation which could be induced by parasitic

or bacterial infection but related to malignancy due to their chronicity. The longer the inflammation persists the more likely are the chances of malignancy developing (Payne, Nowak, and Blumberg, 1992). *H. pylori* infections of the gastrointestinal tract have for some years been linked with carcinogenesis associated with an inflammatory process. Once established the infection can persist for decades. The International Agency for Research on Cancer (IARC) considers *H. pylori* a definite cause of gastric cancer development and in 2019 declared it a group 1 carcinogen (France, 2019).

The association between bacterial infections and cancer cells development has been explored yet the mechanism of action is not fully understood. Although, the symbiotic relationship between bacteria and induction of cancer could lead to a useful approach of successful management of chemotherapy.

### **1.5) Concept of drug design and discovery**

The development of new pharmaceutical agents following the mono-therapy approach is expensive and laborious along with subsequent clinical trials receiving before FDA approval takes about 15 years which makes it more important to find a feasible approach which should be economically efficient. Including these, drug resistance has been a major problem leading to failure of chemotherapy practices in cancer patients (Sutendra, *et al.*, 2011). However, combination of two or more therapeutic approaches to target cancer cells has become a cornerstone in cancer chemotherapy (Giaccone *et al.*, 2004) as it is economically effective therapeutic approach (DiMasi, Hansen and Grabowski, 2003) to reduce the incidence of resistance in cancer cells.

The oxidative property of cancer cells and multi-drug resistance (MDR) due to overexpression of P-gp resulting in increased efflux of drug candidates through cancer cell (Wu *et al.*, 2017) promote the need of a biophysical drug delivery system (Guilhelmelli *et al.*, 2013). The major concept of drug design and development of anticancer and antibacterial prodrugs has been based upon the targeted drug delivery directly into mitochondria of cancer cells to induce mitochondrial oxidative

damage of tumors without effecting the normal cells and into bacterial cells to hinder the growth of bacterial population.

### 1.5.1) Ciprofloxacin (CIPRO)

CIPRO is an FDA approved and widely prescribed broad spectrum antibiotic that belongs to the fluoroquinolone class (Mandell *et al.*, 1994). Structure activity relationship (SAR) has revealed the pharmacological importance of CIPRO in microbiology and oncology.

CIPRO is pharmacologically active against both strains of bacteria by targeting primarily to topoisomerase II (Gellert *et al.*, 1977), DNA-gyrase (Gellert *et al.*, 1976) in Gram-negative bacteria, and topoisomerase IV in Gram-positive bacteria through a non-covalent binding (Ficker, Paolucci and Christensen, 2017; Shindikar and Viswanathan, 2005).

CIPRO is known regarding the possible effects of substitutions on the ring system to inhibit the growth of both Gram-negative and Gram-positive bacteria. The presence of carboxylic acid (-COOH) at position-3 and carbonyl group at position-4 are essential for antimicrobial activity (**Figure 1.8**). However, substitution at position-7 is also important to maintain specificity and serum half-life (Tillotson, 1996).

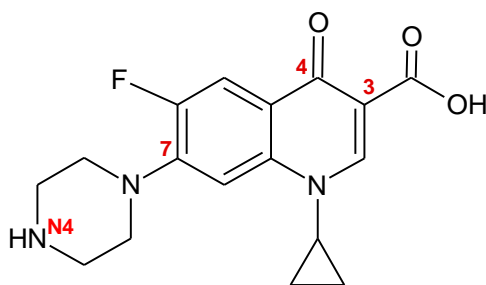


**Figure 1.8:** Chemical Structure of ciprofloxacin

Structure activity relationships (SAR) have shown that position-7 (**Figure 1.8**) improves lipophilicity, broadening the antibacterial spectrum, safety, potency, and pharmacokinetic properties of CIPRO (Koga *et al.*, 1980). MDR has decreased the efficacy of antibiotics through different mechanisms such as expulsion of antibiotics via efflux pump. There is a need to develop an approach of antimicrobials to

overcome MDR impacting on pathological ways such as through a biophysical drug delivery system, drug modification and drug combination methods (Guilhelmelli *et al.*, 2013). Significantly, SARs have also reported the substitution of CIPRO at the C-3 position could be an imperative choice to enhance anticancer potential of CIPRO (Ahadi *et al.*, 2020). Likewise, considering the similarities between mitochondrial and bacterial membranes, two derivatives of TPP<sup>+</sup>-conjugated with CIPRO through an ester and an amide bond at position-3 (**Figure 1.9**) have been developed to increase the efficacy of CIPRO as an antibacterial targeting the bacterial membranes which has successfully established the efficacy of TPP<sup>+</sup>-CIPRO hybridization to combat MDR bacteria (Kang *et al.*, 2020).

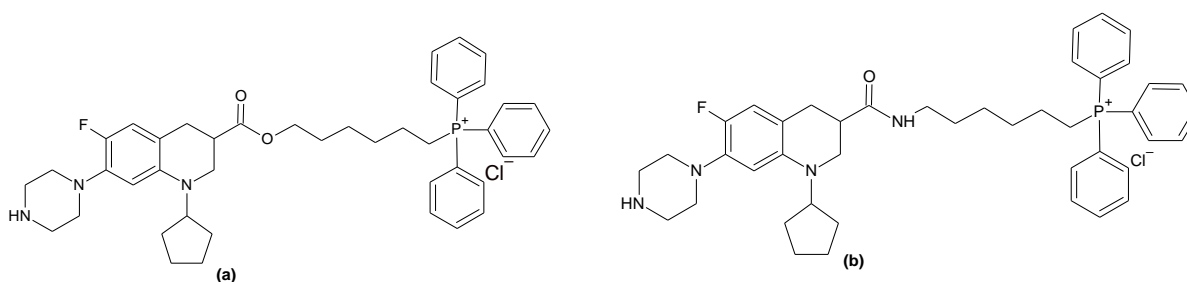


**Figure 1.9:** Chemical structures of TPP<sup>+</sup>-conjugated with ciprofloxacin through (a) an ester bond and (b) amide bond

It is also previously investigated and documented that an introduction of a substituent on N4-piperazine moiety can dramatically improve the biological and physiological potential of CIPRO as antibacterial and anticancer agent (Gootz *et al.*, 1994) including lipophilicity of the compound.

For example, 7-((4-substitued) piperazin-1-yl) derivatives of ciprofloxacin (**Figure 1.10**) have been synthesized which are non-toxic and showed potent antitumour activity which demonstrates that the cytotoxic activity of CIPRO could be potently modulated by the addition of simple substituents on N4-piperazinyl ring (Azéma *et al.*, 2009).

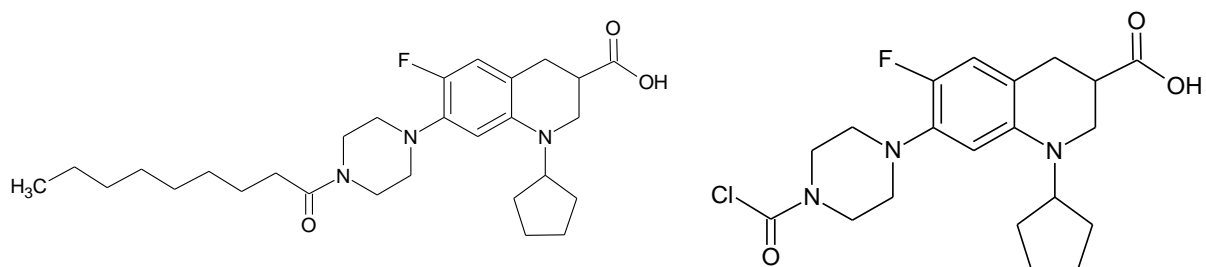


**Figure 1.10:** Chemical structure of 7-((4-substituted)piperazin-1-yl) derivatives of ciprofloxacin

Including CIPRO there are other antibiotics that have effects upon cancer cell metabolism and mitochondrial biogenesis. Levofloxacin (**Figure 1.11**) is one of those broad-spectrum FDA-approved antibiotics that synergistically acts with chemotherapeutics as an attractive combination to treat breast cancer. Biologically, it has been proven that breast cancer cells have higher mitochondrial biogenesis than normal breast cells.

The mechanism of action of levofloxacin as anticancer agent acts through the inhibition of mitochondrial biogenesis which is associated with the deactivation of signalling pathways responsible for the growth and development of breast cancer (Yu, Li and Zhang, 2016).

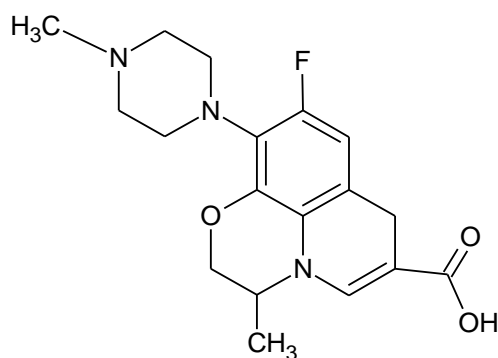


**Figure 1.11:** Chemical structure of Levofloxacin

The cytotoxic potential of CIPRO is revealed by the induction of apoptosis and inhibition of cancer cell progression by cell cycle arrest. Very recently it has been employed in adjuvant chemotherapy and are also recognized to regulate the stemness of cancer cells (**Figure 1.12**). CIPRO has made a unique element among all other family members of antibiotics due to its recognized property of apoptosis and G2 cell cycle arrest of several cancer cell lines (Smart *et al.*, 2008) such as

U87MG (Glioblastoma), Panc-1 (pancreatic cancer), MLC9981 (prostate cancer), MDA MB-231 (breast cancer), H460 (lung cancer), HTB9 (bladder cancer), HT-29 (colorectal carcinoma) and K562 (leukemia cells) (Gürbay *et al.*, 2005; Reuveni *et al.*, 2008).

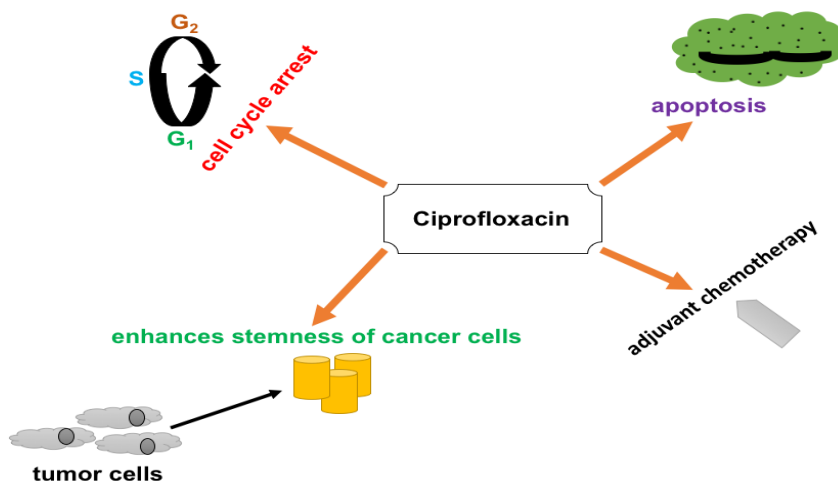


**Figure 1.12:** Anticancer potential of ciprofloxacin

There are several approaches such as derivatization, cyclization and bio-steric replacement could be applied to design CIPRO-based anticancer and antibacterial agents.

Likewise, tetracycline and tigecycline belonging to the same class of antibiotics have also been recognized as anticancer agents on acute myeloid leukemia (AML) through the induction of mitochondrial degeneration and cell-cycle arrest.

Tetracycline (**Figure 1.13**) and derivatives have long been investigated as anticancer agents on Hela cell lines with a significant inhibitory action and an effect on mitochondrial structure (Buy and Showacre, 1961).

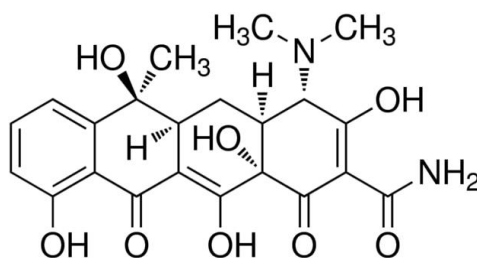


**Figure 1.13:** Chemical structure of Tetracycline

However, the main effect of Tigecycline (**Figure 1.14**) on cancer cells is the inhibition of cell-proliferation, cell cycle arrest and mitochondrial dysfunction. It also helps via autophagy to induce apoptosis and inhibits angiogenesis on solid tumours (Škrtić *et al.*, 2012).

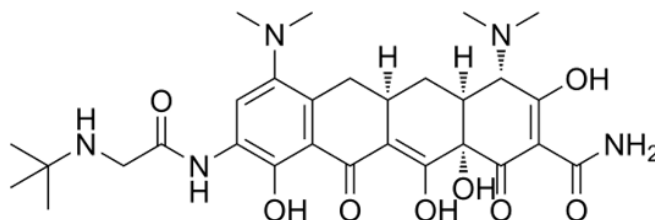


**Figure 1.14:** Chemical structure of Tigecycline

Structure activity relationships of CIPRO have revealed the fact that CIPRO could be a dynamic choice to regulate cancer cells' death. Good penetration ability of CIPRO into different tissues and glands has also made it eligible for both anticancer and antibacterial studies. In fact, in-vitro studies have established the need of high concentration of CIPRO to gain cytotoxic potential (Kassab and Gedawy, 2018; Yadav *et al.*, 2015) as it was found to induce apoptosis at a higher concentration while at a lower concentration it could inhibit the proliferation of Jurkat cells but not cell death (Kloskowski *et al.*, 2012).

To focus on biological importance of CIPRO, it is therefore particularly aimed to design a CIPRO hybrid with a structural modification at C-3 and N4-piperazine ring having both anticancer and antibacterial potential.

### 1.5.2) Dichloroacetic acid (DCA)

The interest in the therapeutic use of dichloroacetate (DCA) (**Figure 1.15**) has been increasing as an anticancer agent (Sun *et al.*, 2010) which is a mitochondrial-targeting agent, metabolically acts to switch the metabolism of cancer cells from anaerobic glycolysis to aerobic glycolysis by inhibiting the activity of mitochondrial enzymes (PDK) and metabolizing the activity of pyruvate dehydrogenase (PDH) (Bonnet *et al.*, 2007).

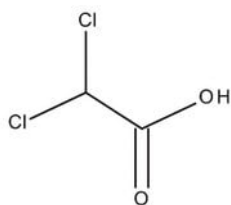


**Figure 1.15:** Chemical structure of DCA

DCA activates the release of pyruvate dehydrogenase enzyme (PDH) by inhibiting pyruvate dehydrogenase kinase (PDK) in mitochondria of cancer cells that fosters the mitochondrial oxidation of pyruvate and interrupts in the metabolic advantage of cancer cells (Stacpoole, Handerson, Yan and James, 1998) which leads to mutation in mitochondrial DNA resulting in respiratory chain dysfunction by the release of cytochrome-c through oxidative phosphorylation (**Figure 1.16**).

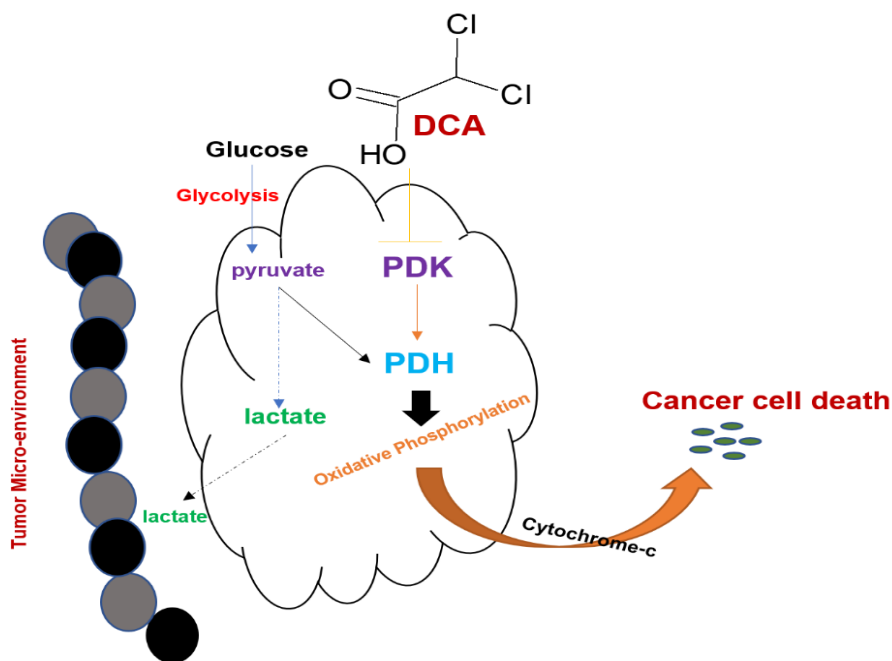


**Figure 1.16:** Mechanism of action of DCA

There are numerous drugs targeting cancer cells' metabolism, yet DCA has been recognized as highly reactive due to its positive effect to chemotherapy (Pathak *et al.*, 2014; Ward and Thompson, 2012) as it plays a key role to induce apoptosis in cancer cells by increasing mitochondrial oxygen species (ROS). It is a small molecule (150 Da) that can penetrate to all types of cells and tissues. It acts as a lactate lowering drug that has a counteractive effect on the acidosis state of tumor



microenvironment by inhibiting the tumour growth and dissemination (Papandreou, Goliassova and Denko, 2011; Stockwin *et al.*, 2010). The presence of pyruvate in mitochondria causes an increased efflux of cytochrome c, apoptotic-inducing factors and upregulates the level of ROS resulting in consequent reduction in the viability of cancer cells (**Figure 1.16**) (Ruggieri *et al.*, 2015).

The biological activity of DCA as a single candidate is not considered to be ideal, therefore there is a need to modify DCA to enhance its potential (Yang *et al.*, 2010). Such as DCA was conjugated with CIPRO through a structure-based conjugation reaction and the resulting conjugate has been proved to be effective against Gram-negative and Gram-positive bacteria with highly potent antimicrobial property (**Figure 1.17**) (Seliem *et al.*, 2019).

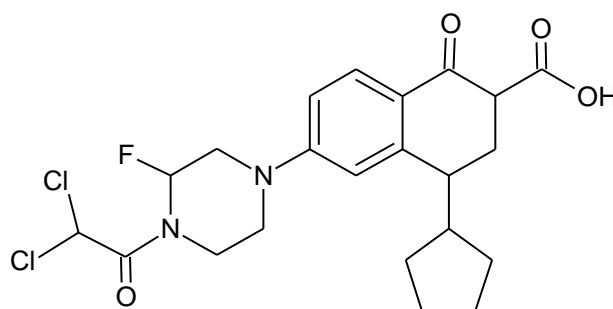


**Figure 1.17:** Chemical structure of DCA derivative of ciprofloxacin

DCA can inhibit the growth of cancer cells and initiate cancer cell death, yet its cytotoxic potential is quite low ( $IC_{50} > 1000 \mu M$ ) and because of this, is a starting candidate for improving cytotoxic activity which has led to the synthesis of a variety of DCA derivatives. Notably, the cytotoxic activity of DCA has been successfully augmented by conjugating it with triphenyl phosphonium cation ( $TPP^+$ ) to afford a conjugate denoted as 'Mito-DCA' through a direct translocation to mitochondria of cancer cells to induce apoptosis (**Figure 1.18**) (Pathak *et al.*, 2014).

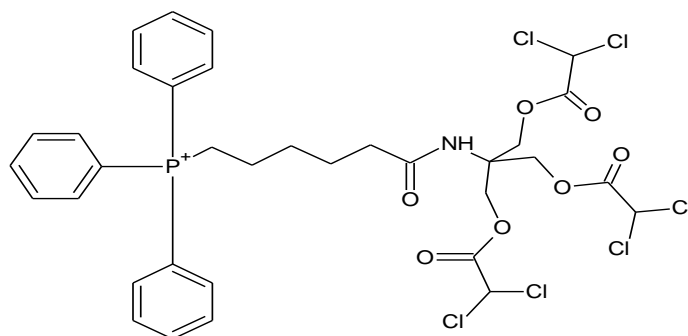


**Figure 1.18:** Chemical structure of Mito-DCA

The synergistic effect of DCA with other chemical agents and reduction in adverse effects has also made it an eligible candidate in biomedicine practices (Stander, Stander and Joubert, 2015). The number of tested strategies of different cancer cell types is too limited to report about the efficacy of DCA, yet *in-vitro* and *in-vivo* study of DCA on xeno-transplant models has revealed its apoptotic effect and decreased tumour growth (Sutendra *et al.*, 2013).

Based upon the pharmacological evidence of DCA as anticancer agent and increasing antimicrobial potency of antibiotics has led to a hopeful achievement of conjugating DCA with CIPRO to exhibit both anticancer and antibacterial properties in a single candidate, during this research programme.

### 1.5.3) Anthraquinones (AQ)

Anthraquinones (AQ) have extensive therapeutic effects on cancer cells that are related to angiogenesis, metastasis, and invasion, reversing multi-drug resistance, promoting tumor apoptosis, and increasing sensitivity to chemotherapy (Ge and Russell, 1997).

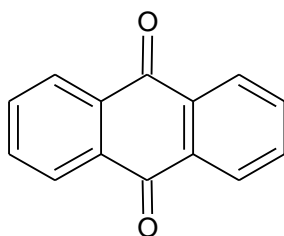


**Figure 1.19:** Chemical structure of anthraquinone

The structural core of anthraquinone (**Figure 1.19**) has attracted the interest as an anticancer agent (Fan, Shi and Lowary, 2007) as they can uncouple mitochondrial OXPHOS causing mechanistic investigation in their redox chemistry. Additionally, the antioxidant property of anthraquinone have increased their importance in chemotherapy to induce cancer cell death through oxidative stress mechanism by increasing the concentration of ROS (Ge and Russell, 1997).

It is generally believed that cytotoxic activity of anthraquinone work through DNA interaction. However, the mechanism of interaction is not fully understood. The

anthraquinone related anticancer drugs could interact with mitochondrial DNA (mtDNA), preferentially at the rich sites of guanine and cytosine. This cleavage can cause conformational changes in the mtDNA which could lead to inhibition of mtDNA replication in cancer cells and may cause mtDNA damage (El-Gogary, 2002). On the other hand, anthraquinones have been shown to inhibit the activity of mitochondrial topoisomerase II which could lead to DNA damage. Mitochondrial topoisomerases II are one of the essential enzymes to control the topological state of mitochondrial DNA involve in genetic process such as replication and transcription which are activated in cancer cells' growth. Therefore, mitochondrial topoisomerase II could be an important cellular target to control the growth of cancer cells to design new antineoplastic drugs (Kou *et al.*, 2012).

Additionally, anthraquinone have the biological activity to modulate ROS-mediated mechanism in cancer cells which could evaluate their antioxidant activity in cancer cells and trigger cell death by reaching the level of ROS to toxic threshold level (Hancock, Desikan and Neill, 2001). Anthraquinone exhibit antibacterial activity through the disruption of redox process of bacteria. High concentration of anthraquinone can disrupt bacterial membrane agents (Chan, Zhang, and Chang, 2011). Molecules having anthraquinone compounds can inhibit bacterial DNA gyrase through the exhibition of their toxicity on bacterial cell by stabilizing the double-stranded break of DNA which is created by gyrase to block the transcription (Williamott *et al.*, 1994). In general, anthraquinone could be a better choice to design the framework of novel anticancer compound.

To develop potent antitumour agents, a series of anticancer agents have been designed and developed having anthraquinone as a base component due to its reported antioxidant and anticancer activities (Bhasin *et al.*, 2013) with a possible mode of interaction following the disruption of cellular redox process (Fukuda *et al.*, 2009). For example, a doxorubicin analogue has been successfully synthesized having TPP<sup>+</sup> and DCA attached in it and investigated for its cytotoxic potential on DOX-resistant xenograft tumor model (**Figure 1.20**) (Sharma *et al.*, 2018).

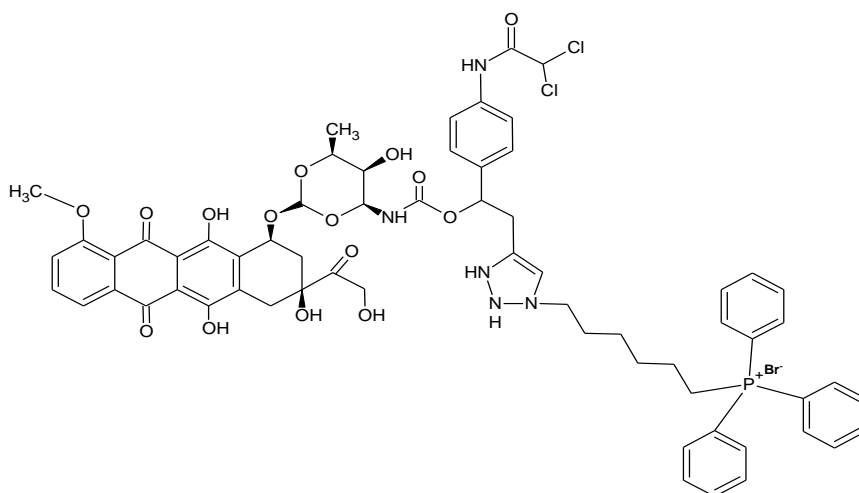


**Figure 1.20:** Chemical Structure of doxorubicin analogue with TPP<sup>+</sup>-cation and DCA

#### 1.5.4) Triphenylphosphonium cation (TPP<sup>+</sup>):

Lipophilic cations such as triphenyl phosphonium (TPP<sup>+</sup>) cations (**Figure 1.21**) have the capability to target mitochondria in cancer cells through a biophysical means of drug delivery system. TPP<sup>+</sup>-cations can accumulate several hundred-folds in mitochondria in the absence of transporters to cross mitochondrial membranes. The hydrophobic surface of TPP<sup>+</sup>-cations make it eligible to enter mitochondrial matrix probably due to high mitochondrial membrane potential ( $\Delta\psi_m$ ) in malignant cells (Millard *et al.*, 2010).

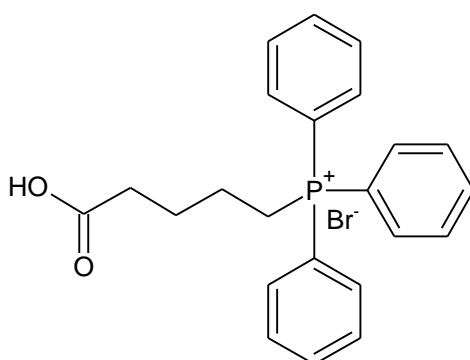


**Figure 1.21:** Chemical Structure of (4-carboxybutyl)triphenylphosphonium bromide

The structure activity relationship of TPP<sup>+</sup> conjugates has revealed the mystery that lipophilicity of TPP<sup>+</sup>-cations enable them to target mitochondria in cancer cells. Accordingly, lipophilic TPP<sup>+</sup>-cations have been widely used as a probe to target mitochondria. In addition to these, malignant cells are highly oxidative due to high electron transport chain and TCA cycle that could offer a biophysical drug delivery

system in mitochondrial matrix. This has raised the possibility of TPP<sup>+</sup>-cations having large surface area to cross mitochondrial membranes and accumulate in mitochondrial matrix. TPP<sup>+</sup> based lipophilic cations can sufficiently delocalize the positive charge to cross the large surface area and therefore there is no need to apply a further specific transporter for mitochondrial translocation (Jonnalagadda *et al.*, 2020).

TPP<sup>+</sup>-cations cross inner and outer membranes of cancer cells through traversing the high mitochondrial membrane potential directly the mitochondria of malignant cells. The membrane can prevent non-cancerous cells from being damaged as commonly affected by chemotherapy. The positive ion of TPP<sup>+</sup> can delocalize at the hyperpolarized state of cancer cells which diminishes the need of specific translocators to target mitochondria of cancer cells (Dong *et al.*, 2013) (**Figure 1.22**).

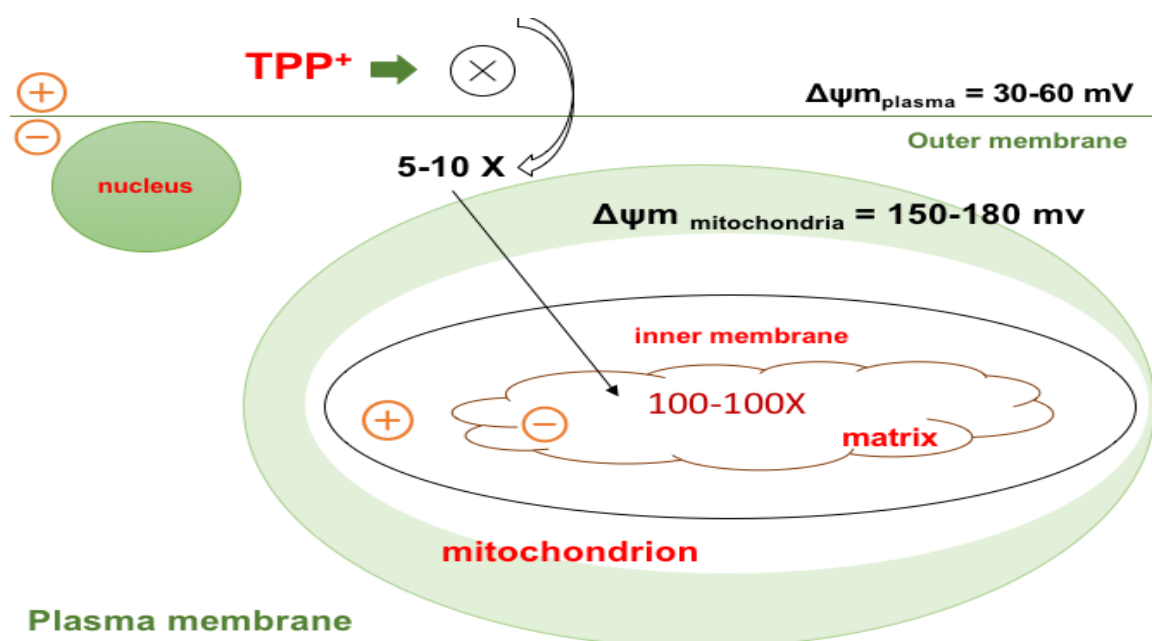


**Figure 1.22:** Translocation of triphenyl phosphonium cation to mitochondria of cancer cells

In earlier work from this laboratory, focusing on the mechanism of action of the TPP<sup>+</sup>-cation, a series of novel anthraquinone TPP conjugates was synthesized, including an ester-linked amino-anthraquinone-triphenylphosphonium (AQ-TPP) conjugate code-named SH1 (**Figure 1.23**) that was shown to accumulate inside mitochondria to circumvent P-gp mediated resistance which was tracked by using MitoTracker<sup>FM</sup> tracer dye. Furthermore, SH1 was proved to be equally cytotoxic in

the highly resistant HCT-15 colon cancer and relatively sensitive MCF-7 breast cancer cell lines (MCF-7) (Mohammed, 2021), and was not found in the nucleus.

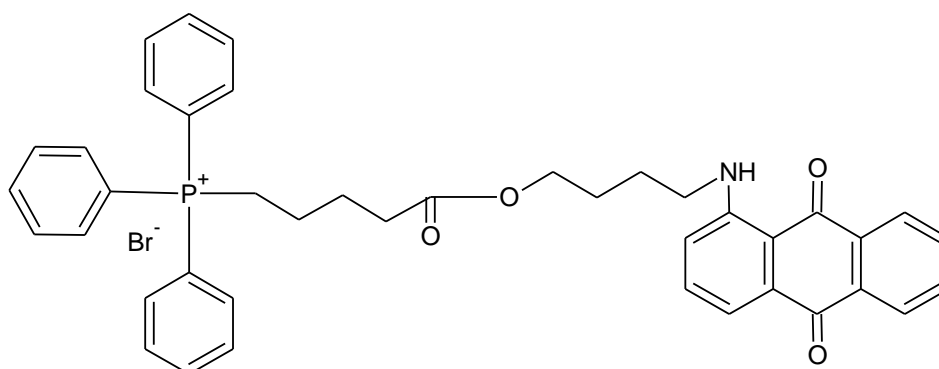


**Figure 1.23:** Chemical structure of **SH1** (Mohammed, 2021)

The observation that the anthraquinone-TPP conjugate SH1 selectively accumulated in the mitochondria of cancer cells provided a prototype to aid the rational design of the more complex hybrid conjugates incorporating CIPRO both with and without additional coupling to DCA.

## Chapter 2

### Results and Discussion

#### 2.1) Background

This chapter presents the results and discussion of experiments to design, discover and evaluate novel intracellularly targeted compounds having variously, anticancer and antibacterial activity to overcome MDR. The intracellularly targeted drugs were specifically designed to target the mitochondria of cancer cells by exploiting the high mitochondrial membrane potential in cancer cells and/or the lipid membranes of bacteria. A major reason to target bacteria in the context of cancer therapy is that intra-tumoural bacteria are known to promote resistance of tumour cells to chemotherapy drugs by metabolizing the respective active drug and drug candidates into inactive forms (Xi *et al.*, 2022).

The anticancer activity of some chemotherapeutics could be potentiated by the administration of antibiotics in patients but chemoresistance via microbe-induced drug-detoxification could be lethal in cancer patients on chemotherapy (Lehouritis *et al.*, 2015). Therefore, the design of a chemical moiety following a combination strategy of a dual antibacterial and anticancer drug candidate could be an imperative choice to overcome the failed impacts of chemotherapy due to MDR.

Pursuing this dual approach in this programme of research, the rational drug design and synthetic strategy towards novel anticancer and antibacterial compounds are explained including the synthesis, purification and characterization details and biological evaluation of selected synthesized compounds in antibacterial and anticancer activity assays.

#### 2.2) Rational drug design

There is a growing need to design and develop new strategies that allow therapeutic interventions in difficult drug targets. Multiple approaches are needed to develop a

drug, these approaches are the basis of rational drug design (Fuller, Burgoyne and Jackson, 2009).

To date many approaches have been proposed to overcome multi-drug resistance (MDR) such as repositioning of drug molecules, combination of different drugs or adoption of improved (targeted) drug delivery mechanisms. Many new chemical agents inhibiting both microbes and cancer cells have been suggested for targeting the molecular mechanisms of MDR. Notably, various approaches based on using cationic polymers or inhibitory integral proteins have been recognized to be effective against both Gram-negative and Gram-positive bacteria (Baker *et al.*, 2018).

It is also necessary to identify a functional relationship between cancer cells and cytotoxic agents which leads to the selection of chemical moieties due to the presence of multiple ways of targeting of mitochondria of cancer cells. Many chemical modifications have been made to clinically used drugs to identify the compounds with defined intracellular targets, decreased general toxicity and circumvention of drug resistance, particularly the anthracycline class, typified by doxorubicin (adriamycin). The most important structural moiety responsible for therapeutic properties of anthracyclines is the anthraquinone core. Therefore, anthraquinones and their analogues are widely used as scaffolds for the design of anticancer drug candidates. Drug modifications have been made to escape resistance mechanisms (Shchekotikhin, *et al.*, 2016); afford differential binding with mtDNA (EI-Gogary, 2002), achieve selective inhibition of mitochondrial topoisomerases II (Kou *et al.*, 2012); block metabolic pathways of cancer cells to induce apoptosis (Bonnet *et al.*, 2007) and modulate the generation of ROS species (Hancock, Desikan and Neill, 2001).

Broadening the spectrum of biological activity by creating hybrid molecules composed of different agents that exert their pharmacological effects by different molecular mechanisms has proved a viable approach. For example, novel anthraquinone-quinazoline hybrids have emerged as anticancer drug candidates with promising multitargeted biological activities (Liang, *et al.*, 2020).



In the research described in this thesis, the major concept of drug design and development of anticancer and antimicrobial hybrids has been based upon targeted drug delivery to induce mitochondrial damage in tumour cells without damaging the healthy cells, and concomitantly into bacterial cells to hinder the growth of bacterial populations associated with the tumour microenvironment of solid tumours.

Modification in the chemical structure of the anthraquinone scaffold and derivatization of CIPRO were combined with the aim to optimize the therapeutic effects and physico-chemical properties, which could lead to the generation of a new series of clinical candidates in chemotherapy practices.

The general structure of the target compounds in this work, is shown in its simplest diagrammatic form in **Figure 2.1**. The figure depicts a tri-component (tripartite) system that contained the anthraquinone scaffold, orthogonally connected to a mitochondrial-targeted TPP<sup>+</sup> vector and a ciprofloxacin-DCA conjugate, thus introducing the pharmacophores with anticancer and antibacterial potential and an organelle-seeking and bacterial membrane-penetrating targeting group.

Targeting mitochondria of cancer cells has been a promising focus to improve the efficiency of chemotherapy, yet high mitochondrial membrane potential hinders the accumulation of drugs in cancer cells. The oxidative property of cancer cells and multi-drug resistance (MDR) due to overexpression of P-gp resulting in increased efflux of drug candidates through cancer cells (Wu *et al.*, 2017), promote the need of a biophysical drug delivery system such as the TPP<sup>+</sup> cation.

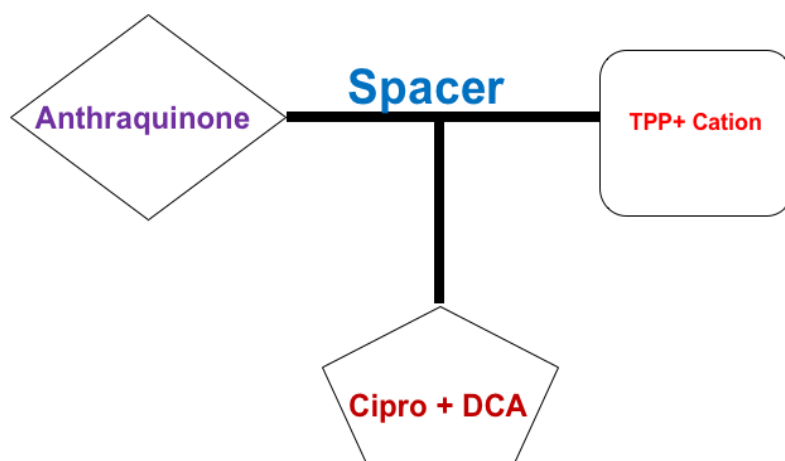


**Figure 2.1:** Rational design of novel dual anticancer and antibacterial hybrid drugs

Conjugation of a drug candidate with a triphenylphosphonium (lipophilic) cation is a promising approach which would accumulate the drug ~10 times greater in cancer cells than normal cells as a consequence of the differential mitochondrial membrane potential of cancer cells that is more negative ( $\sim -220$  mV) than healthy cells ( $\sim -160$  mV). It is hypothesized that structure-based conjugation of drug-candidates by exploiting a biophysical drug delivery system would cause a physical damage to mitochondria of cancer cells leading to selective anticancer and antibacterial effects to overcome the effects of MDR (Smith *et al.*, 1999).

Sharma *et al.* reported a cancer-selective multicomponent conjugate that triggers an oncogene-directed reprogramming of mitochondrial metabolism to restore mitochondrial OXPHOS, which promoted active doxorubicin (Dox) translocation from mitochondria to the nucleus and significantly increased apoptosis and in both Dox-sensitive and Dox-resistant tumour models, including simultaneous circumvention of drug-efflux pumps (Sharma *et al.*, 2018).

The encouraging results in the published literature, outlined above, to target mitochondria and broaden the spectrum of biological activity of a drug, provided in part the motivation to design a new hybrid compound of some complexity, having CIPRO as a main component, and predicted to possess both antibacterial and anticancer properties.

### 2.2.1) Synthetic strategy

The main purpose to synthesize TPP<sup>+</sup>-targeted drug is the translocation of novel anticancer and antibacterial agent through a biophysical drug delivery system which would be possible by the conjugation of CIPRO molecule with triphenyl-phosphonium cation (TPP<sup>+</sup>).

Following the above approach, in this research programme a synthetic strategy was proposed (**Figure 2.2**) to design a new dual TPP<sup>+</sup>-targeted anticancer and antibacterial agent. Starting with commercially available 2-chloroanthraquinone, a piperazine substituent was introduced in 2 steps to synthesize KA2. Further, KA1 was conjugated to lysine in order to introduce two points of attachment for both the TPP carrier (on the alpha amino group) and (later) Boc-protected ciprofloxacin (at the epsilon amino group), affording intermediate KA9. Subsequently, deprotection of the Boc group (standard removal with trifluoroacetic acid) in KA9, followed by conjugation to DCA gave the ultimate target compound KA11.

Amide bonds would be formed where possible to assemble the individual pharmacophores into their hybrid conjugates to prevent enzymatic breakdown that might occur if ester bonds were used. In this research project, several derivatives of anthraquinone derivatives have been synthesized through nucleophilic substitution reactions (on commercially available chloroanthraquinones) leading to the formation of anthraquinones substituted with secondary amines that give enzymatically stable tertiary amides upon reaction with carboxylic acids. Furthermore, it has been reported that presence of nitrogen atoms plays an important role in binding with mtDNA and maintaining a drug-mtDNA complex in cancer cells (Niedziałkowski *et al.*, 2019).

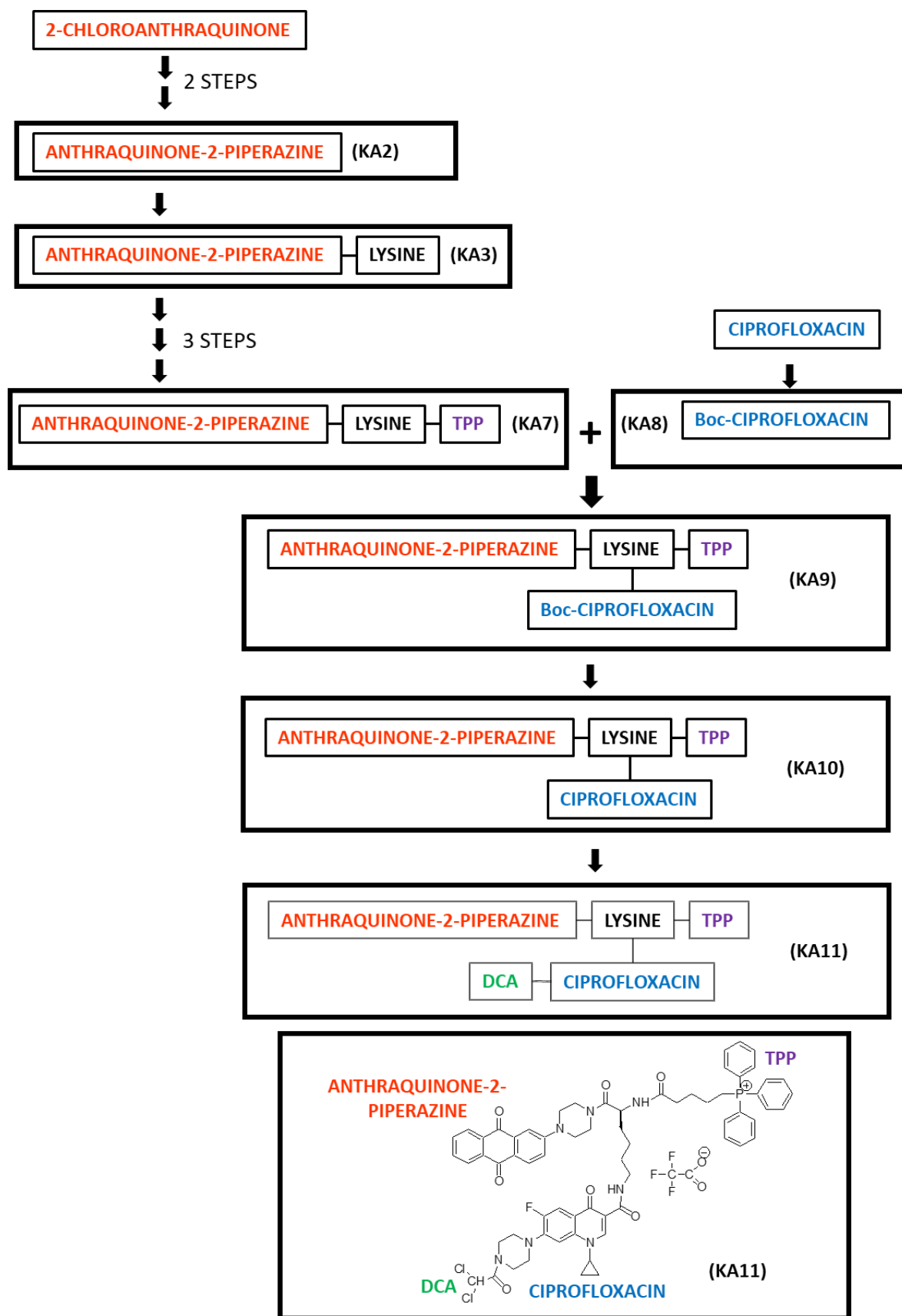
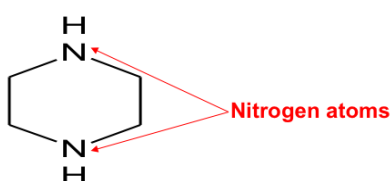


Figure 2.2: Overview of the proposed synthesis of target compound KA11

Anthraquinones (anthracene-9,10-diones) which are a structural core of the anthracycline antibiotics, have attracted great interest for their proven or potential applications (Fan, Shi and Lowary, 2007) as chemotherapeutics (Schneeweiss *et al.*, 2019). However, alteration in the chemical structure of anthraquinones may adversely affect their electrochemical properties which can lead to a change in their mechanism of action and their redox properties. It is necessary to consider the type of substituent which would be used to generate anthraquinone derivatives (Lehmann and Evans, 2001). The position of a substituent on an anthraquinone moiety along with its stereochemistry (if present) but not a concern in this research, and precise functional groups leading to specific binding of the compound with the target receptor molecule, are all factors that may lead to a large change in antitumor activities of the compound (Tripathi *et al.*, 2001).

In a related but limited number of studies, has been reported that anthraquinone hybrids containing the piperazine ring as a substituent at different positions exhibit anticancer properties (Niedziałkowski, *et al.*, 2019). The piperazine ring structure plays an important role in many pharmaceuticals and biological research (Lien *et al.*, 1997). The effect of the piperazine ring as a substituent depends upon the chemical moiety directly attached to one or both of its nitrogen atoms (**Figure 2.3**) (Ganushchak *et al.*, 1971); equally, including the number of substituents on an anthraquinone moiety, given anthraquinone derivatives with a single piperazine ring has been proved to be highly cytotoxic as compared to two piperazine substituents (Niedziałkowski *et al.*, 2019).



**Figure 2.3:** Chemical structure of piperazine ring showing the points of attachment to other groups

Singh *et al.*, have emphasized the versatility of the piperazine ring system as a biological scaffold in a recent review and its use as a nucleophile in a number of settings (Singh *et al.*, 2022). The piperazine has the unique feature of ease of functionalization for research targets in chemistry which has made it an important

candidate in medicinal chemistry to search for new chemicals with a therapeutic impact (Solankee *et al.*, 2010).

Piperazine can be used to replace chlorine in 2-chloroanthraquinone by nucleophilic displacement, involving an addition-elimination process (**Figure 2.4**). The electron-withdrawing effects of the carbonyl groups in the quinone make the C-2 carbon atom of the anthraquinone susceptible to nucleophilic substitution (normally a difficult process to achieve in simple aromatic systems). A piperazine nitrogen atom adds on to C-2 with loss of its proton; this is followed by elimination of a chloride ion to give the desired product.

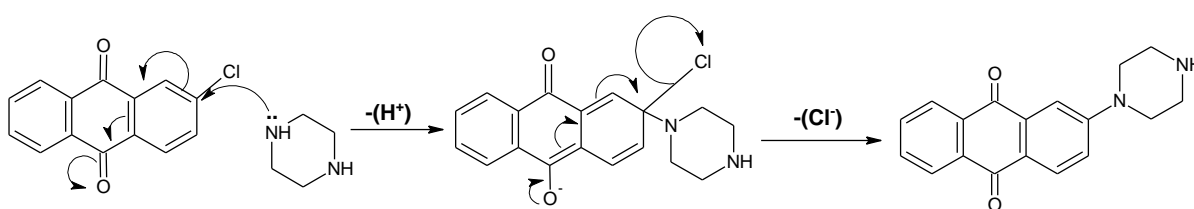


**Figure 2.4:** Nucleophilic displacement of chlorine by piperazine (an addition-elimination sequence)

A drawback with using piperazine as the free base is the possibility of obtaining unwanted reaction at each of its nitrogen, whereas we require only the mono-substituted 1:1 anthraquinone-piperazine adduct. A further difficulty is the general poor solubility of anthraquinone-based spacer compounds of this type in organic solvents, making their isolation and purification difficult. Consequently, in this research, a partially protected derivative of piperazine (possessing a Boc-protecting group on one nitrogen) was used to favour the desired product (Section 2.3.1).

Conjugation of drugs with a TPP<sup>+</sup> molecule to facilitate uptake into mitochondria of cancer cells is not a new concept and various chemical agents have been synthesized with TPP<sup>+</sup>-cations, including antioxidants (Cheng *et al.*, 2016).

The advantage of TPP<sup>+</sup> based drug delivery over other drug delivery systems is the stability of TPP<sup>+</sup> cation in biological systems and ease of conjugation (Zielonka *et al.*, 2017). The delocalized TPP<sup>+</sup>-cation is usually linked through a spacer or an alkyl chain which modulates the lipophilicity, cellular uptake and site of mitochondrial sequestration. Some of the published chemical methodology was therefore used as starting points for establishing reaction conditions and adapted to the molecules

used in the present study, keeping in mind the overall design principles (**Figure 2.5**) and the 'in-house' prototype anthraquinone-TPP conjugate SH1.

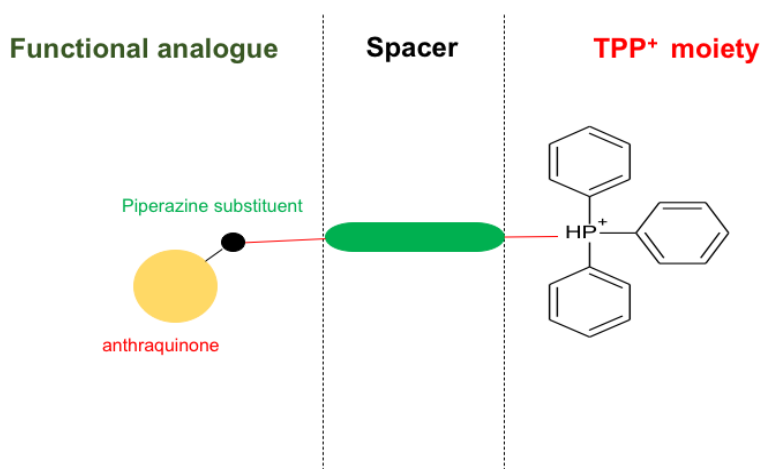


**Figure 2.5:** Anatomy of TPP<sup>+</sup>- based functional analogues of SH1

In this rational drug design and development, DCA (a mitochondrial targeted agent that inhibits pyruvate dehydrogenase kinases) is a strong candidate to develop its cytotoxic potential (Sun *et al.*, 2010) because of its modulating action on a major metabolic component of (cancer) cells (Bonnet *et al.*, 2007). Additionally, the possibility of achieving a synergistic effect with DCA provides motivation for conjugating DCA with other anticancer agents via a structure-based modification (Seliem *et al.*, 2019). Further, good penetration ability of CIPRO has made it an eligible candidate for chemotherapy practices (Ahadi *et al.*, 2020).

### **2.3) Synthesis of hybrid anthraquinone, TPP<sup>+</sup>, ciprofloxacin and DCA conjugates**

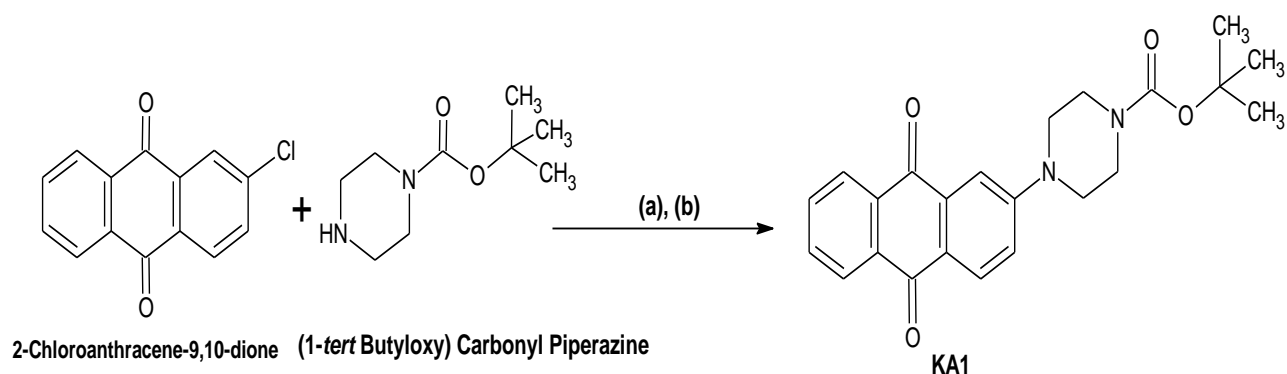
#### **2.3.1) Synthesis of AQ-PIP-BOC (KA1)**

KA1 was synthesized by reacting 2-chloroanthracene-9,10-dione with 1-*tert* butyloxycarbonyl-piperazine (**Scheme 01**). The reaction was successfully performed at 40°C by the use of DMSO as a solvent.

The synthesis of KA1 was confirmed by TLC using the solvent system (dichloromethane: ethyl-acetate 9:1). The compound was isolated by solvent extraction with water and dichloromethane and purified by column chromatography.

The pure fractions of KA1 were collected, filtered and dried. The orange precipitate of KA1 was formed by the addition of diethyl ether. KA1 was obtained in low yield (34%) but the conditions were not optimised; the compound was deemed pure by chromatographic analysis and NMR spectroscopy, and used for subsequent reactions.

The structure of KA1 was confirmed by high resolution electrospray (+) mass spectrum showing a clear signal (100%) at  $m/z$  393.1805, corresponding to the expected molecular weight of KA1 (392.44766 Da) (**Figure 2.6**). Additionally, good correlation was found between theoretical isotope and observed data of  $C_{23}H_{24}N_2O_4$  (**Figure 2.7**).



**Scheme 01:** Chemical synthesis of KA1; **(a)** = Boc-piperazine **(b)** = DIPEA

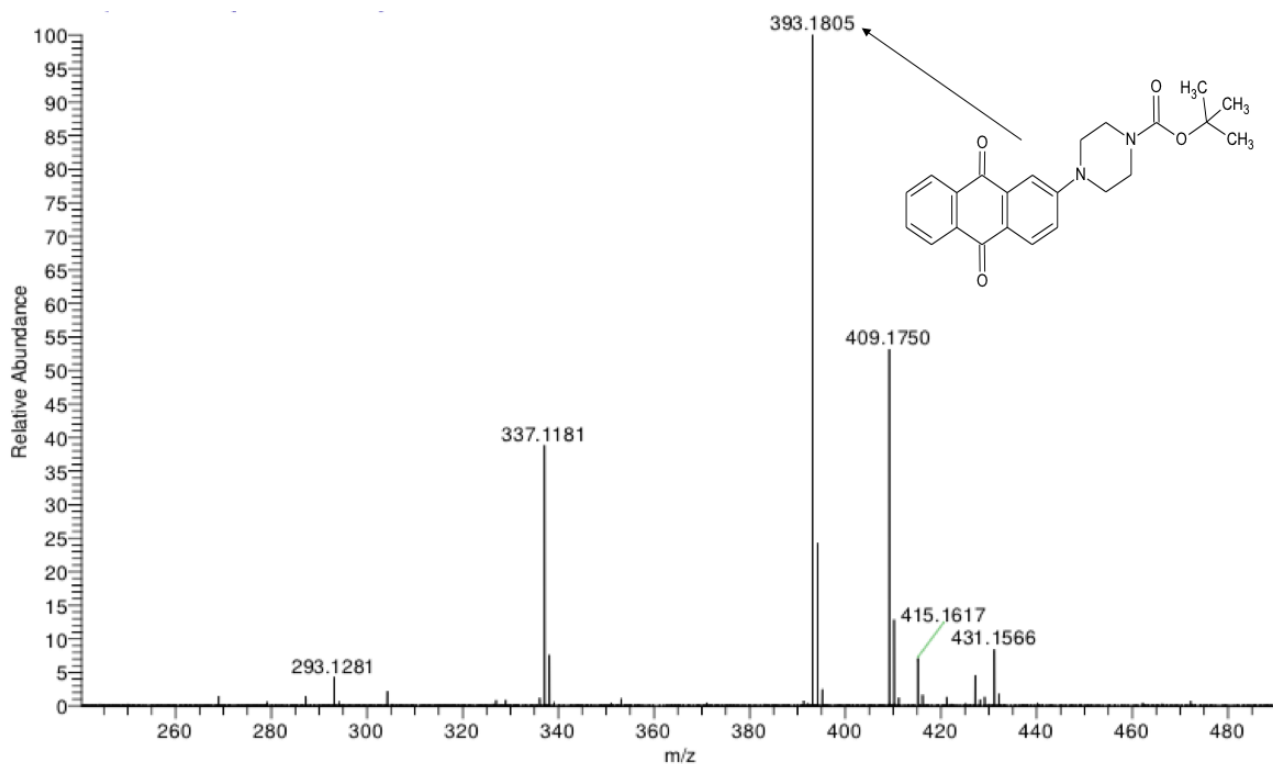




**Figure 2.6:** The high-resolution ESI (+) mass spectrum of KA1

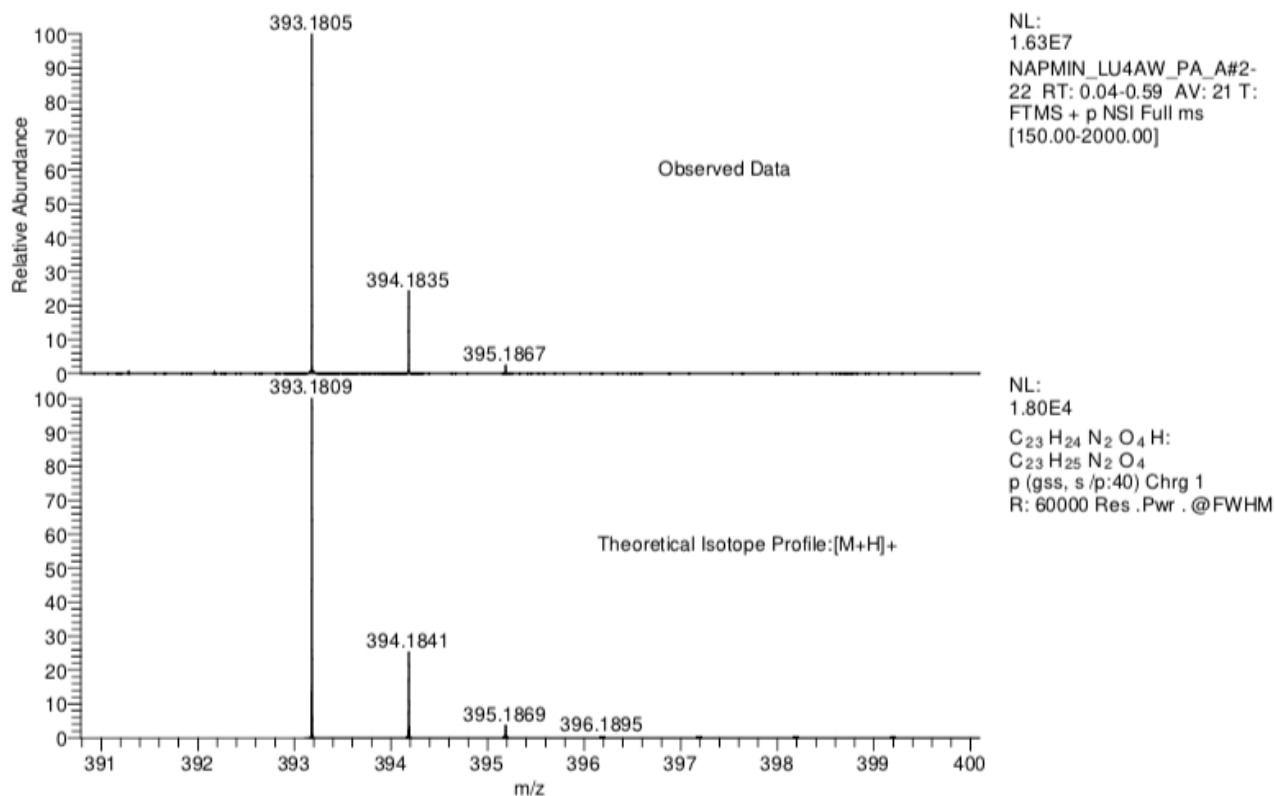


**Figure 2.7:** Correlation between observed data and theoretical <sup>13</sup>C isotope profile of KA1

In addition to mass spectrometry, KA1 was characterized by its <sup>1</sup>H NMR spectrum (in CDCl<sub>3</sub>). A nine-proton singlet at 1.52 ppm was assigned to the three equivalent methyl groups of the Boc protecting group. The four methylene groups of the piperazine spacer gave signals at 3.52 and 3.62 ppm. All aromatic protons were successfully assigned; H-3 and H-4 gave one proton doublets at 7.18 and 8.22 ppm, respectively. A one proton singlet at 7.65 ppm was assigned to H-1. The H-6 and H-7 protons were present at 7.76 ppm and the H-5 and H-8 protons at 8.28 ppm (Figure 2.8).

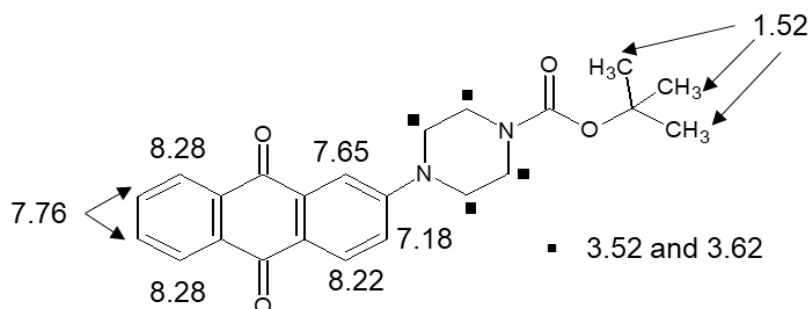


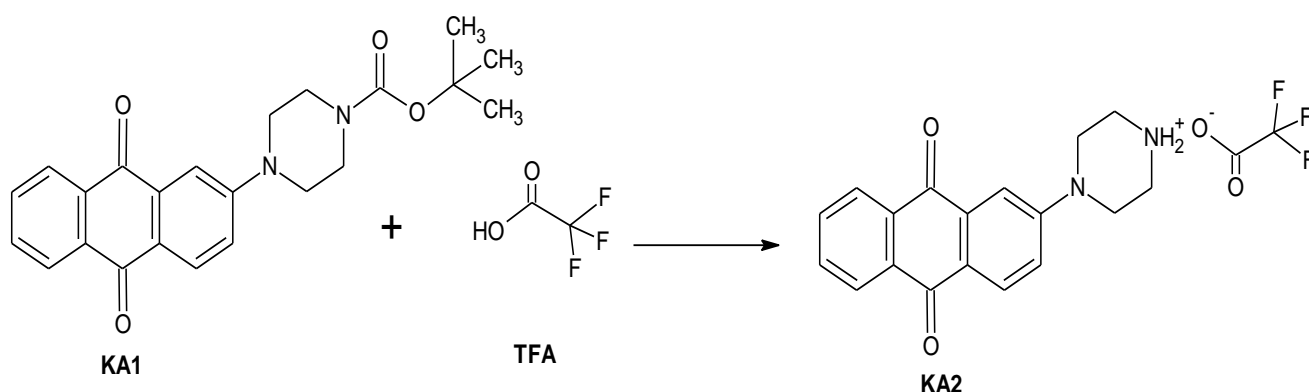
**Figure 2.8:** NMR assignments and peak positions in ppm for KA1 (AQ-2-pip-Boc)

### 2.3.2) Synthesis of AQ-PIP-TFA (KA2)

KA2 was synthesized by the dissolution of KA1 in TFA for 30 minutes at room temperature. In this step of chemical synthesis, deprotection of KA1 results the KA2, with complete removal of the Boc-protecting group and otherwise, gaseous products. The yield was virtually quantitative and because the trifluoroacetic acid acts both as a reagent and solvent, upon evaporation, the first-formed free base is converted to its trifluoroacetate salt form (stable) by protonation of the piperaziny amino group in the excess acid (**Scheme 02**). This offers a convenient way to store the amine in its stable salt form.

The formation of KA2 was confirmed by TLC using a solvent system of dichloromethane: ethyl-acetate (9:1). The trifluoroacetate salt KA2 was obtained in solid form under diethyl ether and dried in vacuo. The compound was homogeneous on TLC.

The structure of KA2 was confirmed by high resolution electrospray (+) mass spectrum showing a clear signal (100%) at  $m/z$  293.1282 calculated for the cation  $C_{18}H_{17}N_2O_2^+$  (**Figure 2.9**). Additionally, good correlation was found between the carbon 13 theoretical isotope model and observed data for  $C_{18}H_{17}N_2O_2^+$  (**Figure 2.10**).



**Scheme 02:** Synthesis of KA2 (by TFA mediated deprotection of KA1)

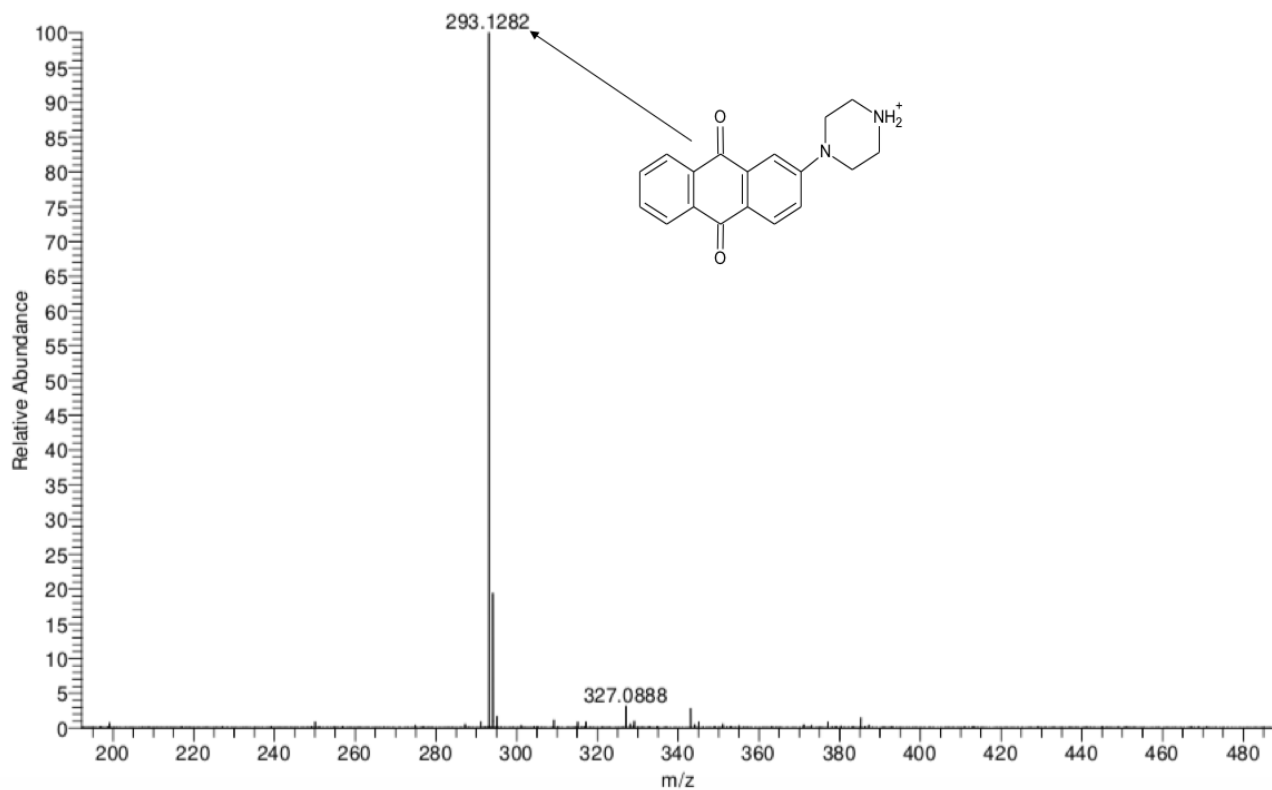


Figure 2.9: The high-resolution ESI (+) mass spectrum of KA2

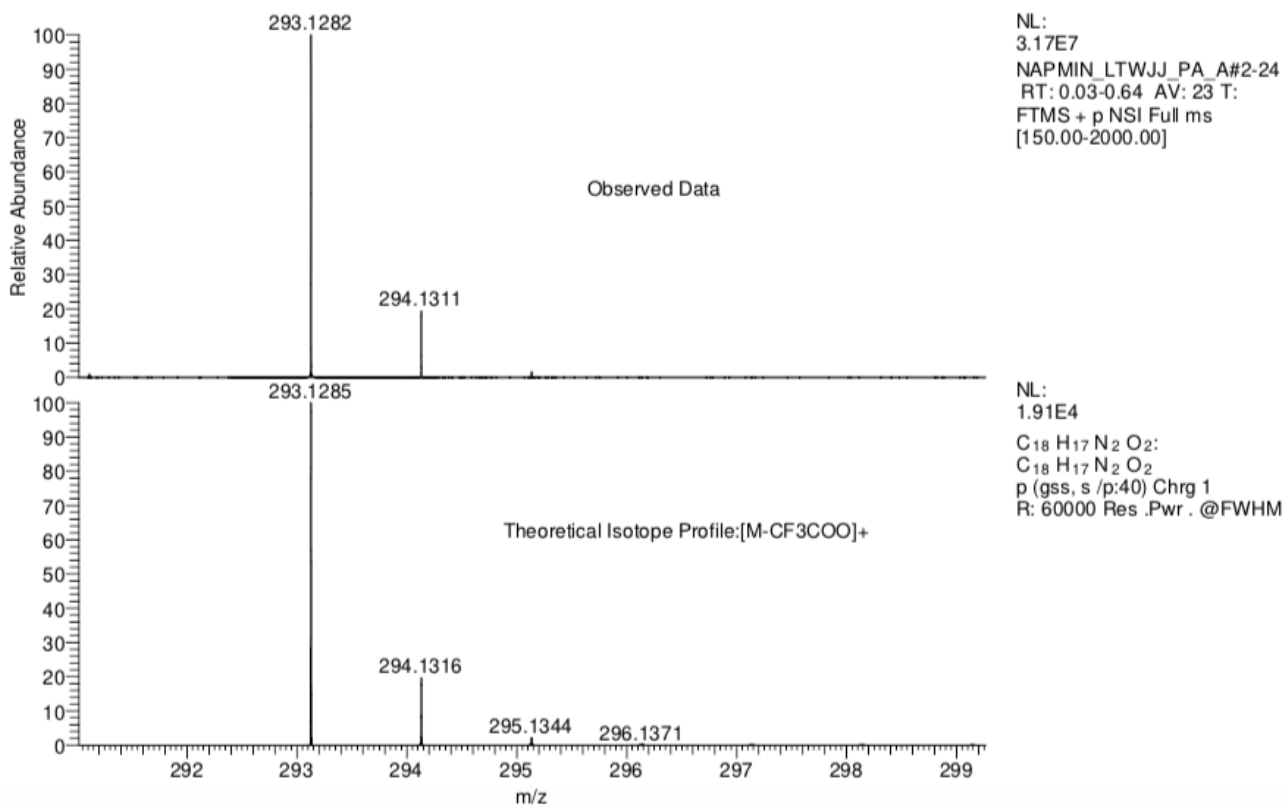


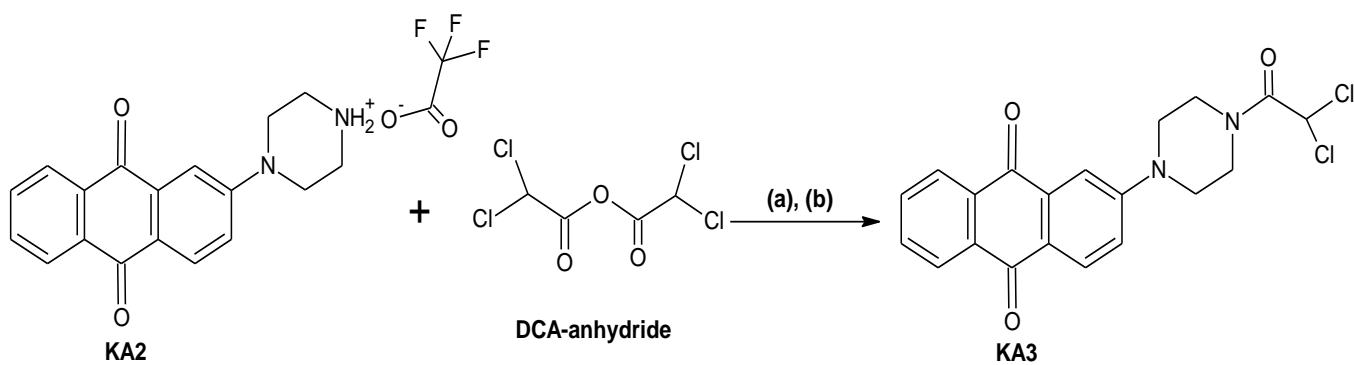
Figure 2.10: Correlation between observed data and the theoretical  $^{13}\text{C}$  isotope of KA2

### 2.3.3) Synthesis of AQ-PIP-DCA (KA3)

KA3 was synthesized by the dropwise addition of DCA-anhydride to a solution of KA2 in dichloromethane, with potassium carbonate acting as a base. The main difference between KA2 and KA3 is the addition of DCA through a tertiary amide bond (**Scheme 03**). The main purpose to synthesize such a DCA-AQ hybrid was to establish the best reaction conditions in what was potentially a model compound, so that optimised conditions could be applied to more complex hybrids in subsequent experiments. However, the model compound KA3 could be of interest in itself; DCA conjugation in some cases could potentiate the antitumour activity (here, of an aminoanthraquinone) by increasing the generation of ROS reported in other series (Hossain *et al.*, 2020). The lipophilicity of anthraquinones could be further increased, as DCA plays an important role to enhance the lipophilicity of different anticancer agents that have included metal-salts, ammonium salts, amides and esters (Yang *et al.*, 2010) aiding passage through biological membranes.

The synthesis of KA3 was confirmed by TLC using a solvent system of dichloromethane: ethyl acetate (9:1), having  $R_f$  0.70. The white crystals of potassium carbonate were filtered off, and the mixture was extracted using equal portions of dichloromethane: water (1:1) then dried. However, TLC showed a coloured impurity which was removed through purification of KA3 by column chromatography. The pure fractions containing KA3 were collected, filtered and dried. The orange precipitate of KA3 was formed by the addition of diethyl ether.

The structure of KA3 was confirmed by a high-resolution electrospray (+) mass spectrum showing a clear signal (100%) at  $m/z$  403.0611 corresponding to the expected molecular weight of KA3 (402 Da) (**Figure 2.11**). Additionally, good correlation was found between the theoretical isotope model and observed data for  $C_{20}H_{17}Cl_2N_2O_3$  (**Figure 2.12**)



**Scheme 03:** Synthesis of KA3; (a) = potassium carbonate, (b) = dichloromethane

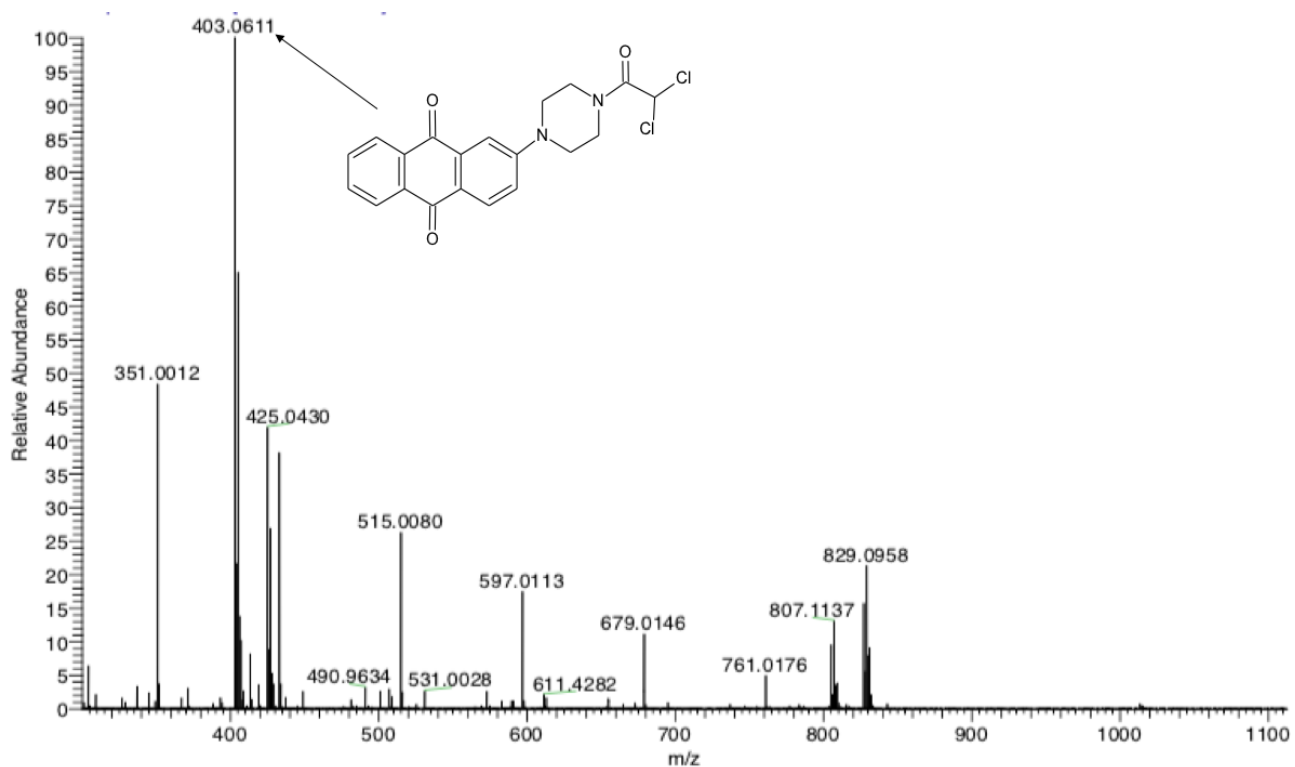


**Figure 2.11:** The high-resolution ESI (+) mass spectrum of KA3

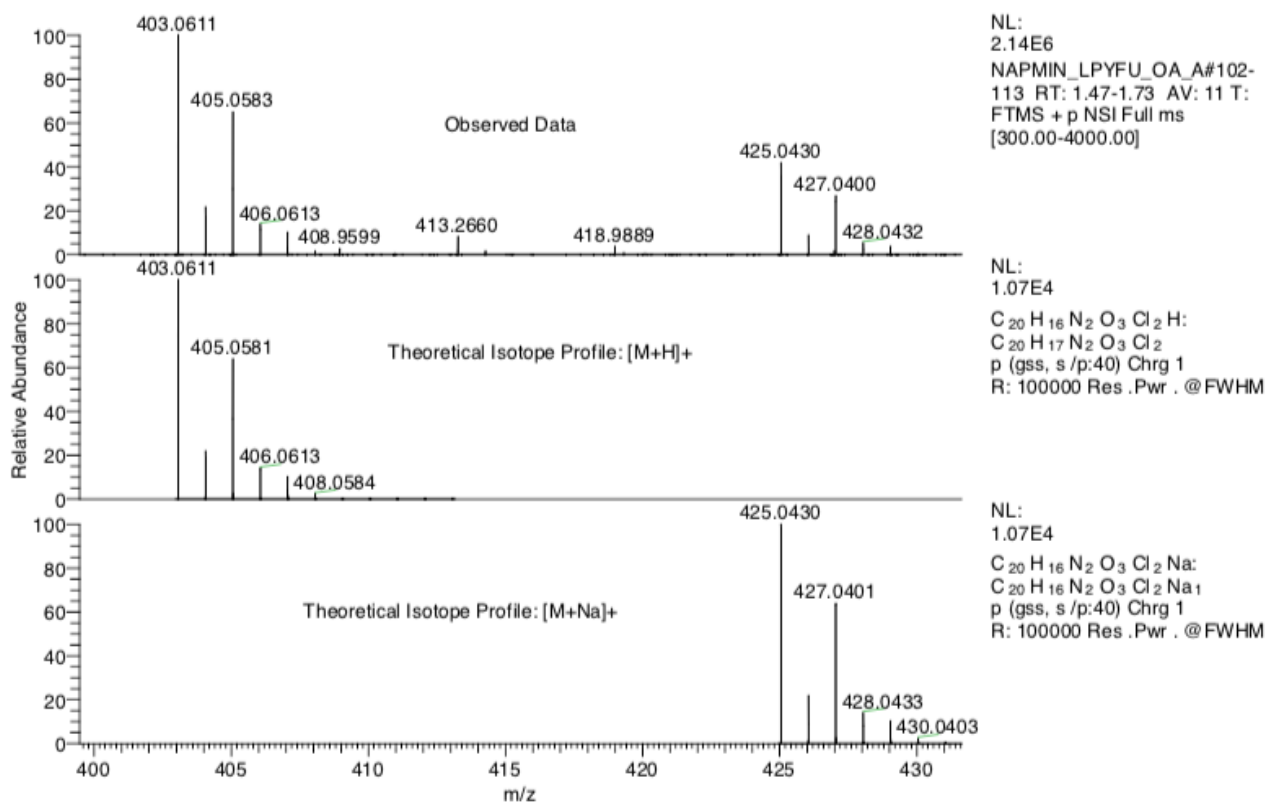


**Figure 2.12:** Correlation between observed data and  $^{13}\text{C}$  theoretical isotope profile of KA3

KA3 was further characterized by its  $^1\text{H}$  NMR spectrum (in  $\text{DMSO-}d_6$ ). The four methylene groups of the piperazine spacer gave signals between 3.56 and 3.84 ppm. The methine proton of DCA was assigned to a one proton singlet at 7.31 ppm. All aromatic protons were successfully assigned; H-3 and H-4 gave one proton doublets at 7.39 and 8.02 ppm, respectively. A one proton singlet at 7.51 ppm was assigned to H-1. The H-6 and H-7 protons were present at 7.87 ppm and the H-5 and H-8 protons at 8.18 ppm.

#### 2.3.4) Synthesis of AQ-PIP-Lys (BOC)-Fmoc (KA4)

Synthesis of KA4 was by formation of an amide bond between the secondary amino group of KA2 and the carboxylic acid group of Fmoc-Lys (BOC)-OH. The Fluorenylmethoxycarbonyl protecting group (Fmoc) is a protecting group which is widely used in organic synthesis to protect amino groups. The most attractive feature of the Fmoc protective group is its stability under acid conditions in contrast to a Boc-

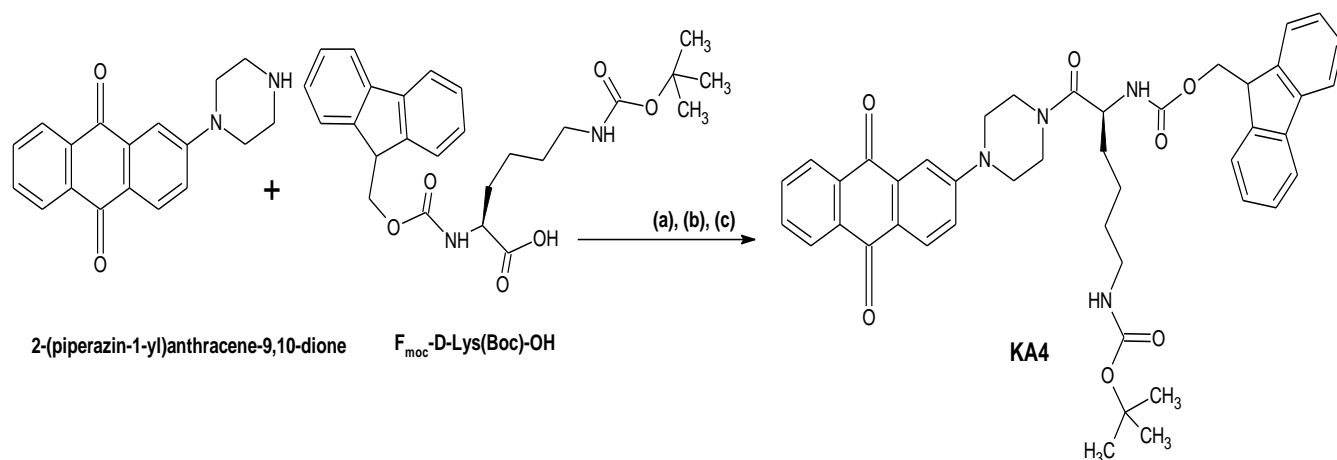
group (and vice-versa). Fmoc groups are stable to TFA and removed by 20% piperidine in DMF.

The reaction was carried out at room temperature in DMF in the presence of coupling agents [Hexafluorophosphate Azabenzotriazole Tetramethyl Uronium (HATU)] and using diisopropylethylamine as a base (**Scheme 04**).

The Fmoc is a protective group that is normally removed by base (*i.e.*, the secondary amine, piperidine) but has excellent acid stability, meaning that a Boc group can be selectively removed by acid, typically TFA, leaving the Fmoc group in place. This is known as orthogonal protection.

KA4 was obtained in good yield in a pure form, confirmed by TLC using a solvent system of chloroform: methanol (4: 1) with  $R_f$  0.70. The reaction solution of KA4 was extracted using dichloromethane and water (1:1), dried and purified through column chromatography. The pure fractions of KA4 were collected, filtered and dried. KA4 was precipitated by the addition of diethyl ether.

The structure of KA4 was confirmed by high resolution electrospray (+) mass spectrum which showed a signal at  $m/z$  743.3451 which corresponded to the species  $[M+H]^+$  (**Figure 2.13**). Furthermore, a good correlation was found between observed data and theoretical isotope model of  $C_{44}H_{47}N_4O_7$  (**Figure 2.14**).



**Scheme 04:** Synthesis of KA4; (a) = HATU, (b) = DMF, (c) = DIPEA

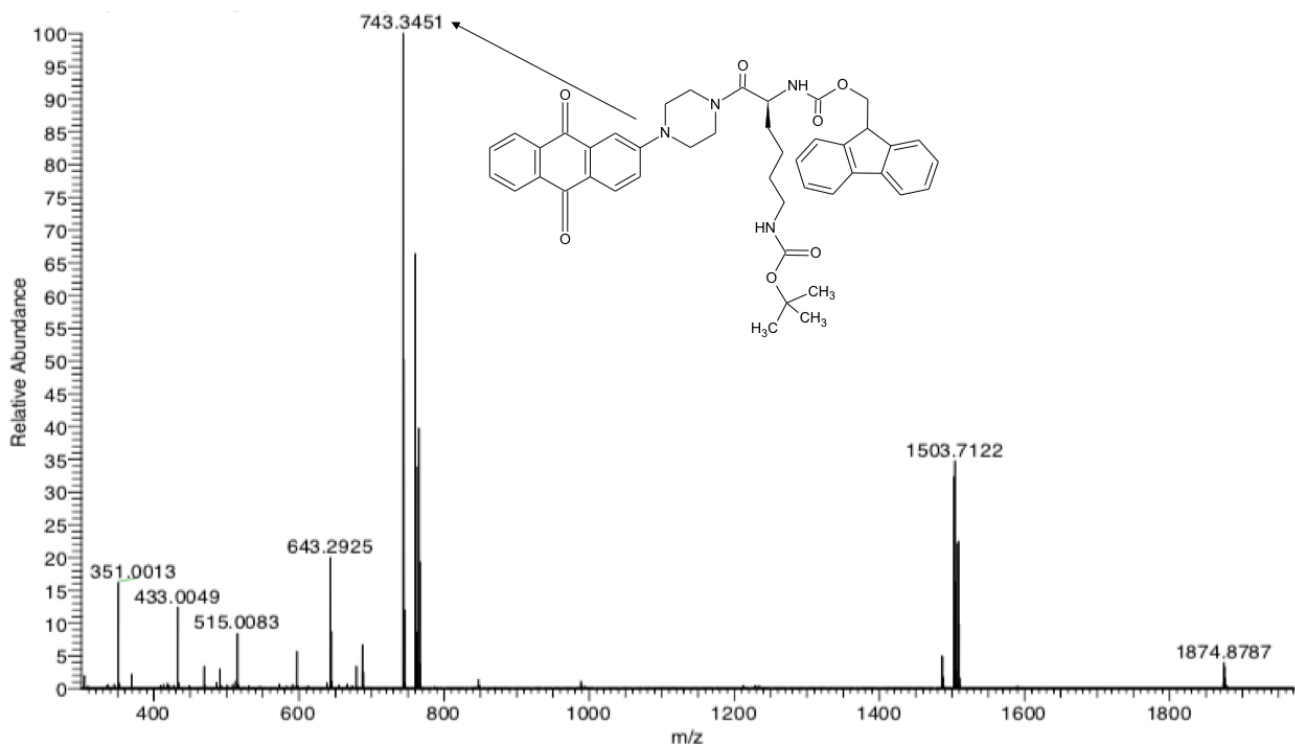


**Figure 2.13:** The high-resolution ESI (+) mass spectrum of KA4

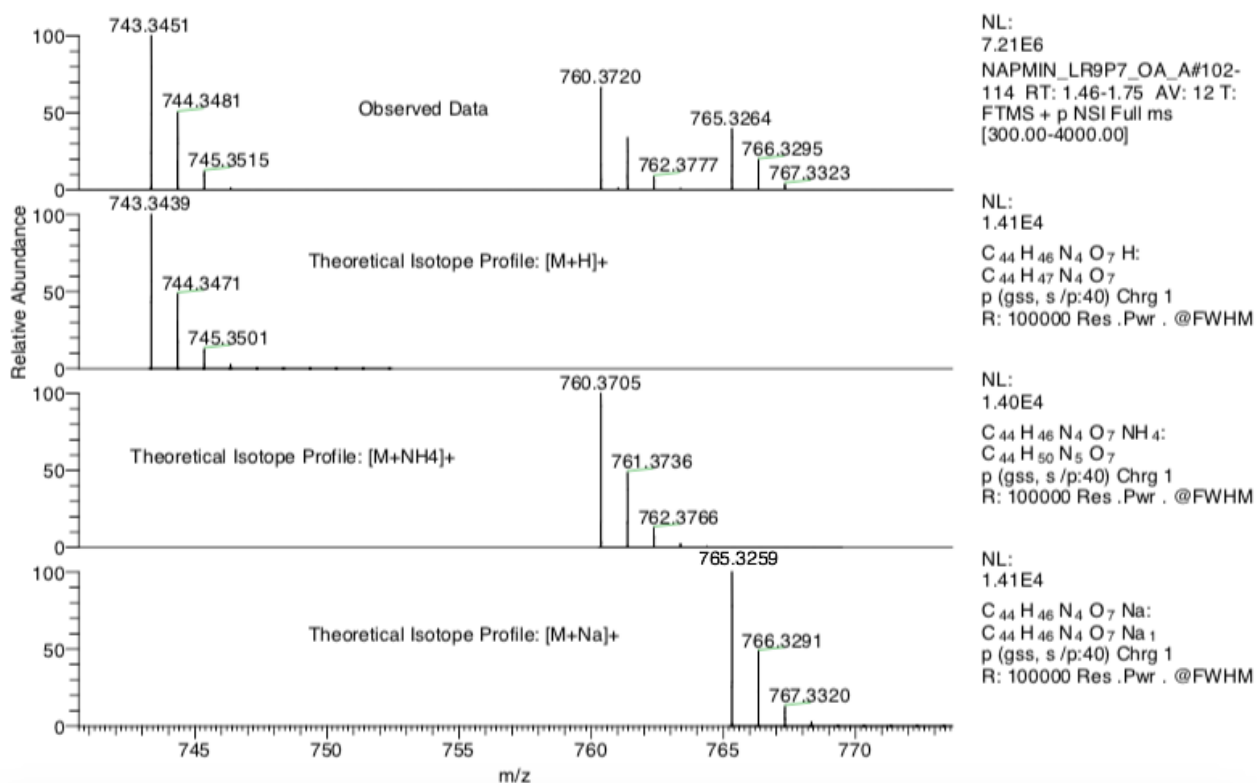


**Figure 2.14:** Correlation between observed data and the <sup>13</sup>C theoretical isotope model of KA4

KA4 was additionally characterized by its <sup>1</sup>H NMR spectrum (in CDCl<sub>3</sub>). Signals for the Boc protecting group and the β-, γ- and δ- methylene groups of lysine were found



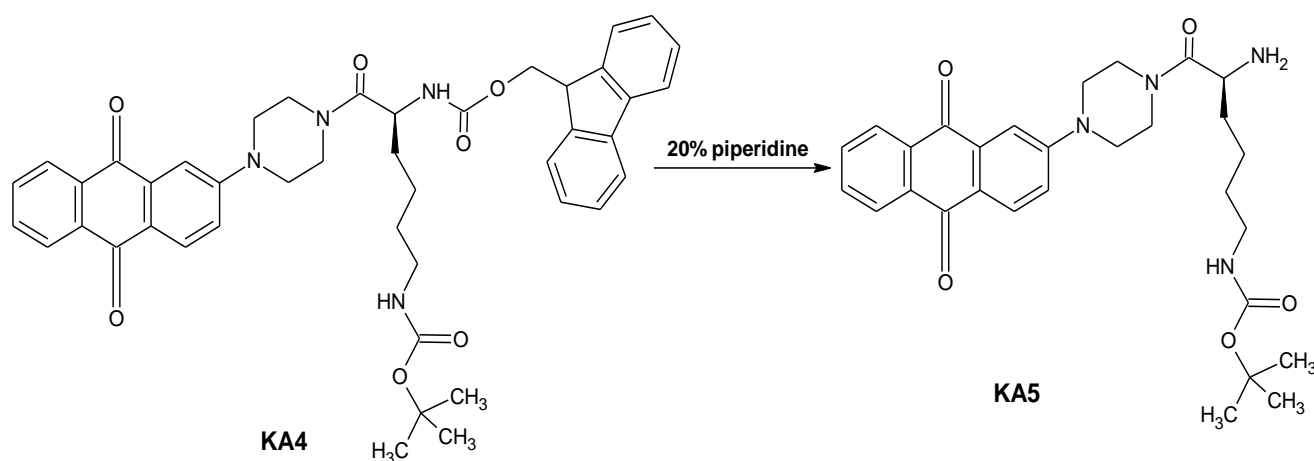
between 1.38 and 1.80 ppm, with  $\epsilon$ -CH<sub>2</sub> at 3.22 ppm. The four methylene groups of the piperazine spacer gave signals between 3.55 and 3.98 ppm. The alpha proton of lysine gave a one proton multiplet at 4.25 ppm. A two-proton doublet at 4.42 ppm was assigned to the Fmoc methylene group. A one proton doublet at 5.75 ppm was assigned to the amide of the Fmoc protecting group. All aromatic anthraquinone and Fmoc protons were accounted for.

### 2.3.5) Synthesis of AQ-PIP-Lys (BOC) (KA5)

The chemical structure of KA4 had an Fmoc group on the alpha amino group of lysine which required removal prior to TPP conjugation. The deprotection of the Fmoc was carried out by treating KA4 with the base piperidine (**Scheme 05**). KA5 was synthesized by dissolving KA4 in DMF with 20% piperidine with yield 60%.

The reaction mixture subjected to solvent extraction and the organic phase was dried. KA5 was purified by column chromatography using gradient elution (chloroform: methanol; 19:1; 9:1; 4:1) respectively. The pure fractions were collected, filtered and dried. Diethyl ether was added to form a precipitate of KA5.

The chemical structure of KA5 was confirmed by high resolution electrospray (+) mass spectrum which showed a clear signal at  $m/z$  521.2753 which was corresponded to the expected molecular mass of KA4 (520.61994 Da) (**Figure 2.15**). Also, good agreement was found between observed data and theoretical isotope model of C<sub>44</sub>H<sub>47</sub>N<sub>4</sub>O<sub>7</sub> (**Figure 2.16**).



**Scheme 05:** Synthesis of KA5 (deprotection of KA4 with piperidine)

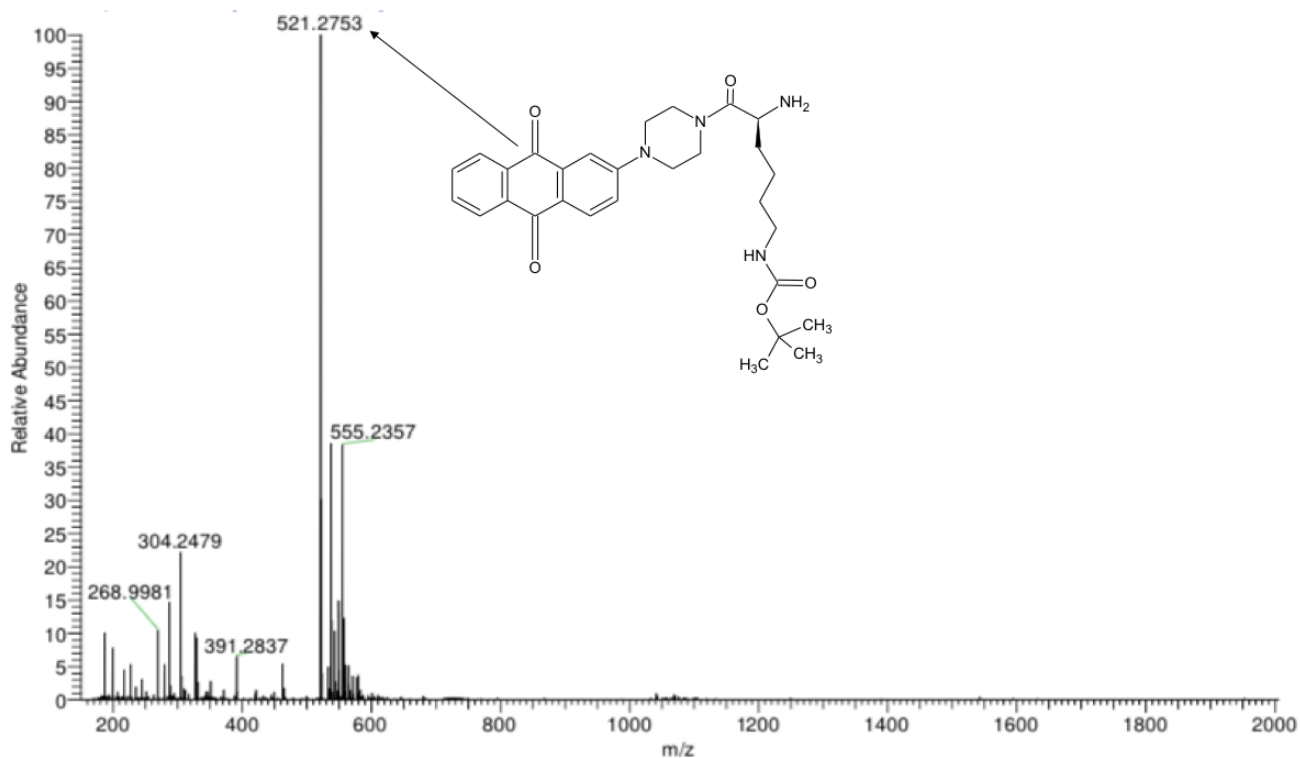


Figure 2.15: The high-resolution ESI (+) mass spectrum of KA5

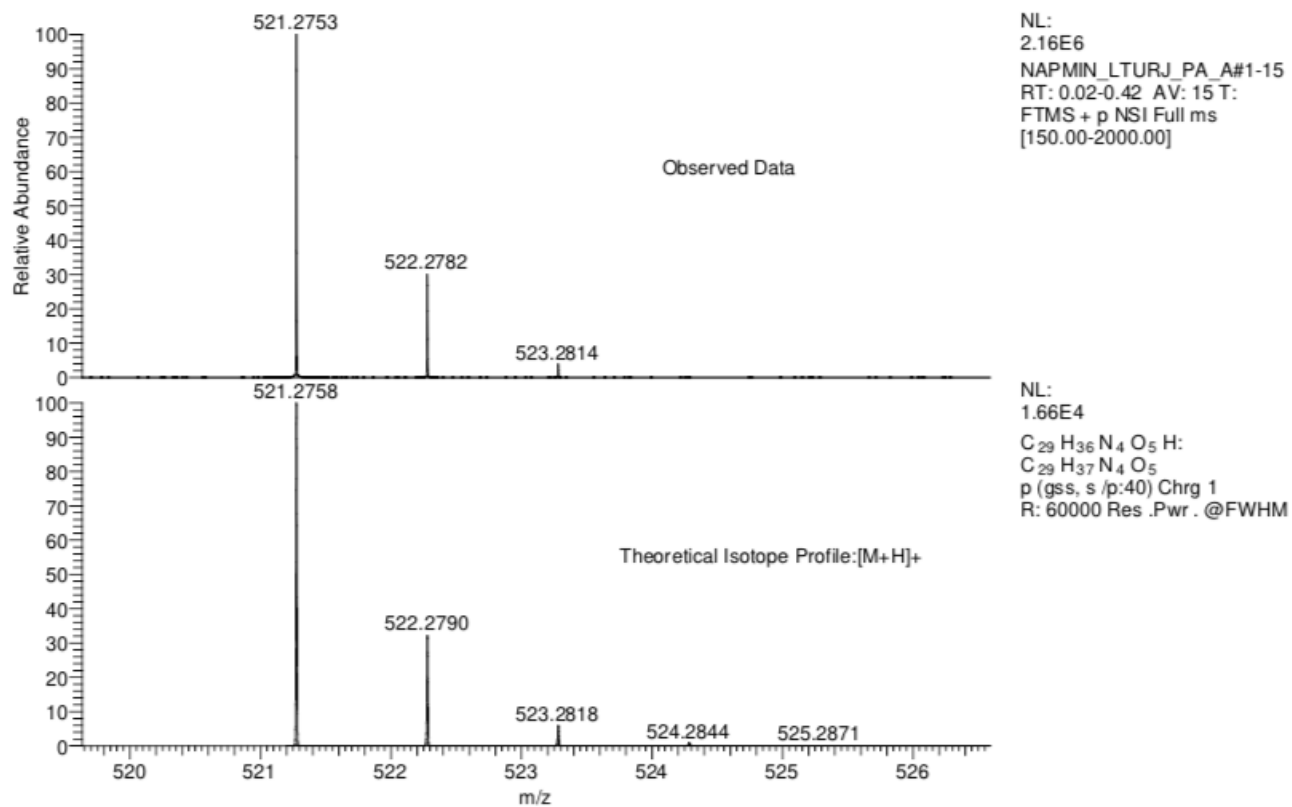


Figure 2.16: Correlation between observed data and  $^{13}\text{C}$  theoretical isotope of KA5 for cation  $[\text{M}+\text{H}]^+$

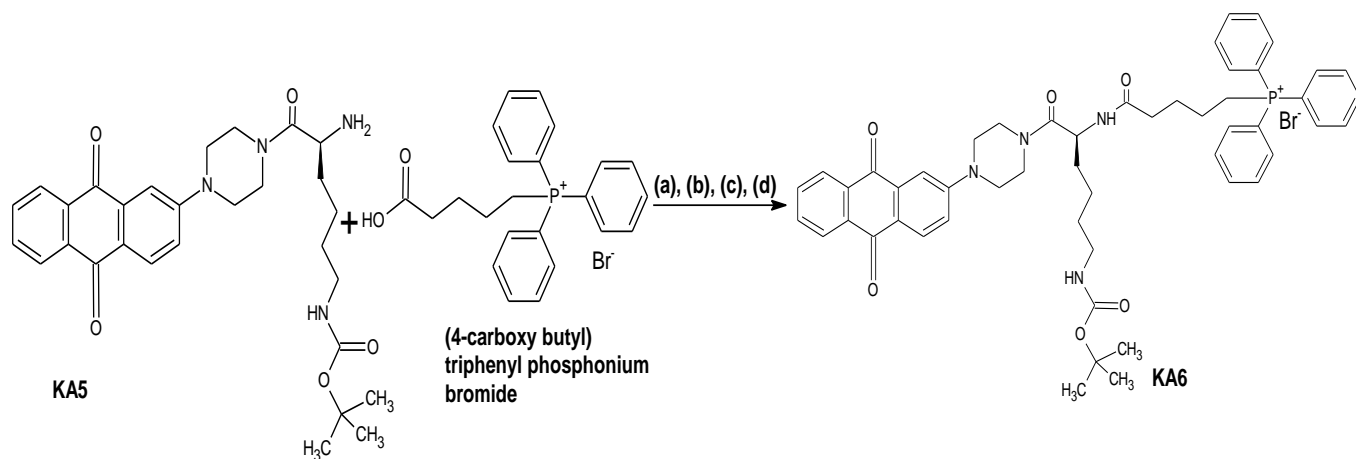
KA5 was characterized by its  $^1\text{H}$  NMR spectrum (in  $\text{CDCl}_3$ ). Signals for the Boc protecting group and the  $\beta$ -,  $\gamma$ - and  $\delta$ - methylene groups of lysine were found between 1.40 and 1.72 ppm, with  $\varepsilon\text{-CH}_2$  at 3.15 ppm. The four methylene groups of the piperazine spacer gave signals between 3.52 and 3.88 ppm. The alpha proton of lysine was a one proton multiplet at 4.62 ppm. All aromatic protons were successfully assigned; H-3 and H-4 gave one proton doublets at 7.17 and 8.20 ppm, respectively. A one proton singlet at 7.65 ppm was assigned to H-1. The H-6 and H-7 protons were present at 7.74 ppm and the H-5 and H-8 protons at 8.28 ppm.

### **2.3.6) Synthesis of AQ-PIP-Lys (BOC)-TPP (KA6)**

KA6 (yield, 63%) was synthesized by reaction of KA5 with (4-carboxy-butyl)triphenylphosphonium bromide (TPP) in DMF, under basic conditions and in the presence of coupling agents (PYBOP, HOBT) at room temperature (**Scheme 06**).

The TPP<sup>+</sup>- cation is an excellent membrane penetrating agent whose positive charge is delocalised due to the presence of three aromatic rings (Kelso, *et al.*, 2001). The synthesis of KA6 was confirmed by TLC with  $R_f$  0.46. Solvent extraction was carried out using dichlorométhane : water (1 :1) and KA6 was purified through column chromatography. The pure fractions were collected, filtered and dried. Diethyl ether was added to obtain KA6 in solid form.

The structure of KA6 was confirmed by high resolution electrospray (+) mass spectrum showing a clear signal at  $m/z$  865.4088 corresponding to the expected molecular mass of the cation of KA6 (**Figure 2.17**). Additionally, good agreement was found between observed data and theoretical isotope model of  $\text{C}_{52}\text{H}_{58}\text{O}_6\text{N}_4\text{P}$  (**Figure 2.18**).



**Scheme 06:** Synthesis of KA6; (a) = HOBT, (b) = PYBOP, (c) = DIPEA, (d) = DMF



**Figure 2.17:** The high-resolution ESI (+) mass spectrum of KA6

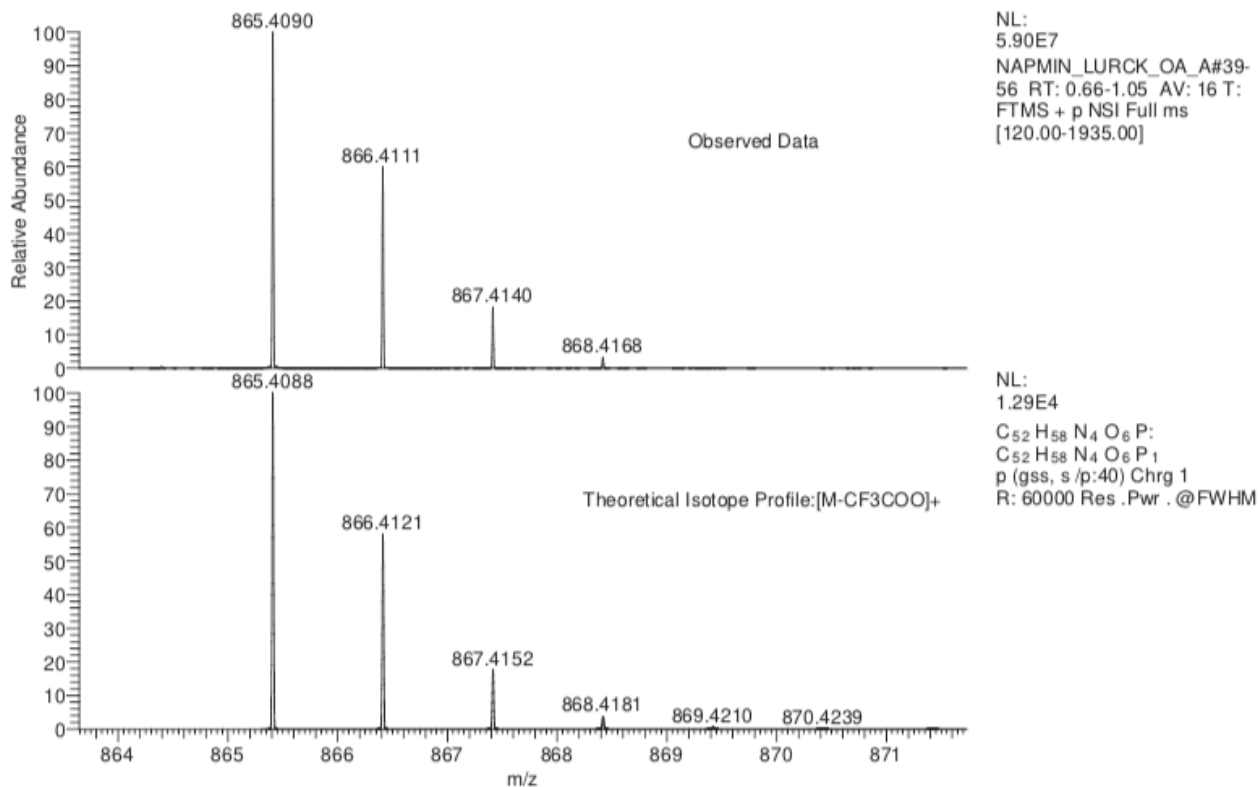
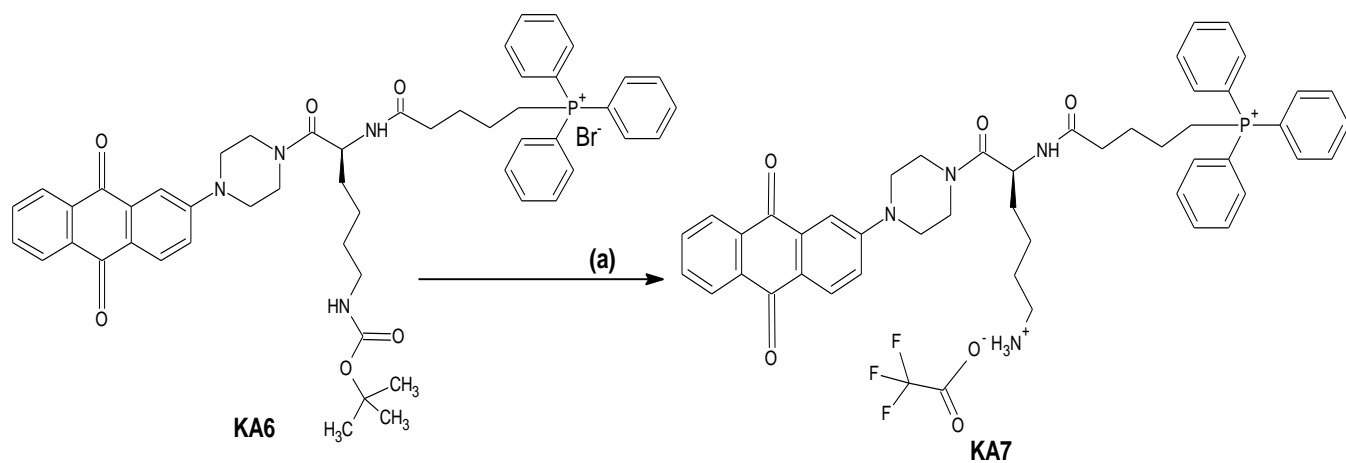


**Figure 2.18:** Correlation between observed data and theoretical <sup>13</sup>C isotope profile of KA6

### 2.3.7) Synthesis of AQ-PIP-Lys (TFA)-TPP (KA7)

KA7 was synthesized by (quantitative) removal of the Boc protecting group from the epsilon amino group of lysine in KA6. This was carried out by dissolving KA6 in trifluoroacetic acid at room temperature for 30 min (**Scheme 07**). The reaction mixture was dried and KA7 was precipitated by the addition of diethyl ether.

The structure of KA7 was confirmed by high resolution electrospray (+) mass spectrum showing a clear signal at m/z 765.3567 corresponding to the expected molecular mass of the KA7 cation (**Figure 2.19**). A good correlation was found between observed data and theoretical isotope model of C<sub>49</sub>H<sub>50</sub>N<sub>4</sub>O<sub>6</sub>F<sub>3</sub>P (**Figure 2.20**).



**Scheme 07:** Synthesis of KA7; deprotection of KA6 (a) = TFA

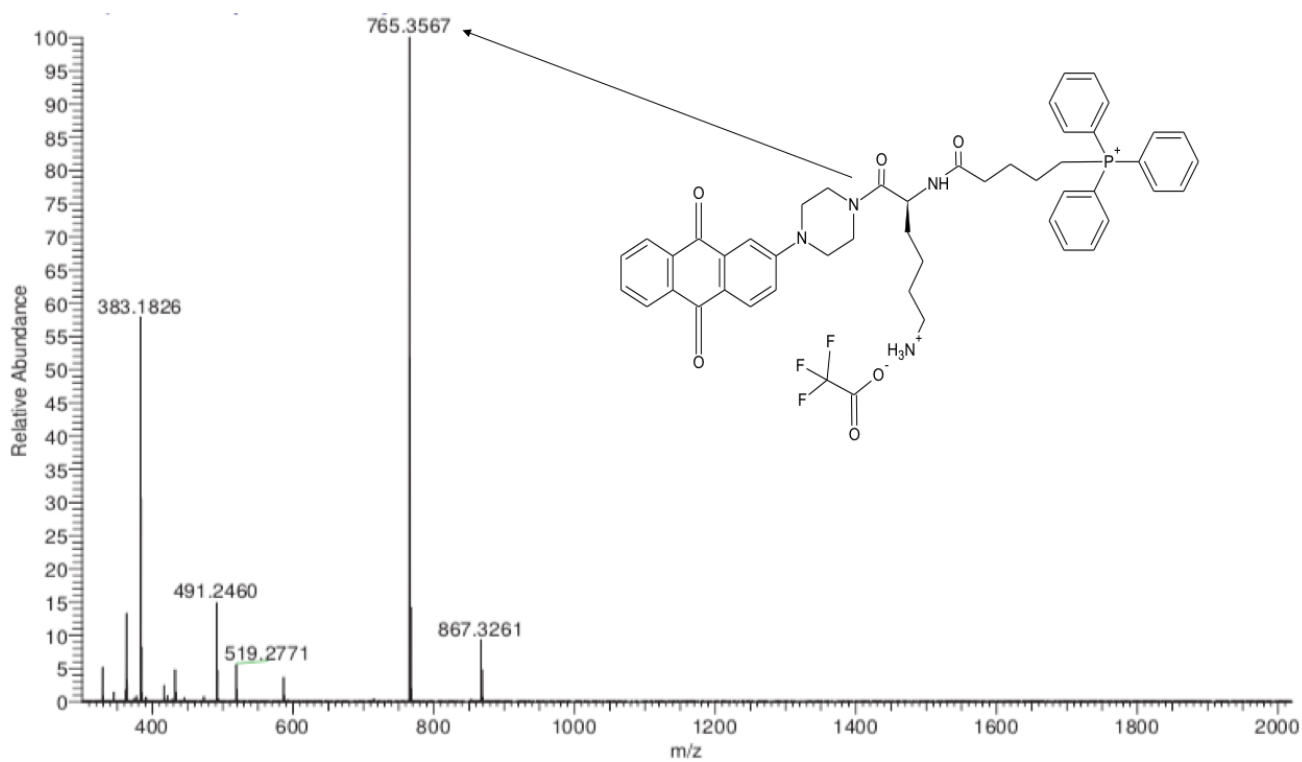


**Figure 2.19:** The high-resolution ESI (+) mass spectrum of KA7

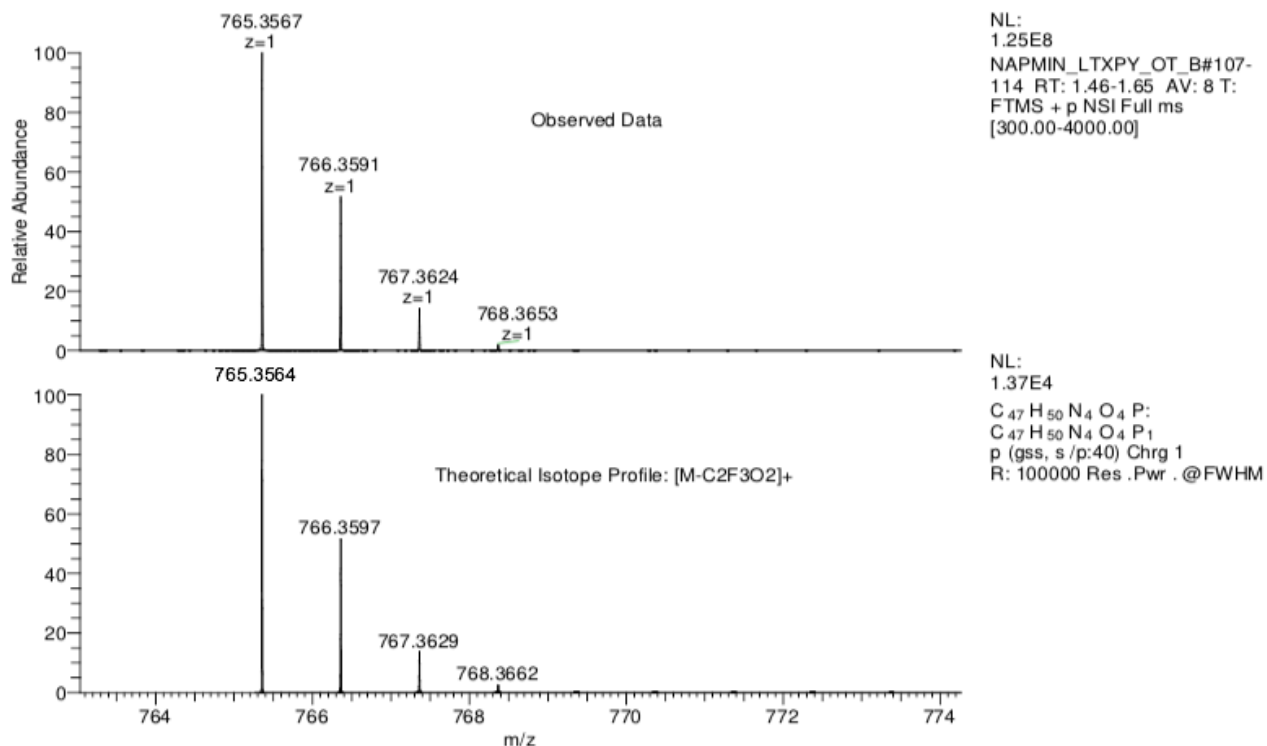
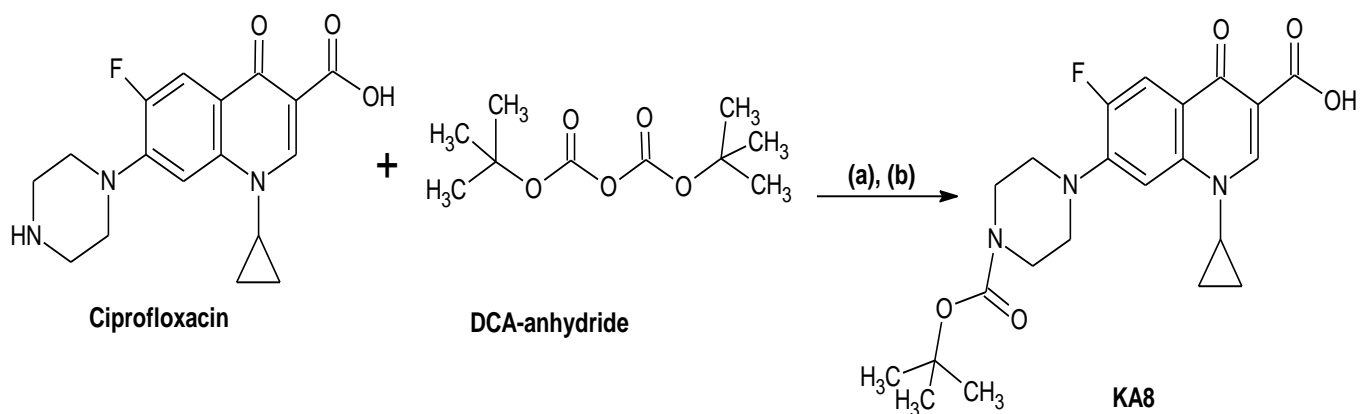


**Figure 2.20:** Correlation between observed data and theoretical isotope of KA7

### 2.3.8) Synthesis of CIPRO-BOC (KA8)

The synthesis of KA8 is shown in **Scheme 08**. KA8 was synthesized by dropwise addition of di-*tert*-butyl dicarbonate to a solution of CIPRO and THF: H<sub>2</sub>O (1:1) at room temperature for 30 minutes. The synthesis of KA8 was confirmed by TLC with R<sub>f</sub> 0.75. White precipitate of KA8 was formed by the addition of ice-cold water to the reaction mixture, filtered, washed and dried (yield 80%).

The structure of KA8 was confirmed by high resolution electrospray (-) mass spectrum showing a clear signal at m/z 430.1788 corresponded to the expected molecular mass of KA8 (431.4573432 Da) (**Figure 2.21**). Additionally, a good correlation was found between observed data and theoretical isotope model of C<sub>22</sub>H<sub>26</sub>FN<sub>3</sub>O<sub>5</sub> (**Figure 2.22**).



**Scheme 08:** Synthesis of KA8; **(a)** = THF: H<sub>2</sub>O, **(b)** = sodium bicarbonate

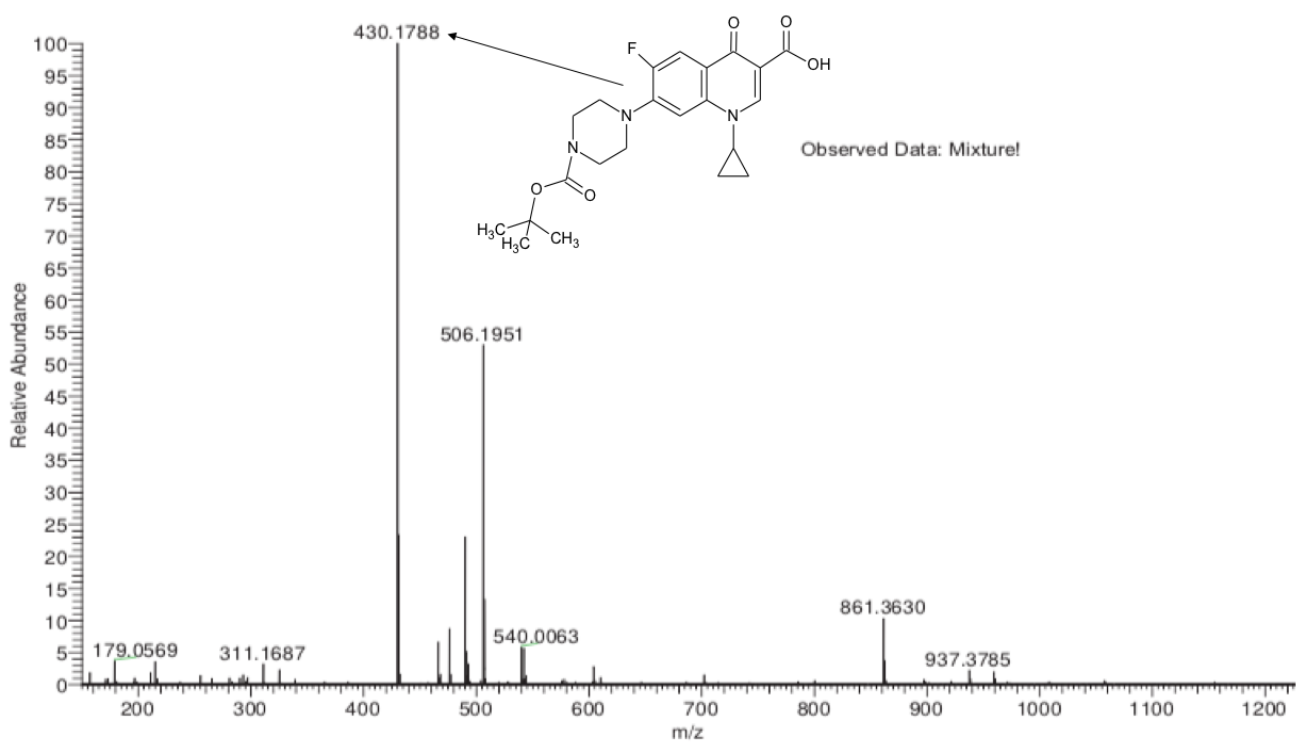


**Figure 2.21:** The high-resolution ESI (+) mass spectrum of KA8



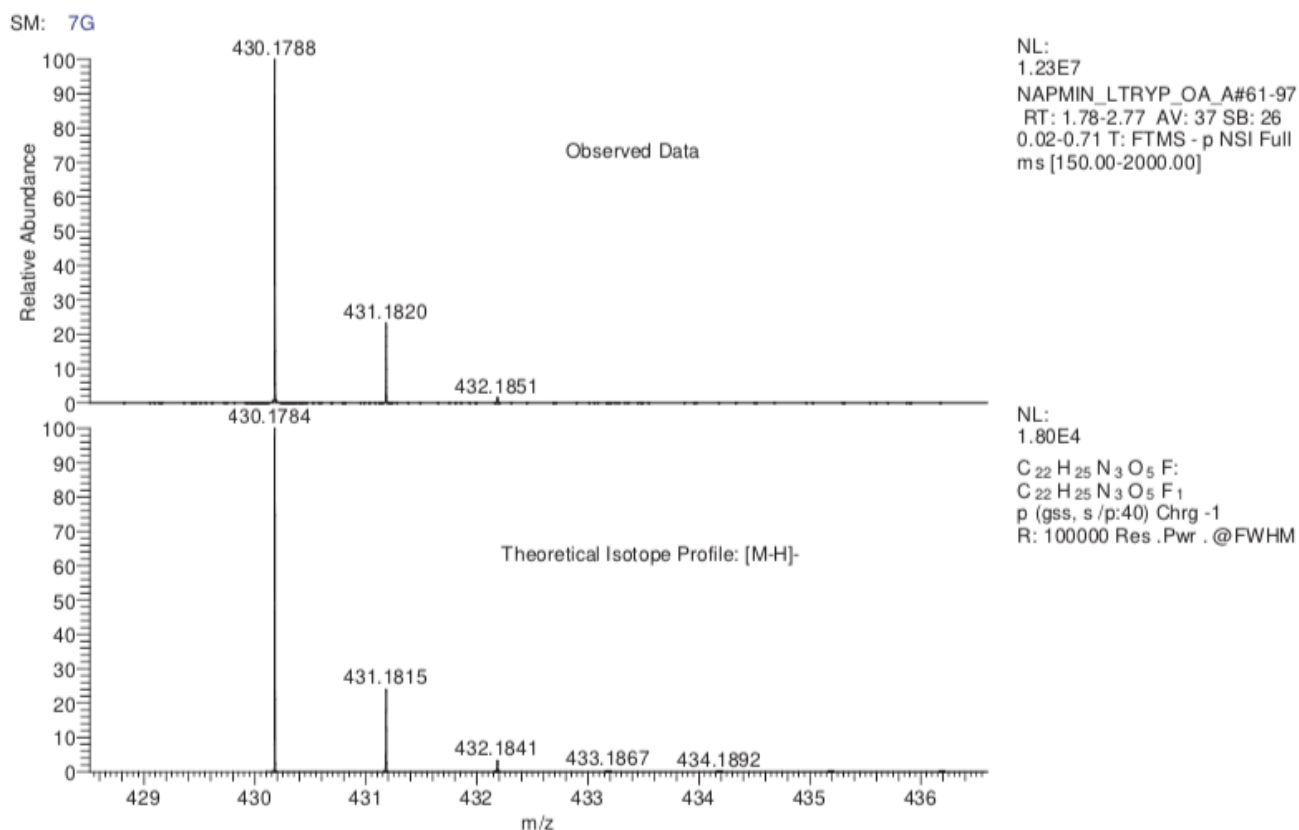
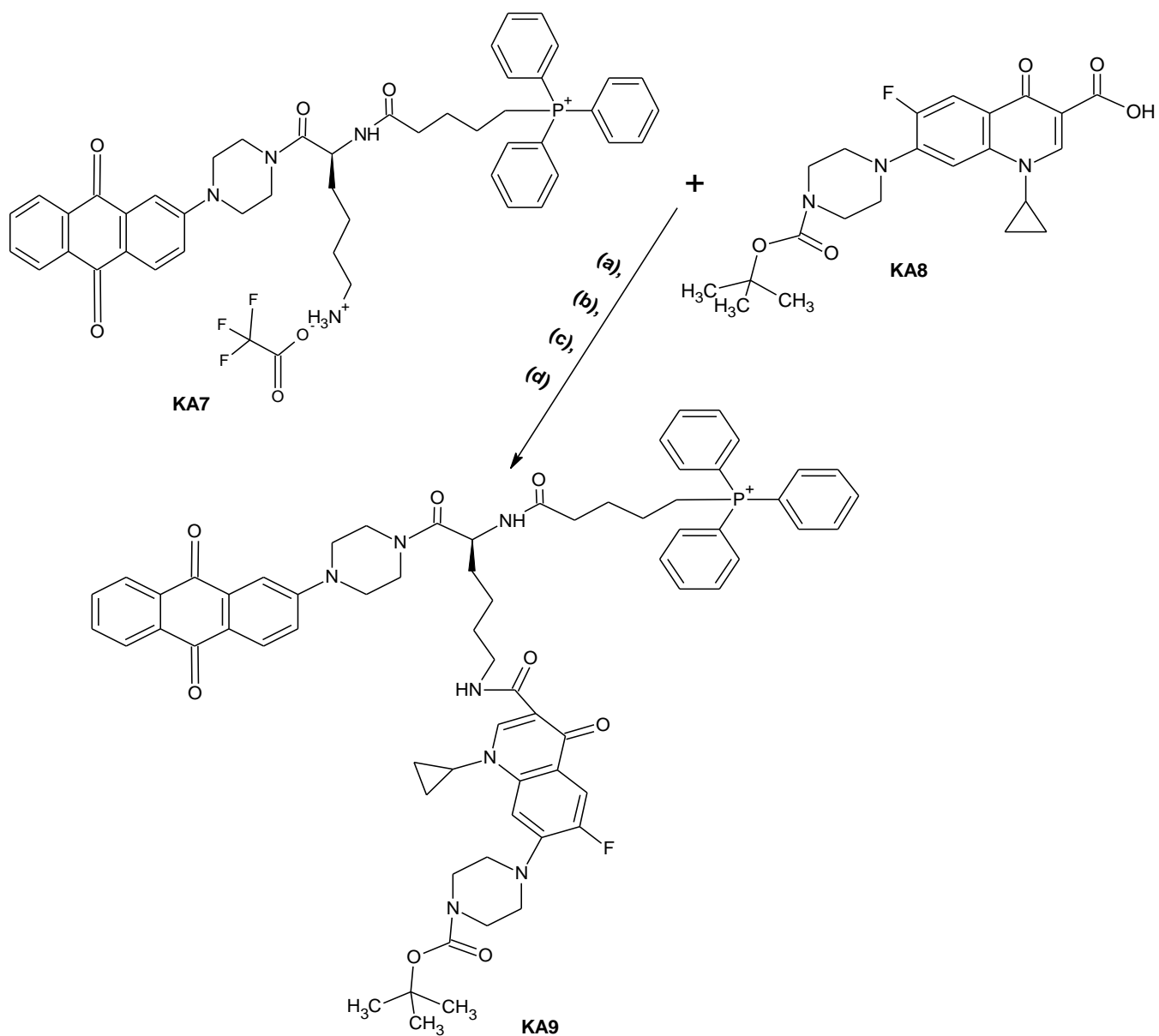


**Figure 2.22:** Correlation between observed data and theoretical <sup>13</sup>C isotope profile of KA8

### 2.3.9) Synthesis of AQ-TPP-CIPRO-BOC (KA9)

KA9 is the anthraquinone-piperazine-lysine-(ciprofloxacin)-TPP hybrid. In this reaction, Boc-ciprofloxacin was conjugated to the epsilon (side chain) amino group of lysine in KA8 through an amide bond (**Scheme 09**) using standard peptide coupling conditions. The synthesis of KA9 was confirmed by TLC. The coupling reaction between KA7 and KA8 afforded KA9 in high yield. The reaction mixture was extracted using dichloromethane and water and the product purified by column chromatography using a relatively polar solvent system (dichloromethane: methanol; 4:1). The pure fractions were collected, dried and precipitated by the addition of diethyl ether.

The chemical structure of KA9 was confirmed by high resolution electrospray (+) mass spectrum showing a clear signal at  $m/z$  1178.5287 corresponded to the expected molecular mass of the KA9 cation (**Figure 2.23**). Also, a good correlation was found between observed data and theoretical isotope model of C<sub>71</sub>H<sub>74</sub>N<sub>7</sub>O<sub>10</sub>F<sub>4</sub>P (**Figure 2.24**).



**Scheme 09:** Synthesis of KA9; (a) = HOBT, (b) = PYBOP, (c) = DMF, (d) = dichloromethane

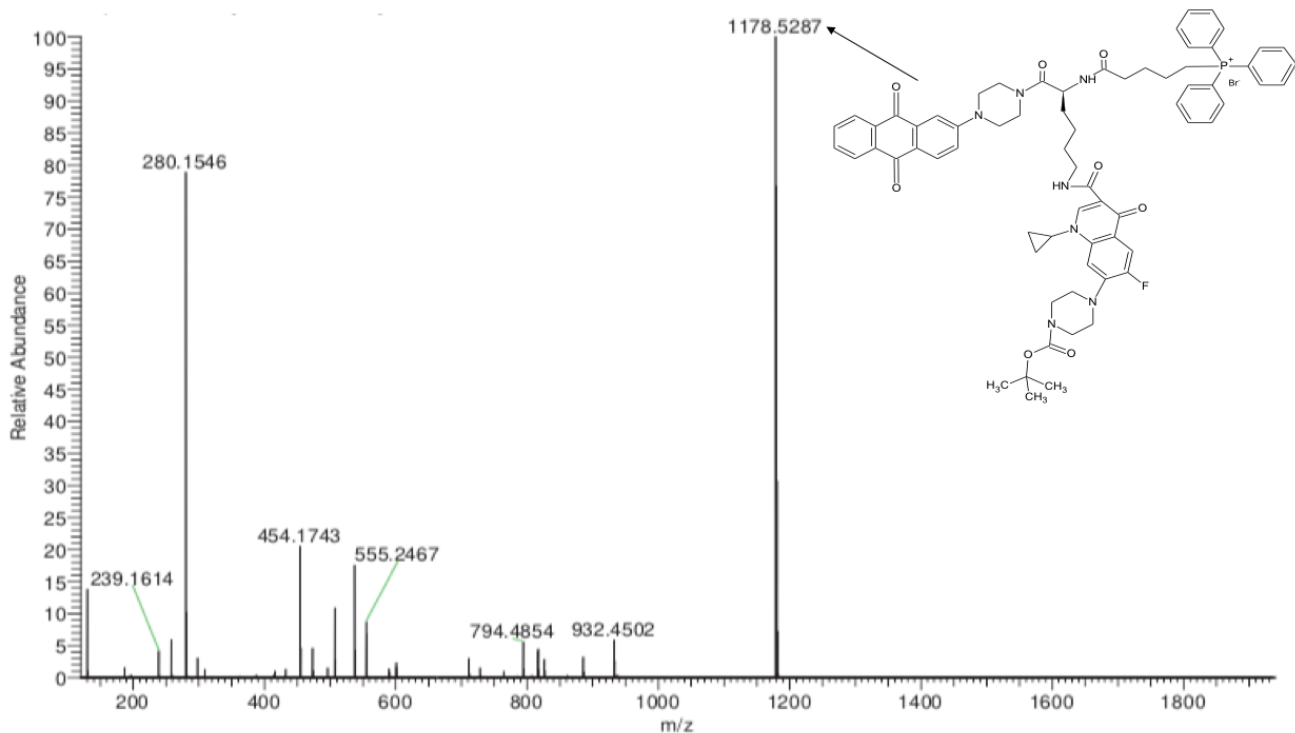


**Figure 2.23:** The high-resolution ESI (+) mass spectrum of KA9

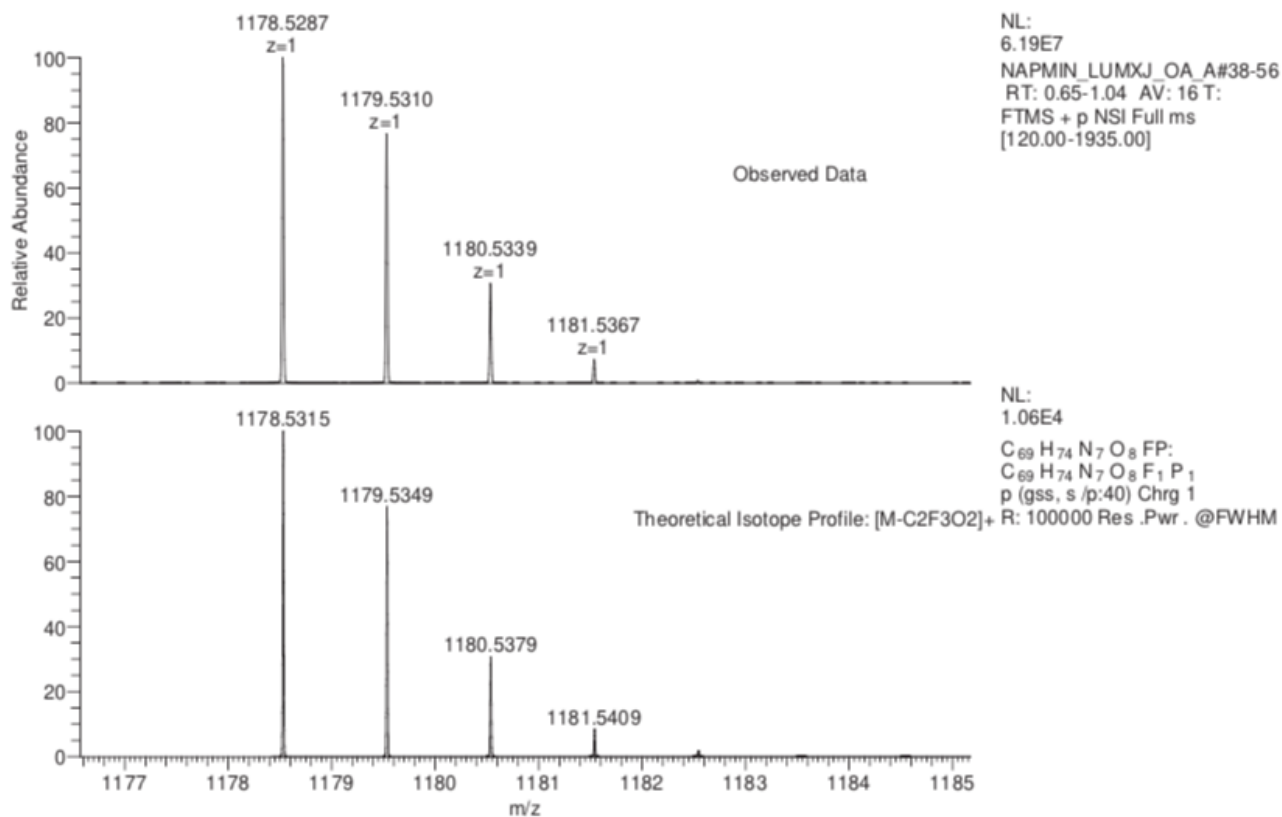
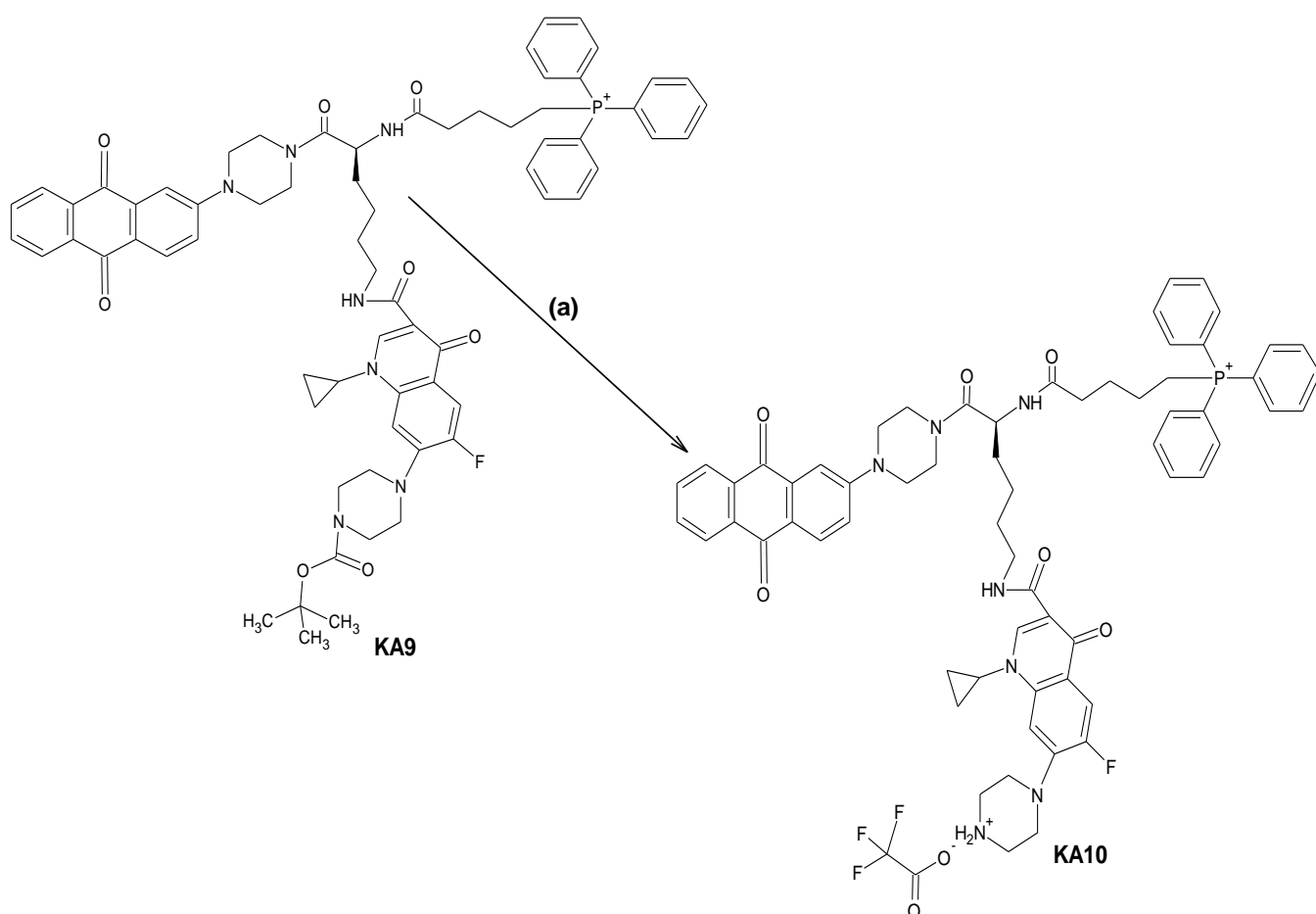


**Figure 2.24:** Correlation between observed data and  $^{13}\text{C}$  theoretical isotope profile of KA9

### 2.3.10) Synthesis of AQ-TPP-CIPRO-TFA (KA10)

KA10 is the compound formed by removal of the Boc protecting group of KA9 using TFA. The purpose is to free the piperazine moiety of CIPRO (**Scheme 10**). The synthesis of KA10 was confirmed by TLC ( $R_f$  0.46). The precipitate of KA10 was formed by the addition of diethyl ether. The structure of KA10 was confirmed by high resolution electrospray (+) mass spectrum with a clear signal at  $m/z$  1078.4791 which was corresponding to the expected molecular mass of the KA10 cation (**Figure 2.25**). Also, a good correlation was found between observed data and theoretical isotope model of  $C_{64}H_{66}F_1N_7O_6P$  (**Figure 2.26**).



**Scheme 10:** Synthesis of KA10 (Boc-deprotection of KA9); (a) = trifluoroacetic acid

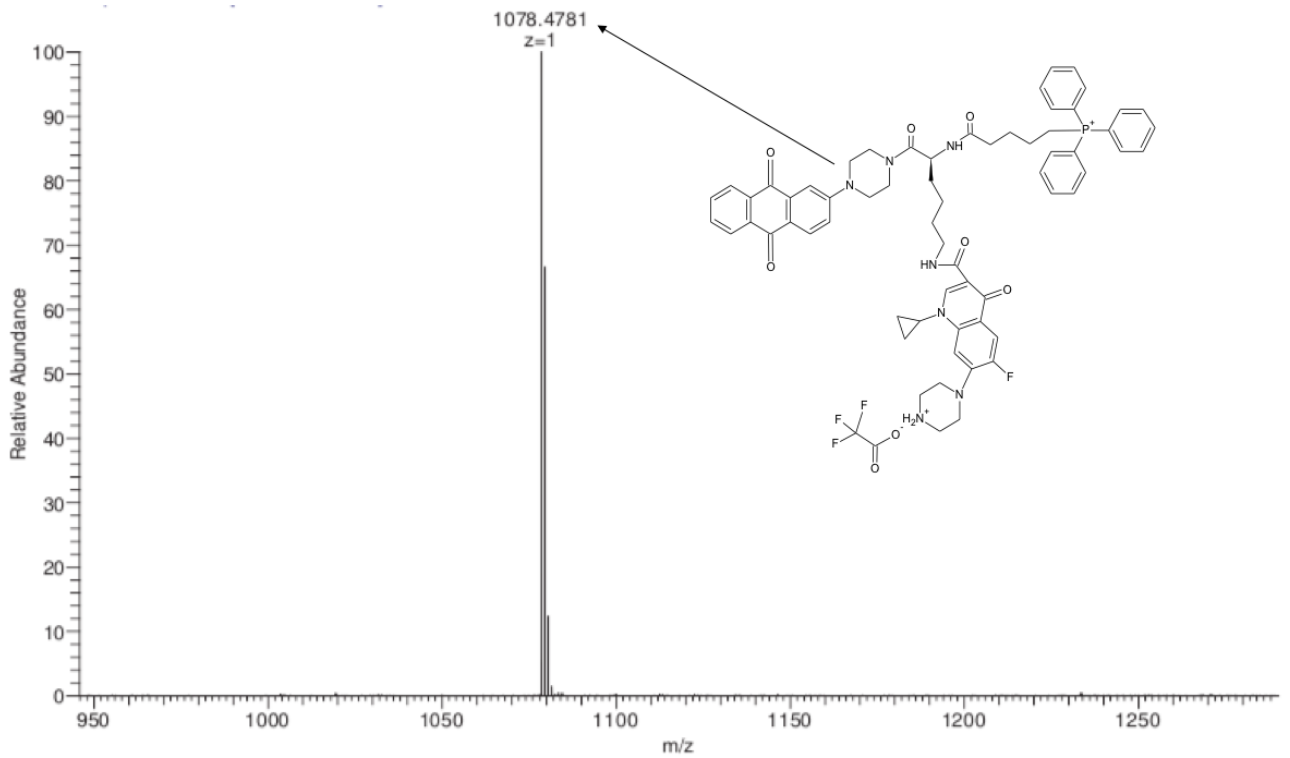


**Figure 2.25:** The high-resolution ESI (+) mass spectrum of KA10

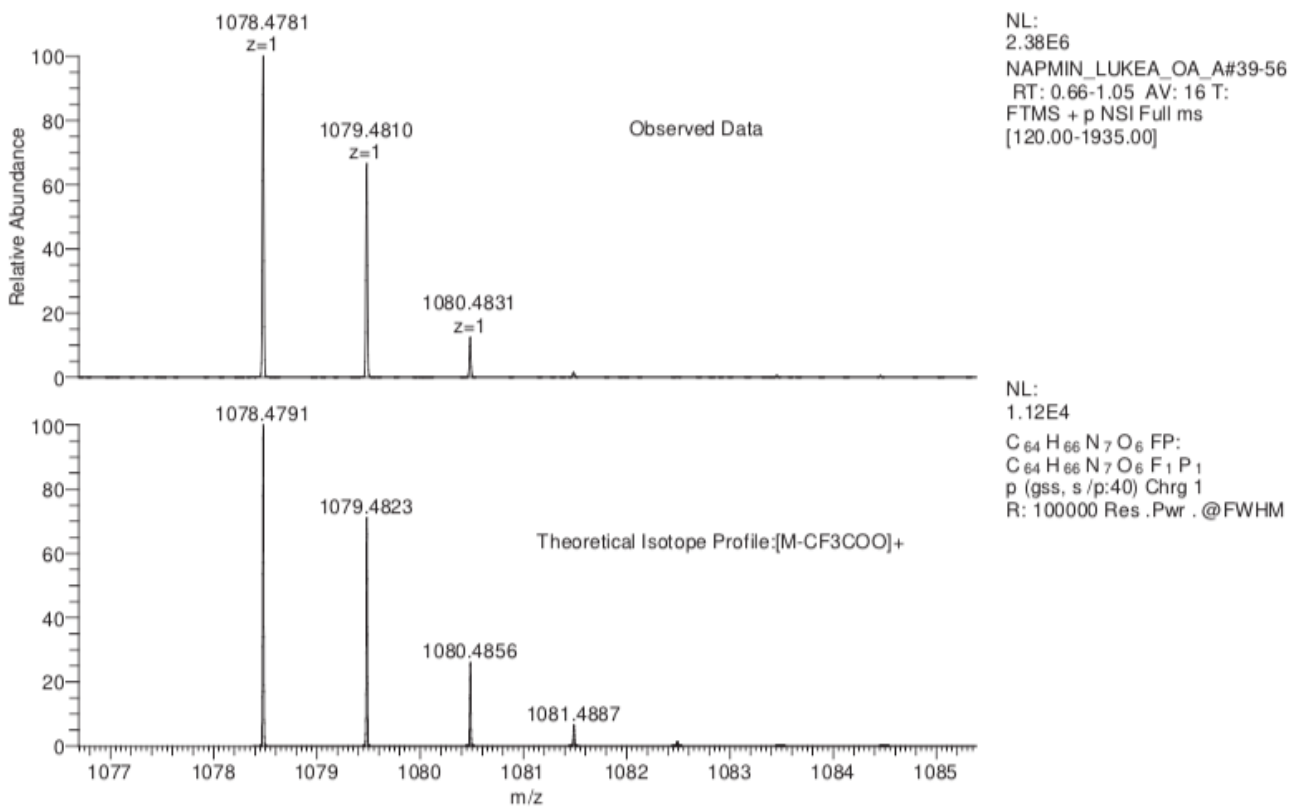


**Figure 2.26:** Correlation between observed data and the  $^{13}\text{C}$  theoretical isotope profile of KA10

### 2.3.11) Synthesis of AQ-TPP-CIPRO-DCA (KA11)

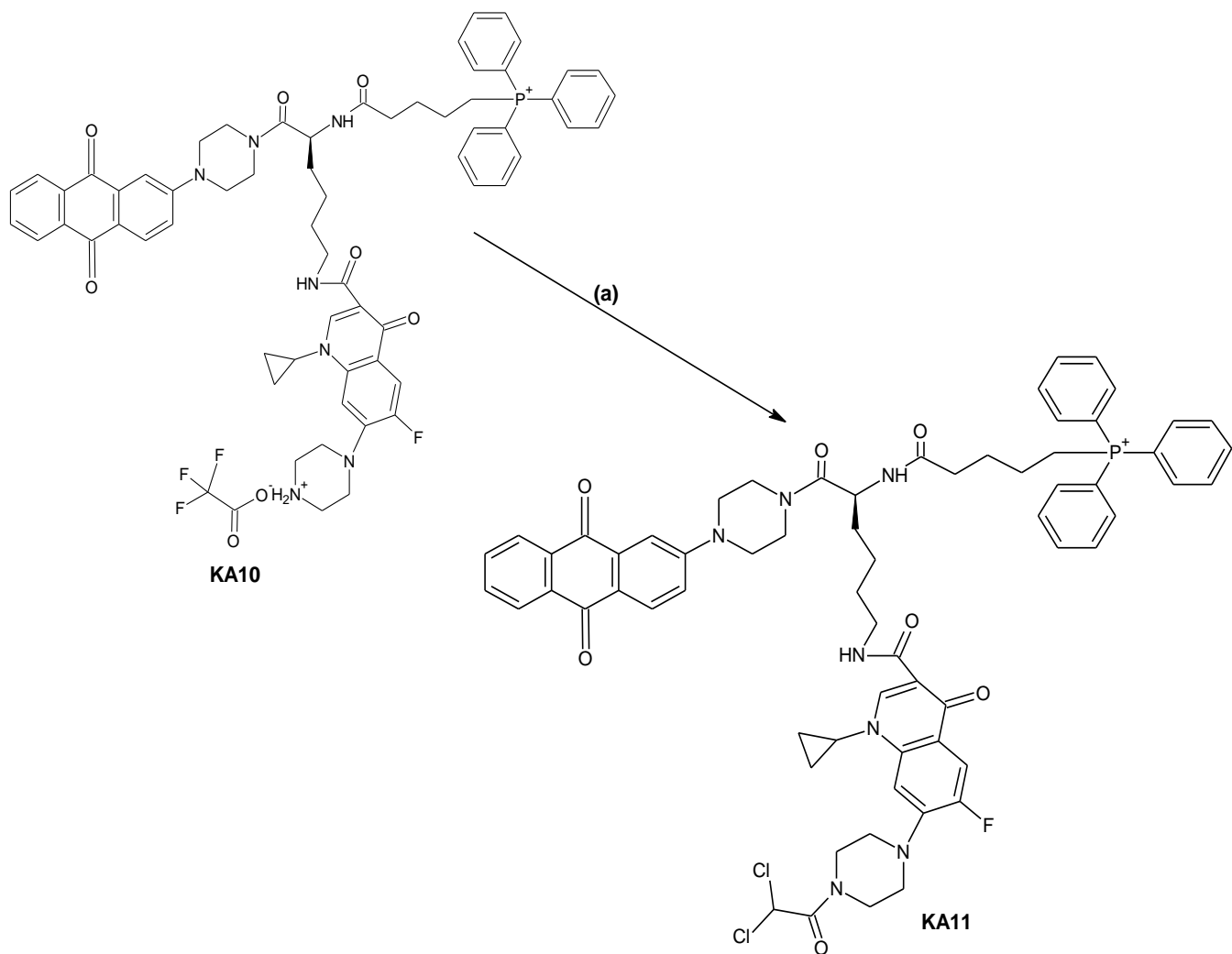
KA11 (the ultimate and most complex hybrid target conjugate) was synthesized by the dropwise addition of dichloroacetic acid anhydride (DCA-anhydride) to a solution of KA10 followed by 2 hours stirring at room temperature to afford the complex target hybrid containing all the planned features of an anthraquinone and the mitochondrial-targeting TPP vector, together with the incorporation of the antibiotic CIPRO and the known mitochondria-targeting anticancer agent dichloroacetate.

The introduction of the DCA moiety at this final step was accomplished via an amide bond linking the carboxylic acid group of the DCA to the free piperazine nitrogen in KA10. (**Scheme 11**) The amide formation lowered the polarity and increased the liposolubility of the DCA residue.

In simple DCA derivatives, N-phenylamide formation to decrease the polarity and increase lipid solubility led to increased anticancer potency in cancer cell lines compared to the free dichloroacetic acid (Yang, *et al.*, 2010).

The synthesis of KA11 was confirmed by TLC. Solvent extraction and purification by column chromatography afforded pure fractions of KA11. Diethyl ether was added to residues of evaporated fractions of KA11 to form precipitates at 4°C that were combined, filtered and collected. The removal of the Boc group in KA10 to afford KA11 (the target hybrid conjugate) proceeded quantitatively.

The structure of the target compound KA11 was confirmed by its high-resolution electrospray (+) mass spectrum showing a clear signal at  $m/z$  1188.4095 corresponding to the expected molecular mass (1194.2544976 Da) of KA11 (**Figure 2.27**). Additionally, a good correlation was found between the observed data and theoretical carbon 13 isotope model of  $C_{66}H_{66}Cl_2FN_7O_7P^+$  (**Figure 2.28**).



**Scheme 11:** Synthesis of KA11; **(a)** = dichloroacetic anhydride

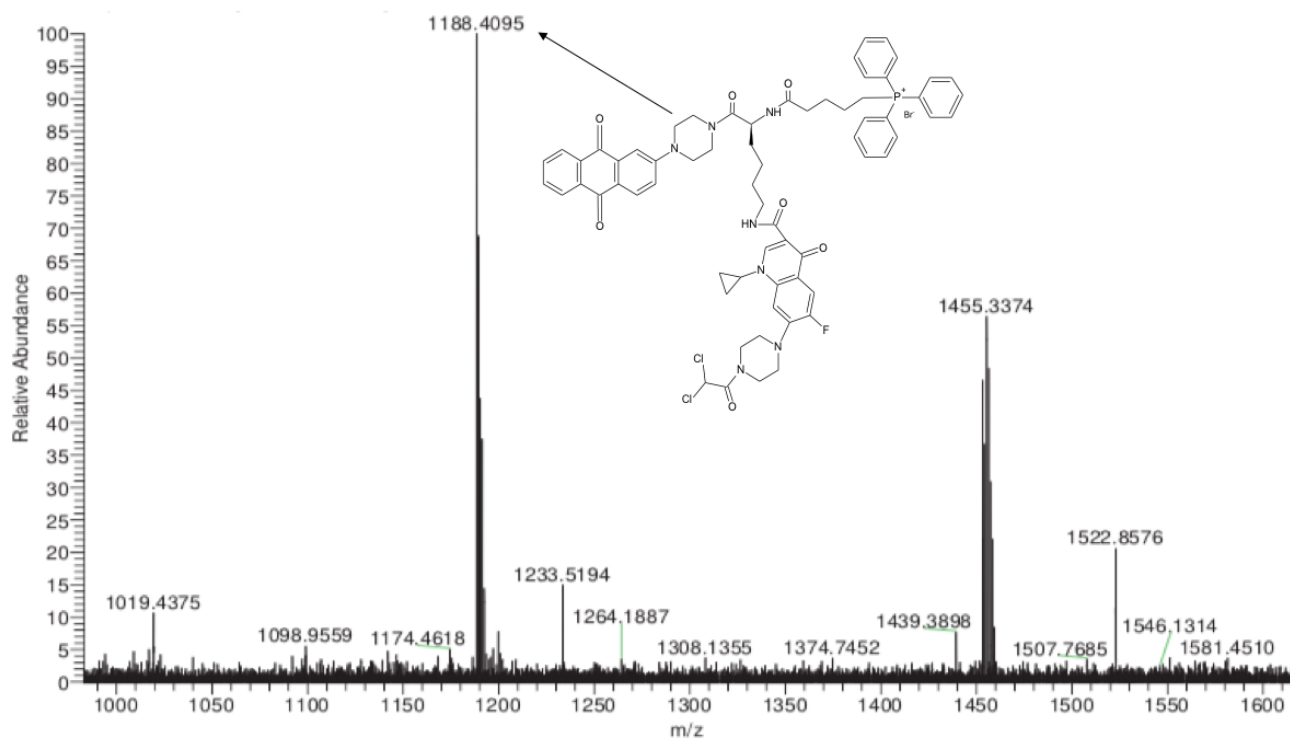


Figure 2.27: The high-resolution ESI (+) mass spectrum of KA11

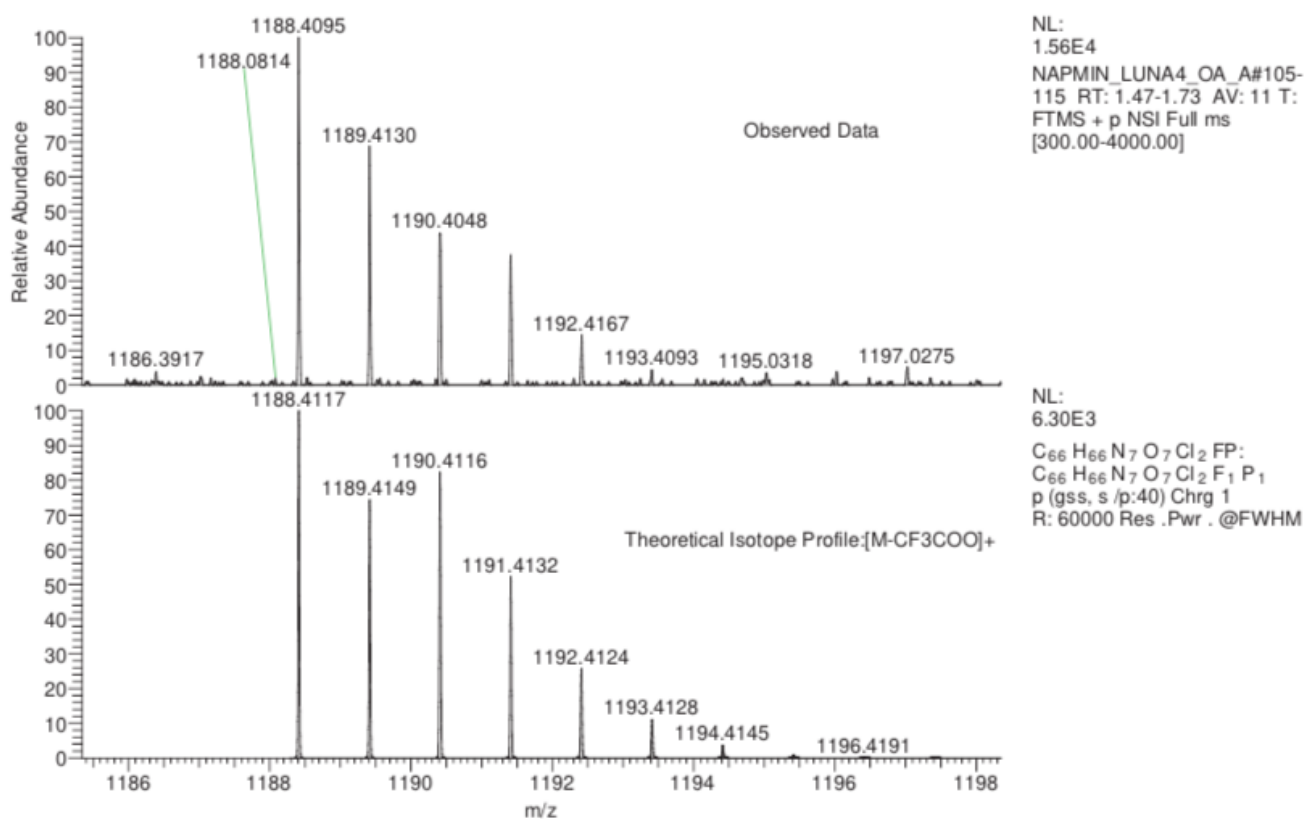


Figure 2.28: Correlation between observed data and theoretical  $^{13}\text{C}$  isotope profile of KA11



## 2.4) In-vitro biological assays

### 2.4.1) Antibacterial activity

#### i) Measurement of minimum inhibitory concentrations (MIC) and minimum bactericidal concentration (MBC)

Chemical hybrids (KA11, KA10, KA7 and KA3) were subjected to antibacterial assay to determine the minimum inhibitory concentration (MIC) and minimum bactericidal concentration (MBC) against resistant and sensitive strains of *S. aureus* and *E. coli*. ATCC47055 was the sensitive culture collection strain of *E. coli* and LIB213 was an environmental isolate which was previously isolated and provided by Dr Donald Morrison (Edinburgh Napier University) and used as a resistant strain of *E. coli*. NCTC 6571 (82) was the sensitive culture collection strain of *S. aureus* (MSSA) and NCTC 13616 (83) was the resistant cultured strain of *S. aureus* (MRSA).

Minimum inhibitory concentration of tested compounds (KA3, KA7, KA10 and KA11) was determined after 24 of incubation (**Table1**) while MBC value was determined later on based on the 24 h incubation of inhibitory concentrations of tested compounds. Full details of the experimental protocols are located in Chapter 3 Experimental, Section 3.4.1.01.

**Table 2.1: In-vitro minimum inhibitory concentration (MIC) of novel compounds on *E. coli* & *S. aureus* for 24 h incubation period**

MIC Values ( $\mu\text{g/mL}$ )				
Bacterial Strains	KA11	KA10	KA7	KA3
<i>E. coli</i> ATCC47055	256	0.5	115 $\pm$ 28.62	>256
<i>E. coli</i> LIB213	>256	11.2 $\pm$ 3.2	256	>256
<i>S. aureus</i> NCTC6571	256	3.2 $\pm$ 1.09	64	>256
<i>S. aureus</i> NCTC13616	>256	64	128	>256

According to **Table 2.1**, it is clear that modification of CIPRO could be effective to overcome bacterium induced resistance in cancer cells by inhibiting the growth of adverse bacteria. KA10 and KA11 were the ciprofloxacin-based anthraquinone derivatives that showed significant activity against bacterial strains. KA10

(ciprofloxacin-based anthraquinone hybrid with TPP<sup>+</sup>-cation) displayed enhanced *in-vitro* activity against both strains of Gram-positive and Gram-negative bacteria. Among all tested chemical moieties KA10 showed the lower MIC value of 0.5 µg/mL and 3 µg/mL against sensitive culture strain of *E. coli* ATCC47055 and *S. aureus* NCTCC6571.

The highest MIC value of KA10 to inhibit the growth was 64 µg/mL against resistant strain of Gram-positive bacillus, while 8 µg/mL was the inhibitory concentration of resistant strain of Gram-negative bacillus (**Table 2.1**). However, KA10 surprisingly showed bactericidal effect on both Gram-negative and Gram-positive bacillus at different concentrations. The minimum bactericidal concentration (MBC) was found to be at 0.5 µg/mL against the sensitive strain of *E. coli*.

KA11 displayed antimicrobial activity at 256 µg/mL against sensitive strains of Gram-positive and Gram-negative bacillus (**Table 2.1**). The minimum bactericidal concentration of KA11 was 256 µg/mL against *E. coli* ATCC47055.

The inhibition growth rate of KA3 and KA7 was not unexpected due to the absence of CIPRO in their chemical structure. KA3 showed no activity against Gram-positive and Gram-negative bacteria which represents that KA3 might not cross the biological membranes of bacteria. KA7 showed inhibitory activity at a minimum value of 64 µg/mL (**Table 2.1**) and proved to be bactericidal at 256 µg/mL which would be consistent (indirect evidence) with the TPP<sup>+</sup> cation actively transferring KA7 passing through the biological membranes of bacteria. Further work is required to establish this speculation.

#### **2.4.2) Anticancer activity**

##### **i) MTT assay**

The MTT (3-[4, 5-dimethylthiazol-2-yl]-2, 5 diphenyl tetrazolium bromide) assay is based on a tetrazolium salt, yellow in colour, and the assay is performed metabolically on viable cells depending upon the conversion of the tetrazolium salt into a Formazan dye (purple). The conversion is processed by mitochondrial oxidoreductase, a mitochondrial enzyme of viable cells, and is quite evident if the

cells are alive (Larkin and Aukim-Hastie, 2011). Successful application of the MTT assay relies on the conversion of tetrazolium dye (water soluble) to Formazan (dark-purple water insoluble) crystals (**Figure 2.29**). These Formazan crystals accumulate in viable cells to measure their mitochondrial activity (Fotakis and Timbrell, 2006), mechanically by the measurement of concentration of Formazan dye through a microplate reader which could detect the increase or decrease of viable cell number.

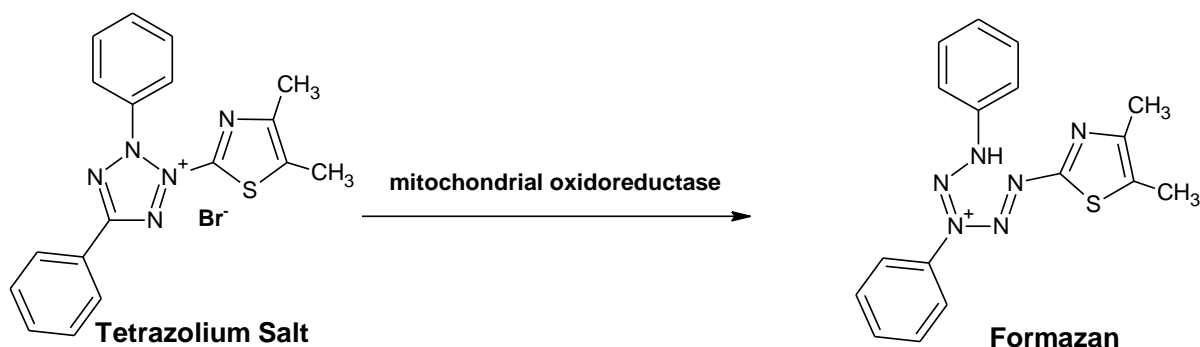


**Figure 2.29:** Conversion of tetrazolium salt to formazan

Hence, MTT assay, widely used for screening the antiproliferative activities of newly synthesised compounds, could be used to measure the toxicity of drug candidates by the reduction in number of viable cells which would indicate the growth inhibition rate. Drug potency is reported by determining the concentration of drug to produce 50% inhibition (IC<sub>50</sub>) of treated viable cells in comparison with the growth rate of untreated control cells (Larkin and Aukim-Hastie, 2011) and can be used to compare different compounds and rank them in order of in vitro potency.

Using an MTT assay, growth inhibition rate was determined by the treatment of viable colon cancer cell lines (relatively resistant HCT-15) with a range of concentrations of test compounds. The selected compounds were KA3, KA7, KA10 and KA11. The reason to use colon carcinoma cells (HCT-15) for the determination of growth inhibition of novel compounds is that they are well characterised by the Developmental Therapeutics Program which was collaborated with various experienced investigators who have measured protein levels, mutation status and activity levels of enzyme on 60 human tumour cell lines and have been shown to possess high levels of P-gp, the most common form of drug efflux transporter (<http://dtp.cancer.gov/default.htm>). Measurement of MDR1 levels relative to actin

RNA for RT-PCR RNA [Experiment id: 20103, pattern id: MT1614] deduced that levels in HCT-15 were 17-fold higher than other cell lines, including MCF-7 (breast carcinoma). Thus, HCT-15 cell lines were ideally matched wild type and MDR cell lines which could be used to determine the ability of agents to overcome P-gp induced resistance through the testing of drug candidates.

Hence, comparison of IC<sub>50</sub> values was made between SH1 and tested drugs (KA3, KA7, KA10 & KA11) to determine the potency of compounds (and potential to overcome P-gp induced resistance) by attachment with a TPP<sup>+</sup> cation. *In-vitro* cytotoxicity of KA3, KA7, KA10, KA11 and SH1 was measured after 96 h of incubation by MTT assay. The cytotoxic activity of SH1 on HCT-15 cell lines was already determined and used to compare with tested compounds. The cell growth curves of HCT-15 carcinoma cells against different concentrations of tested compounds are shown in **Figures 2.30, 2.31, 2.32, and 2.33**. Full details of the experimental protocols are located in Chapter 3 Experimental, Section 3.4.2.02.

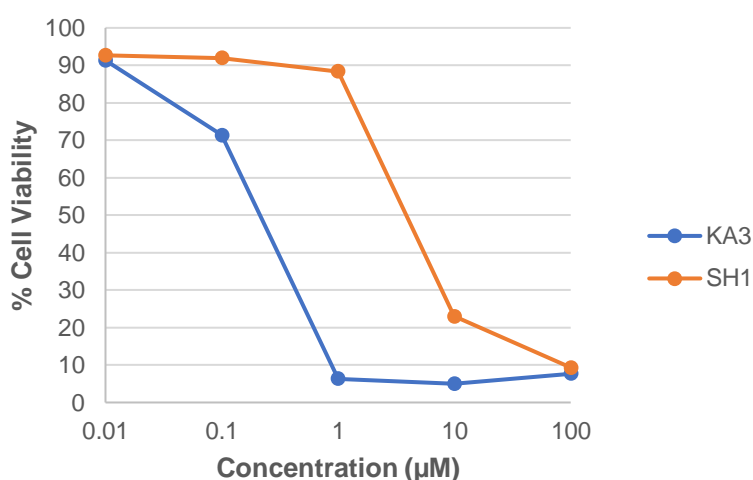


**Figure 2.30:** Comparative Cell Viability analysis of HCT-15 cells between SH1 & KA3

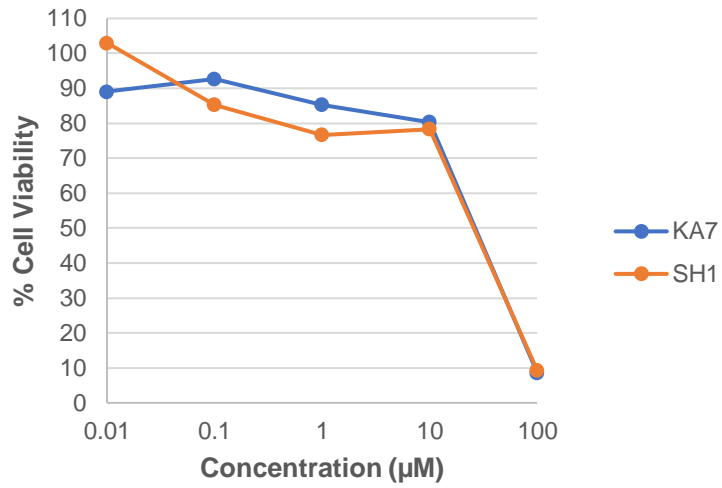


**Figure 2.31:** Comparative Cell Viability analysis of HCT-15 cells between SH1 & KA7

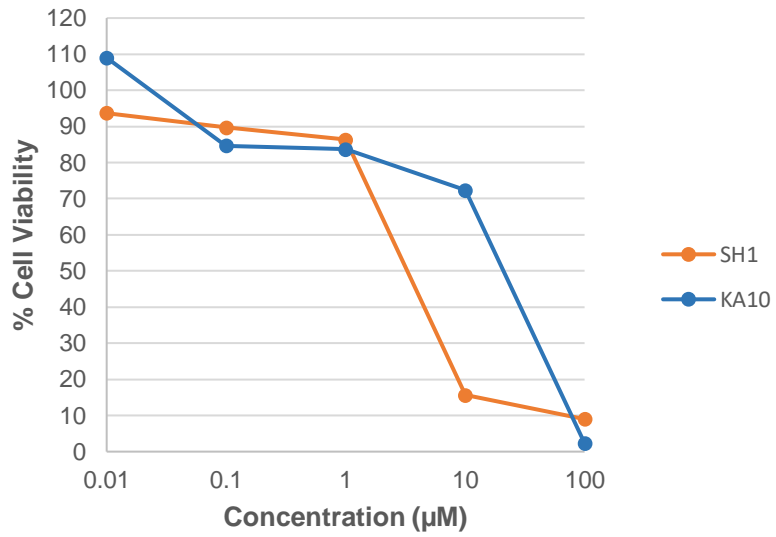


**Figure 2.32:** Comparative Cell Viability analysis of HCT-15 cells between SH1 & KA10

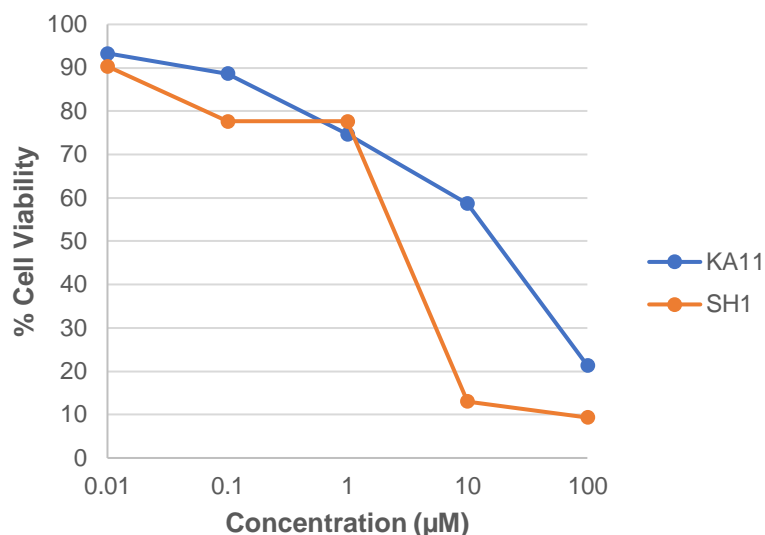


**Figure 2.33:** Comparative Cell Viability analysis of HCT-15 cells between SH1 & KA11

According to the presented results in **Table 2.2** and **Figures 2.29, 2.30, 2.31, Figure** and **2.32**,  $IC_{50}$ -values of KA11 ( $21.33 \pm 5.8 \mu\text{M}$ ), KA10 ( $2.33 \pm 0.29 \mu\text{M}$ ), KA7 ( $8.67 \pm 5.8 \mu\text{M}$ ), KA3 ( $6.33 \pm 2.08 \mu\text{M}$ ) and SH1 ( $9.33 \pm 1.15$ ) suggest that these compounds have retained cytotoxic activity on HCT-15 cells which indicates that these novel-derivatives have anticancer activity against colon carcinoma cells, comparable to SH1. SH1 is an amino-anthraquinone derivative attached to the TPP<sup>+</sup> cation with proven capacity to evade P-gp mediated efflux in cancer cells. However, mitoxantrone ( $IC_{50} 0.082 \pm 0.02$ ) is a more potent anthraquinone against the HCT-15 cell line (Mohammed *et al.*, 2016) (Literature value from this laboratory). This was not used in these experiments due the (anticipated) large difference in potency and instead SH1 was adopted as an internal control.

**Table 2.2: Determination of  $IC_{50}$  of tested compounds against the HCT-15 cell line**

Tested Compound	$IC_{50}$ of HCT-15 cells	Inter-assay variability % CV
SH1	$9.33 \pm 1.15$	12.32%
KA11	$21.33 \pm 5.8$	27%
KA10	$2.33 \pm 0.29$	12.60%
KA7	$8.67 \pm 5.8$	16.60%
KA3	$6.33 \pm 2.08$	26.34%

Among all tested compounds, KA10 has the greater potential with the lowest  $IC_{50}$ -value which may indicate that the TPP<sup>+</sup> cation has proven to be effective to target

direct to mitochondria of cancer cells overcoming the incidence of resistance due to P-gp pump. However, in order to obtain evidence for this mechanism, confocal microscopy studies should be carried out using live cancer cells and tracer dyes (e.g., MitoTracker green) to determine any colocalization in the target organelles. KA10 is a salt-based form of CIPRO hybrid with TPP<sup>+</sup>-cation at its C-3 position and trifluoroacetate at N4-piperazinyl moiety. Linkage of CIPRO with TPP<sup>+</sup>-cation at C-3 position has increased the potential of drug to evade P-gp substrates in related compounds (Ahadi *et al.*, 2020) and derivatization at N4-piperazinyl moiety would likely improve the lipophilicity of the compound to target cancer cells (Kassab and Gedawy, 2018). However, the Table represents the calculated value of % co-efficient of tested compounds to measure the consistency of results from plate to plate during the evaluation. The percentage variance of SH1, KA10 and KA7 is generally acceptable due to small percentage of error from plate to plate yet KA11 and KA3 has represented an error percentage more than 15% which represents the inconsistency of untreated cells from plate to plate in the MTT assay.

There is no doubt that CIPRO has confirmed cytotoxic effects on some of cancer cell lines but in non-pharmacological concentrations (Chrzanowska *et al.*, 2020). The cytotoxic potential of CIPRO is due to the inhibition of topoisomerase I & II enzymes (human equivalents to bacterial DNA-gyrase) (Kloskowski, *et al.*, 2012) including cell proliferation due to mitochondrial DNA damage (Kassab and Gedawy, 2018) and may also be due to the generation of free radicals (Wagai and Tawara, 1991). The main focus of scientists was the substitution at N4-piperazinyl moiety of CIPRO to improve anti-tumour effects on different cancer cell lines such as the development of hydrazone derivative of CIPRO linked at N4-piperazinyl moiety showed good *in vitro* anticancer activity on UO-31 cell lines (Kassab and Gedawy, 2018).

KA11 despite having TPP<sup>+</sup>-cation in the chemical structure, might not be a good P-gp substrate due high IC<sub>50</sub>-value and may have the same mechanism of action in HCT-15 cell lines. Ciprofloxacin-derivatives inhibit topoisomerase enzymes yet they have the potential to reverse cell-cycle arrest by decreasing the expression of cyclin B1 and Cdc2 proteins (Azéma *et al.*, 2009) in cancer cells. The difference between KA10 and KA11 is the linkage of DCA-moiety derivatized at N4-piperazinyl moiety of CIPRO which is an active cytotoxic element (Stacpoole, Henderson, Yan, and

James, 1998). According to data in **Table 2.2**, KA11 is a less toxic compound compared to other compounds probably due to some limitations such as poor water solubility, short half-life, and less bioavailability in common with similar compounds (Piplani, Rajak and Sharma, 2017).

Ciprofloxacin derivative has anticancer potential due to the generation of free radicals yet incidence of resistance due to being a P-gp substrate and bacterial populations have led to the possibility of chemical modification of CIPRO to target cancer cells by evading incidence of resistance. Following this therapeutic approach one chemical series of ciprofloxacin derivatives were synthesized, characterized and investigated having bis-hydrazones at C-3 and an N4-piperaziny moiety with an expectation of synergistic effect. Some of hydrazone-based CIPRO moieties showed *in-vitro* cytotoxic activity due to enhanced lipophilicity (Samir *et al.*, 2021). The IC<sub>50</sub>-value of SH1 and KA7 (**Table 2.2**) has revealed the fact that their biological activity may be equally toxic in colon cancer cell lines.

## 2.5) Summary

This study was aimed to design an intracellularly targeted chemical compound (AQ-TPP-CIPRO-DCA) (KA11) having an optimized anticancer and antimicrobial potential to overcome the incidence of resistance due to the overexpression of P-gp and the emergence of bacterial infections. A series of chemical reactions were performed to synthesize (AQ-TPP-CIPRO-DCA) (KA11). Some of the exploratory reactions were performed at first to analyze the conjugation between chemical agents, leading to the synthesis of KA3 (AQ-PIP-BOC). KA3 was successfully synthesized in three simple steps, following nucleophilic substitution and addition reaction between 2-chloroanthracene-9, 10-dione and a piperazine moiety.

Further, it was necessary to develop biophysical drug delivery system to translocate the chemical hybrid directly into mitochondria of cancer cells (Guilhelmelli *et al.*, 2013). Therefore, TPP<sup>+</sup>-derivatives of an anthraquinone moiety were synthesized by the attachment of a spacer with anthraquinone through different chemical reactions leading to the synthesis of KA7 (AQ-PIP-Lys (TFA)-TPP). The main goal was to conjugate CIPRO moiety with KA7 (AQ-PIP-Lys (TFA)-TPP) for which the free amine



of CIPRO was protected with BOC resulting in the synthesis of KA8 (CIPRO-BOC). CIPRO-BOC (KA8) and AQ-PIP-Lys (TFA)-TPP (KA7) were combined through a base catalyzed chemical reaction leading to the synthesis of KA9 (AQ-TPP-CIPRO-BOC). KA9 was deprotected further by reacting it with TFA leading to the synthesis of KA10 (AQ-TPP-CIPRO-TFA) which was reacted with DCA-anhydride to synthesize KA11 (AQ-TPP-CIPRO-DCA).

Synthesized compounds were satisfactorily and successfully characterized by Swansea University in the laboratory of National Mass Spectrometry Facility through Thermo-Scientific LTQ Orbitrap XL using DCM and MEOH. Four synthesized compounds (KA3, KA7, KA10 & KA11) were investigated for antibacterial activity following the reference protocols of Baltzer, 2017 and cytotoxic potential was evaluated through MTT assays (Mosmann, 1983).

The results of antibacterial assay have revealed that the presence of CIPRO is necessary to overcome the resistance caused by bacterial infections. Compounds having CIPRO (KA7, KA10 & KA11) showed inhibitory activity against Gram-negative and Gram-positive bacteria. KA3 (AQ-PIP-DCA), the chemical hybrid of anthraquinone and DCA, showed no inhibition against bacteria which may mean that KA3 might not reduce the emergence of bacterial infections in cancer cells. However, KA10 (AQ-TPP-CIPRO-TFA) showed significant inhibitory concentration against Gram-negative (*E. coli*) and Gram-positive (*S. aureus*) bacteria.

The results of MTT assay indicated that all tested compounds have significant antiproliferative activity. KA10 (AQ-TPP-CIPRO-TFA) showed the highest cytotoxic potency in the HCT-15 cancer cell line. KA3 (AQ-PIP-DCA) is not a TPP<sup>+</sup>-conjugate but showed high cytotoxic potential on HCT-15 cancer cell lines which may indicate that DCA has the potential to increase the lipophilicity (Hossain, *et al.*, 2020) of the compound to target mitochondria of cancer cells. However, KA11 (AQ-TPP-CIPRO-DCA) did not show good cytotoxic activity against cancer cells which indicates that conjugation of DCA-moiety at N4-piperaziny ring may have decreased its bioavailability due to decreased overall aqueous solubility.

## 2.6) Conclusion

Repositioning of CIPRO to exhibit anticancer and antimicrobial property following biologically oriented drug delivery system is the main purpose of this research project. CIPRO has the potential to inhibit bacterial growth (Koga *et al.*, 1980) and to damage cancer cells (Wagai and Tawari 1991). Incidence of multi-drug resistance (MDR) has increased the uptake of drugs from cancer cells leading to unsuccessful management of chemotherapy practices. It has been essential to promote the need of biologically oriented drug delivery system to target cancer cells overcoming MDR. Emergence of bacteria is also a leading problem in chemotherapy as they increase the resistance of cancer cells to chemotherapeutic drugs through several mechanisms. The basic aim is to design and develop a chemical hybrid to target cancer and bacterial cells evading the incidence of MDR.

Physical and chemical properties (Gootz *et al.*, 1994) of CIPRO has made it a unique element for chemical modification following biophysical drug delivery system. Targeting mitochondria of cancer cells is a promising approach but high mitochondrial potential of cancer cells effects upon accumulation of drugs in cancer cells (Smith *et al.*, 1999). The delocalized positive charge of TPP<sup>+</sup>-cation makes it hydrophobic to freely pass through the phospholipid layers of plasma membrane without the need of special uptake mechanism (Reily, *et al.*, 2013).

Following the above therapeutic approach, hybrids of CIPRO derivatives and anthraquinone derivatives were successfully synthesized and characterized. Some of the novel compounds were evaluated for their anticancer and antibacterial potential. *In-vitro* assay of antibacterial activity was investigated on resistant and sensitive strains of Gram-positive and Gram-negative bacteria. The result of antibacterial assay has shown that KA10 has high potential to inhibit the growth of both Gram-positive and Gram-negative bacteria in cancer cells probably due to the formation of salt-based CIPRO moiety.

## Chapter 3

### Experimental

#### 3.1) General analytical techniques

##### 3.1.1) Thin-layer chromatography (TLC)

The progress of chemical reactions was monitored by thin-layer chromatography (TLC), preceded by a mini-solvent extraction with dichloromethane (DCM) and water (H<sub>2</sub>O) (1:1), where necessary. TLC was performed on pre-coated TLC plates with Kieselgel 60 F<sub>254</sub> aluminium sheets (Merck). Most of the compounds absorbed in the visible region, however some of compounds were visualised through a UV-light (254 nm and 365 nm) detector.

##### 3.1.2) Silica gel column chromatography

Synthesized compounds were purified, using Kieselgel 60 F<sub>254</sub> silica gel, mesh size 0.063-0.200 mm (Merck).

##### 3.1.3) Liquid-liquid extraction

The reaction mixture was equally partitioned between chloroform or dichloromethane and water (1:1; typically, 5 to 100 ml total volume). The organic layer was washed with water three times (3 × 100 ml), filtered and evaporated.

##### 3.1.4) Mass spectrometry

This was carried out by the EPSRC National Mass Spectrometry Service, Swansea University in the laboratory of the National Mass Spectrometry Facility (NMSF). Electrospray ionisation (ESI) was the preferred method and performed on an Orbitrap XL or Xevo G2S instrument. Orbitrap XL is a high-resolution instrument used to provide accurate mass measurement over the full mass range ( $m/z$  2000) in electrospray or in atmospheric pressure chemical ionisation (APCI). Orbitrap XL is

provided through Thermo Scientific with a mass accuracy <3 ppm RMS with external calibration and <2 ppm RMS with internal calibration.

### 3.1.5) Nuclear magnetic resonance (NMR) (<sup>1</sup>H)

<sup>1</sup>H NMR Spectra were recorded on a Bruker AC300 NMR spectrometer at 300.1 MHz, from samples dissolved either in deuterated DMSO or deuterated chloroform.

### 3.2) Synthesis of anthraquinone-DCA conjugate (target KA3)

#### 3.2.1) Synthesis of AQ-PIP-BOC (KA1)

2-Chloroanthracene-9,10-dione (1 g, 4.12 mmol) and 1-*tert* butyloxycarbonyl-piperazine (5.37 g, 28.8 mmol) were dissolved in DMSO (6.625 g, 76 mmol) (dropwise addition), followed by the addition of N, N diisopropylethylamine (DIPEA; 0.789 ml, 0.45 mmol) and then heated on a water bath at 40°C for 7 h. The progress of the chemical reaction was monitored by TLC every 30 min.

The heated chemical reaction was cooled down and then extracted using dichloromethane and water. Silica gel column (25 ×100 mm) chromatography was performed using the solvent system of dichloromethane: ethyl acetate (9: 1) to get the purified form of KA1 [4-(9, 10-dioxo-9, 10-dihydro-anthracen-2-yl)-piperazine-1-carboxylic acid *tert*-butyl ester]. The collected fractions of column chromatography containing the purified product KA1 (analysed by TLC) were combined together, filtered through Whatman filter paper and then evaporated using a rotary evaporator. The orange precipitate of KA1 formed by the addition of diethyl ether (≥ 5ml) was filtered and stored at room temperature. (Yield; 0.34 g, 34%)

TLC (dichloromethane: ethyl acetate ; 9 :1), R<sub>f</sub> 0.46. (Orange) AQ-PIP-BOC (KA1)  
HRMS (ESI) (+) m/z: 293.1281 (4%) [M + Na]<sup>+</sup>, 393.1805 (100%) [M + H]<sup>+</sup>. Calcd for [C<sub>23</sub>H<sub>24</sub>N<sub>2</sub>O<sub>4</sub>]<sup>+</sup>, 393.1805; Found 392.44766.

$^1\text{H}$  NMR ( $\text{CDCl}_3$ , 300 MHz):  $\delta$  (ppm) 1.52 [s, 9H,  $3 \times \text{CH}_3$  ('Boc)]; 3.52 (m, 4H,  $2 \times \text{CH}_2\text{-N}$ ); 3.62 (m, 4H,  $2 \times \text{CH}_2\text{-N}$ ); 7.18 (d, 1H, H-3); 7.65 (s, 1H, H-1); 7.76 (m, 2H, H-6 and H-7); 8.22 (d, 1H, H-4); 8.28 (m, 2H, H-5 and H-8).

### 3.2.2) Synthesis of AQ-PIP-TFA (KA2)

KA1 [4-(9, 10-dioxo-9, 10-dihydro-anthracen-2-yl)-piperazine-1-carboxylic acid *tert*-butyl ester; 0.1243 g, 0.313 mmol] was dissolved in TFA (4 ml) for 30 min at room temperature. The mixture was dried using a rotary evaporator and solidified into an orange precipitate of KA2 through the addition of diethyl ether ( $\leq 5$  ml). The solid was filtered and stored at room temperature (Yield; 0.0001615 g, 47.5%).

TLC (dichloromethane: ethyl acetate ; 9 :1),  $R_f$  0. (Orange) AQ-PIP<sup>+</sup> (KA2).

HRMS (ESI) (+)  $m/z$ : 327.0888 (3%)  $[\text{M} + \text{Na}]^+$ , 293.1282 (100%)  $[\text{M} + \text{H}]^+$ . Calcd for  $[\text{C}_{18}\text{H}_{17}\text{N}_2\text{O}_2]$  293.3392314 Da; Found 293.1282.

### 3.2.3) Synthesis of AQ-PIP-DCA(KA3)

DCA anhydride (0.078 ml, 0.55 mmol) was pipetted dropwise to a solution of KA2 (2-piperidin-1-yl-anthraquinone; 0.0691 g, 0.169 mmol) and potassium carbonate ( $\text{K}_2\text{CO}_3$ ; 0.23 g, 0.166 mmol) in dichloromethane (10 ml) followed by continuous stirring for 2 h. The reaction progress was monitored by TLC every 30 min.

The reaction was extracted through liquid-liquid extraction with dichloromethane: water (1:1), and then dried and further purified through silica gel column (25  $\times$  100 mm) chromatography using the solvent system of dichloromethane: ethyl acetate (9:1). The fractions (monitored by TLC) containing purified KA3 (AQ-PIP-DCA) were combined and evaporated using a rotary evaporator. The purified and solid form of KA3 was precipitated through the addition of diethyl ether. Solid KA3 was stored at an ambient temperature. (Yield; 0.1 g)

TLC (dichloromethane: ethyl acetate, 9:1):  $R_f$  0.70 (Orange), AQ-PIP-DCA (KA3).

HRMS (ESI) (+)  $m/z$ : 490.9634 (6%)  $[\text{M} + \text{Na}]^+$ , 403.0611 (100%)  $[\text{M} + \text{H}]^+$ . Calcd for  $[\text{C}_{20}\text{H}_{17}\text{Cl}_2\text{N}_2\text{O}_3]^+$ , 402; Found 403.0611.

$^1\text{H}$  NMR ( $\text{DMSO-}d_6$ , 300 MHz):  $\delta$  (ppm) 3.56-3.84 (m, unresolved, 8H, 4  $\times$   $\text{CH}_2\text{-N}$ ); 7.31 [s, 1H, H-(Cl) $_2$ ]; 7.39 (d, 1H, H-3); 7.51 (s, 1H, H-1); 7.87 (m, 2H, H-6 and H-7); 8.02 (d, 1H, H-4); 8.18 (m, 2H, H-5 and H-8).

### **3.3) Synthesis of anthraquinone hybrid TPP<sup>+</sup>, ciprofloxacin and DCA conjugates**

#### **3.3.1) Synthesis of AQ-PIP-Lys (BOC)-Fmoc (KA4)**

Fmoc-Lys (BOC)-OH (1.79 g, 3.8 mmol) and HATU (1.56 g, 4.1 mmol) were dissolved in DMF (5 ml), followed by the addition of DIPEA (1.907 ml, 6.3 mmol) and left at an ambient temperature for 15 min, and then added to a solution of AQ-PIP(2 piperazin-1-yl-anthraquinone) (0.8 g, 2.7 mmol) in DMF (6 ml) followed by continuous stirring at rt for 2h and kept overnight.

The resultant product KA4 was purified by silica gel column (10  $\times$  200mm) chromatography with the solvent system of chloroform: methanol (4:1). The purified and collected fractions of KA4 (analysed by TLC) were combined, filtered and evaporated using rotary evaporator. The purified and solid form of KA4 was precipitated at the end by the addition of diethyl ether (< 5mL) and filtered. The end product KA4 was stored at rt. (Yield; 1.00 g)

TLC (chloroform : methanol, 4 :1):  $R_f$  0.70. (Red) AQ-PIP- Lys (BOC)-Fmoc (KA4)  
HRMS (ESI) (+)  $m/z$ : 679.0150 (4%)  $[\text{M} + \text{Na}]^+$ , 743.3451 (100%)  $[\text{M} + \text{H}]^+$ .  
Calcd for  $[\text{C}_{44}\text{H}_{47}\text{N}_4\text{O}_7]^+$ , 742.85864; Found 743.3451.

$^1\text{H}$  NMR ( $\text{CDCl}_3$ , 300 MHz):  $\delta$  (ppm) 1.38-1.80 (m, unresolved, 15H, 3 $\times$   $\text{CH}_3$  ( $^t\text{Boc}$ ),  $\beta\text{-CH}_2$ ,  $\gamma\text{-CH}_2$  and  $\delta\text{-CH}_2$ ); 3.22 (m, 2H,  $\epsilon\text{-CH}_2$ ); 3.55 (m, 4H, 2  $\times$   $\text{CH}_2\text{-N}$ ); 3.70-3.98 (m, unresolved 4H, 2  $\times$   $\text{CH}_2\text{-N}$ ); 4.25 (m, 1H,  $\alpha\text{-CH}$ ); 4.42 (d, 2H,  $\text{CH}_2\text{-Fmoc}$ ); 4.62 (t, 1H,  $\text{CH-Fmoc}$ ); 4.75 (1H, t,  $\text{NHCO-Boc}$ ); 5.75 (1H, d,  $\text{NHCO-Fmoc}$ ); 7.18 (d, 1H, H-3); 7.25-7.52 (m, unresolved, 4H, 4  $\times$   $\text{CH}_{\text{Ar-Fmoc}}$ ); 7.55 (d, 2H, 2  $\times$   $\text{CH}_{\text{Ar-Fmoc}}$ ); 7.62 (s, 1H, H-1); 7.78 [4H, m, (H-6, H-7)-AQ, 2  $\times$   $\text{CH}_{\text{Ar-Fmoc}}$ ]; 8.24 (d, 1H, H-4); 8.30 [2H, m, (H-5 and H-8)-AQ].

### 3.3.2) Synthesis of AQ-PIP- Lys-BOC (KA5)

KA4 (0.6 g, 0.8 mmol) was dissolved in 20% piperidine (3 ml) for 30 min at room temperature. The reaction progress was monitored by TLC. The reaction mixture was extracted by solvent extraction using dichloromethane and water (1:1).

The product KA5 was purified by silica gel column (25 × 100 mm) chromatography with the solvent systems of chloroform: methanol 9:1 and 4:1 respectively. The fractions containing KA5 (analysed by TLC) were combined, filtered and evaporated using a rotary evaporator. KA5 was precipitated by the addition of diethyl ether ( $\leq$  5ml), filtered and stored at room temperature (Yield; 0.36 g, 60%).

TLC (chloroform: methanol ; 4:1):  $R_f$  0.54. (Red), AQ-PIP- Lys-Boc (KA5). HRMS (ESI) (+)  $m/z$ : 555.2357 (37%)  $[M + Na]^+$ , 521.2753 (100%)  $[M + H]^+$ . Calcd for  $[C_{29}H_{36}N_4O_5]$ , 520.61994; Found 521.2753.

$^1H$  NMR ( $CDCl_3$ , 300 MHz):  $\delta$  (ppm) 1.40-1.72 (m, unresolved, 15H, 3×  $CH_3$  ('Boc),  $\beta$ - $CH_2$ ,  $\gamma$ - $CH_2$  and  $\delta$ - $CH_2$ ); 2.00 (m, 2H,  $NH_2$ ); 3.15 (t, 2H,  $\epsilon$ - $CH_2$ ); 3.52 (m, 4H, 2 ×  $CH_2$ -N); 3.60-3.88 (m, unresolved 4H, 2 ×  $CH_2$ -N); 4.62 (m, 1H,  $\alpha$ - $CH$ ); 7.17 (1H, d, H-3); 7.65 (s, 1H, H-1); 7.74 (2H, m, H-6 and H-7); 8.20 (d, 2H, H-4) 8.28 (m, 2H, H-5 and H-8).

### 3.3.3) Synthesis of AQ-PIP-Lys(BOC)-TPP (KA6)

TPP (0.2984 g, 0.67 mmol), HOBT (0.091 g, 0.67 mmol) and PYBOP (0.35 g, 0.67 mmol) were dissolved in DMF (3 ml), followed by the addition of DIPEA (0.352 ml) for 15 min at room temperature and then added to a solution of KA5 (0.3 g, 0.56 mmol) in DMF (3 ml) for 1 h. The progress of the chemical reaction was monitored by TLC after 30 min.

The reaction was extracted through liquid-liquid extraction and purified through silica gel column (25 × 100 mm) chromatography using chloroform: methanol (4:1) solvent system where pure fractions were combined (analysed through TLC), filtered and evaporated using rotary evaporator. The precipitate of KA6 was formed by the addition of diethyl ether ( $\leq$  5 ml) and filtered. (Yield; 0.19 g, 63%).

TLC (Chloroform : Methanol, 4:1),  $R_f$  0.46. (Red) AQ-PIP-Lys (BOC)-TPP (KA6).  
HRMS (ESI) (+)  $m/z$ : 868.4168 (5%)  $[M + Na]^+$ , 865.4088 (100%)  $[M + H]^+$ . Calcd for  $[C_{52}H_{58}O_6N_4 P]$ , 866.0133334; Found 865.4088.

#### **3.3.4) Synthesis of AQ-PIP-Lys (TFA)-TPP (KA7)**

KA6 (0.1 g, 5.6 mmol) was dissolved in TFA ( $\leq 5$  ml) for 30 min at room temperature. The progress of chemical reaction was monitored by TLC. The reaction mixture was evaporated using rotary evaporator. The precipitate of KA7 was formed by the addition of diethyl ether ( $\leq 5$  ml) and filtered and stored at 4°C (Yield; 0.09 g, 100%).

TLC (chloroform : methanol, 4:1),  $R_f$  0.3. (Red) AQ-PIP-Lys (TFA)-TPP (KA7).  
HRMS (ESI) (+)  $m/z$ : 867.3261 (10%)  $[M + Na]^+$ , 765.3567 (100%)  $[M + H]^+$ . Calcd for  $[C_{49}H_{50}N_4O_6F_3P]^+$  880.9282544; Found 765.3567.

#### **3.3.5) Synthesis of CIPRO-BOC (KA8)**

Ciprofloxacin (0.5 g, 1.5 mmol) and sodium bicarbonate (0.126 g, 1.5 mmol) were dissolved in 5-10 ml of THF: H<sub>2</sub>O (1:1) for 30 min and then cooled to 5 °C. Di-*tert*-butyl di-carbonate (0.3274 g, 1.5 mmol) was added dropwise over 10 min to the cold mixture of CIPRO. The progress of the chemical reaction was monitored by TLC. The precipitate of KA8 was formed by the addition of ice-cold water (>10 ml) and filtered. The white precipitates of KA8 were washed with water and dried (Yield; 0.4 g, 80%).

TLC (Chloroform : Methanol, 9:1),  $R_f$  0.75 (white) CIPRO-BOC, (KA8). HRMS (ESI) (+)  $m/z$ : 476.1844 (10%)  $[M + Na]^+$ , 430.1788 (100%)  $[M + H]^+$ . Calcd for  $[C_{22}H_{26}FN_3O_5]^+$  431.4573432; Found 430.1788.



### 3.3.6) Synthesis of AQ-TPP-CIPRO-BOC (KA9)

KA8 (0.066 g, 0.147 mmol) was dissolved in dichloromethane (10 ml) followed by the addition of PYBOP (0.09 g), HOBt (0.025 g) and DIPEA (127  $\mu$ l) for 15 min. The solution of KA8 was added to the solution of KA7 (0.13 g, 0.147 mmol) in dichloromethane (10ml) and reacted for 1 h. The progress of chemical reaction was monitored by TLC.

The reaction mixture was extracted through solvent extraction using dichloromethane and water (1:1). The end product KA9 was purified by Kieselgel 60 F<sub>254</sub> silica gel column (10  $\times$  200mm) chromatography using the solvent system of dichloromethane: methanol (9:1). Pure fractions (monitored by TLC) were combined, filtered and evaporated using a rotary evaporator. The precipitates of KA9 were formed by the addition of diethyl ether and filtered. KA9 was stored at room temperature (Yield; 0.1 g, 99%).

TLC (chloroform : methanol, 4 :1), R<sub>f</sub> 0.46. (Red) AQ-TPP-CIPRO-BOC (KA9).  
HRMS (ESI) (+) m/z: 1181.5367 (10%) [M + Na]<sup>+</sup>, 1178.5287 (100%) [M + H]<sup>+</sup>.  
Calculated for [C<sub>71</sub>H<sub>74</sub>N<sub>7</sub>O<sub>10</sub>F<sub>4</sub>P]<sup>+</sup>, 1179.3395766; Found 1178.5287.

### 3.3.7) Synthesis of AQ-TPP-CIPRO-TFA (KA10)

KA9 (0.17 g, 0.009 mmol) was dissolved in TFA (3-4 ml) for 30 min. The progress of chemical reaction was monitored by TLC. The precipitate of KA10 was formed by the addition of diethyl ether ( $\leq$  5ml) and filtered. KA10 was stored at 4°C (Yield; 0.16 g, 99%).

TLC (Chloroform : Methanol, 9 :1), R<sub>f</sub> 0.14 (Red), AQ-TPP-CIPRO-TFA (KA10).  
HRMS (ESI) (+) m/z: 1080.4831 (10%) [M + Na]<sup>+</sup>, 1078.4791 (100%) [M + H]<sup>+</sup>. Calcd for [C<sub>64</sub>H<sub>66</sub>F<sub>1</sub>N<sub>7</sub>O<sub>6</sub>P]<sup>+</sup> 1194.2544976; Found 1078.4791.

### 3.3.8) Synthesis of AQ-TPP-CIPRO-DCA (KA11)

DCA anhydride (0.007 ml) was dissolved (dropwise addition) onto the solution of KA10 (0.0501 g, 0.0414 mmol) and potassium carbonate (0.01 g, 0.414 mmol) in dichloromethane (10 ml, 156 mmol) for 2 h. The progress of the chemical reaction was monitored by TLC.

KA11 was purified by silica gel column (25 × 100 mm) chromatography using the solvent systems dichloromethane: methanol 9:1 and 4:1. The pure fractions of KA11 (monitored by TLC) were combined, filtered and dried using a rotary evaporator. The precipitate of compound KA11 was formed by the addition of diethyl ether ( $\leq$  5ml), filtered and stored at room temperature (Yield; 0.05 g).

TLC (Chloroform : Methanol, 4 :1),  $R_f$  0.66 (Orange/Brown), AQ-TPP-CIPRO-DCA (KA11). HRMS (ESI) (+)  $m/z$ : 1098.9559 (5%)  $[M + Na]^+$ , 1188.4117 (100%)  $[M + H]^+$ . Calcd for  $[C_{66}H_{66}Cl_2FN_7O_7P]^+$  1190.1505566; Found 1188.4117.

### 3.4) In-vitro biological assays

*In-vitro* assays were used to screen the biological activities (anticancer and antibacterial) of the novel synthesized compounds. These assays were performed on 96-well microtiter plates to calculate the minimum inhibitory concentration (MIC) and minimum bactericidal activity (MBC) (Baltzar and Baltzar, 2017) on two different strains of bacteria (*S. aureus*, *E. coli*) including their susceptible and resistant strains and to analyse the cytotoxic activity (Van Meerloo, Kaspers and Cloos, 2011) on colon cancer cell lines (HCT-15) with a comparative drug SH1 through a microplate absorbance reader (SUNRISE).

### **3.4.1) Antibacterial assay**

#### **3.4.1.01) Measurement of minimum inhibitory concentrations (MIC) and minimum bactericidal concentration (MBC)**

##### **i) Drugs**

Four synthesized derivatives (KA3, KA7, KA10 and KA11) were investigated for antibacterial activity against sensitive and resistant strains of Gram-positive (*S. aureus*) and Gram negative (*E. coli*) bacteria.

The stock solution of each hybrid was prepared in DMSO with (10mg/ml or 1mg/ml). From the stock solution 512mg/L concentration of each drug was prepared by the addition of 512  $\mu$ L of stock solution to 9.9 ml of distilled water.

##### **ii) Material for MIC and MBC**

Muller-Hinton Broth (MHB) and Muller-Hinton Agar (MH-Agar) were prepared by mixing them with distilled water to 500 ml and then autoclaved at 121°C for 30 min, round bottom uncoated microtiter trays, universal bottles were filled with 10 ml of sterilized Muller-Hinton Broth, round shaped colony forming units which were coated with sterilized Muller-Hinton Agar.

##### **iii) Bacterial isolates**

Bacterial cultures of *S. aureus* and *E. coli* bacteria were prepared and stored through Microbank™ at -70°C. Both susceptible and resistant strains were streaked onto MH-agar plates and incubated at 37°C for 18-24 h.

Overnight broth culture was prepared by adding three to five morphologically similar colonies of each strain into 10 ml MHB respectively and incubated at 37°C for 18-24 h. 10  $\mu$ l of overnight broth culture was added into 10 ml of MHB to measure OD450 through a JENWAY 7300 Spectrophotometer.

##### **iv) MIC assay**

50  $\mu$ l of MHB was pipetted into 2-11 lanes of round bottom microtiter plate while 12<sup>th</sup> lane (positive control) was filled with 100  $\mu$ l of MHB. 100  $\mu$ l of prepared drug concentration (512 mg/L) was pipetted onto lane 1 of microtiter plate.

50 µl of synthesized drug was withdrawn from each well of lane, 1 and added into corresponding wells of lane 2. The sample material in all wells of lane 2 was mixed by pipetting up and down 4-6 times and then pipetted 50 µl of each well of lane 2 into corresponding wells of lane 3. The same step was repeated till lane 10 of each well of microtiter plate, however 50 µl solution from lane 10 of each well was discarded at the end.

The next most important step was the addition of bacteria whereas 50 µl of diluted bacterial suspensions of both sensitive and resistant strains were carefully pipetted onto lane 1 to 11 (negative control) as sensitive strain onto A, B & C wells while resistant strain onto E, F, & G wells and then incubated the plate at 37°C for 18-24 h.

#### **v) Plate spreading method**

The exponential growth of bacteria was determined by diluting ( $10^3$ ,  $10^2$ ,  $10^1$ ) the growth culture (10 µl) of any well of lane 11 (negative control) before incubation till 10 ml of MHB ( $10^3$ ) and transferring 10 µl to another 10 ml of MHB ( $10^2$ ) and then repeating the same procedure again for  $10^1$  dilution. 100 µl was taken from each diluted fraction and spread onto respectively labelled MH agar plate and incubated at 37°C for 18-24 h.

The number of colonies were calculated with:

$$\text{Colony Forming Unit} \left( \frac{\text{CFU}}{\text{ml}} \right) = \text{Colony Count} \times 10 \text{ (100 } \mu\text{l added to plate)} \times 10^3 \text{ (dilution factor)}$$

#### **vi) MBC assay**

An aliquot (10 µl) from each well showing no growth was removed after overnight incubation and spotted onto MH-agar plate including spots of positive and negative control on plate which were incubated for 18-24 h at 37°C.

### **3.4.2) Antiproliferative assays**

#### **3.4.2.01) Cell culture**

##### **i) Materials of cell culture**

RPML-1640 medium without L-glutamine (R0883-500 ml) was purchased from SIGMA-ALDRICH life sciences, a combined solution of 10,000 units of penicillin/10,000 µg/ml of streptomycin (REF, 15140-122), foetal bovine serum (FBS), 200 mM L-glutamine (REF, 25030-024), 0.5% Trypsin-EDTA (REF-15400-054) were purchased from Gibco by life technologies, Colon cancer cell lines (HCT-15) were obtained from American Type Culture Collection (ATCC), Primovert microscope (Zeiss); Axicam ERC 5s, 1 × Trypsin (prepared by diluting 1: 9 with phosphate buffer saline), 70% ethanol, Phosphate buffer saline (PBS), and nigrosine blue dye.

##### **ii) Cell culture method**

HCT-15 cell lines were grown in a suspension and kept in RPMI-1640 medium which was supplemented with 10% FBS, 1% penicillin/streptomycin and 1% L-glutamine and stored at a spark proof fridge at 4°C.

HCT-15 cell lines were passaged by trypsination and stored in a humidified incubator at 37°C with 95% air and 5% CO<sub>2</sub>. The cell lines were regularly examined through Primovert light microscope, Axicam 5s.

##### **iii) Growth curves**

HCT-15 cells were recovered from culture and washed with PBS. The cells were counted and seeded at a density of  $1 \times 10^4$  cells/ml in complete 20 ml RPMI-1640 medium which was incubated (5% CO<sub>2</sub>) at 37°C. The growth of cells was regularly monitored with 7-8 day period, counting the number of cells through a haemocytometer.

### **3.4.2.02) Micro-culture tetrazolium assay (MTT)**

#### **i) Drugs**

The novel synthetic intracellularly targeted anticancer agents KA3, KA7, KA10 and KA11 and control compound SH1 were selected to determine their cytotoxic activity.

Stock solution (10 mg/ml or 1 mg/ml) was prepared by the dissolution of all drugs in 10% DMSO. Dilutions were made from each stock solution to get 100  $\mu$ M and 1000  $\mu$ M solutions.

#### **ii) Materials for MTT assay**

DMSO (Fluka), Nigrosine, MTT (3-(4, 5-dimethylthiazole-2-yl)-2, 5-diphenyltetrazoliumbromide), phosphate buffered saline (PBS), A SUNRISE microplate absorbance reader (TECAN).

#### **iii) Pre-treatment phase (Day 1)**

Exponentially growing cells of HCT-15 were washed with PBS, counted and then diluted to get a suspension with a density of  $1 \times 10^4$  cells/ml. 150  $\mu$ l of cells suspension was pipetted into each well of 96-well microtiter plates from lanes 1-12 lanes (except 1<sup>st</sup> three well of lane 1). The blank wells of lane 1 contained medium only. The plates were incubated at 37°C, 5% CO<sub>2</sub> overnight which had allowed the cells to recover before treatment with compounds.

#### **iv) Treatment Phase (Day 2)**

The stock solution of tested drug samples and SH1 were made up at a concentration of 10mg/ml in DMSO and then diluted these down to 1mM in distilled water with a serial dilution of 1:10 with cell culture medium to get five treatment concentrations 400  $\mu$ M, 40  $\mu$ M, 4  $\mu$ M, 0.4  $\mu$ M, 0.04  $\mu$ M of each sample were prepared.

50  $\mu$ l of each treatment concentrations were added to the corresponding wells of lanes 1-12 (used in triplicates). The concentration of drug samples in the wells had been down to 100  $\mu$ M, 10  $\mu$ M, 1  $\mu$ M, 0.1  $\mu$ M, 0.01  $\mu$ M and the microtiter plates were placed into an incubator at 37°C for 1-3 days.

To keep the balance in each well, 50 µl of medium was added to lane 1-3 (triplicates) which were blank, positive control and to lane 10-12 (column A) which was a negative control.

#### **v) MTT Phase (Day 5)**

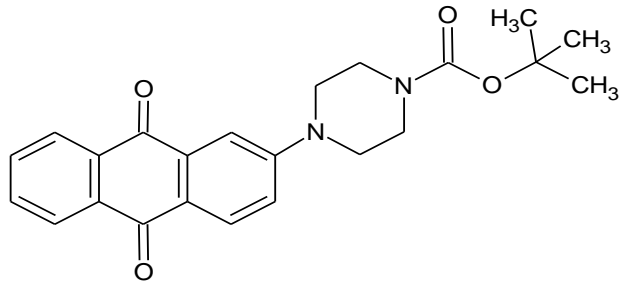
Following the incubation for 96 h, the plate was removed from the incubator and checked the progress of adherent cells. 50 µl of Triton (0.5% in PBS) was added to negative control wells and incubated the plate for 3-5 min at 37°C, 5% CO<sub>2</sub>. All in-use medium was carefully removed from the plate and replaced it with 70 µl of fresh medium.

MTT solution (2 ml of 5 mg/ml MTT in 1 × sterile PBS) was prepared by weighing a minimum of 10 mg of MTT into a sterile bijou and adding 2 ml of PBS. 2 ml of 5mg/ml MTT solution was filtered and added into 5 ml of medium (approx. 1.4 mg/ml useable MTT solution at this point). 50 µl of this solution was added into each well of 96 well plates (approx. 0.5 mg/ml in each well). At this stage, the plate was wrapped in tin foil and incubated at 37°C, 5% CO<sub>2</sub> for 3-4 h.

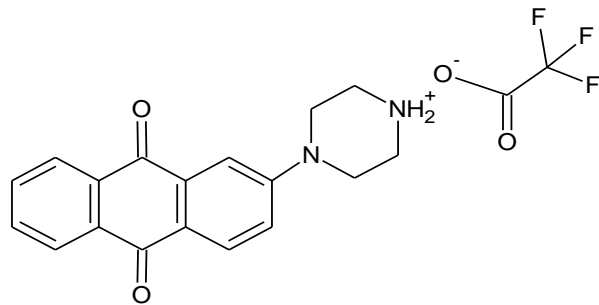
After the incubation period, the plate was carefully removed from the incubator and the medium was replaced with 150 µl of DMSO (mixed it vigorously). The plate was wrapped again with foil and left to settle in a dark place for 30 min.

At the end stage, plate was read at 550 nm through SUNRISE microplate absorbance reader with a reference wavelength of 630 nm. Absorbance values were corrected against absorbance levels of positive, negative control and the IC<sub>50</sub> which was defined as the concentration of drug that would reduce the absorbance to 50% compared with untreated (blank) control cells.

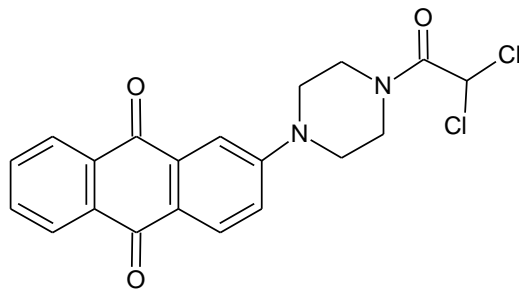
## Structure Library



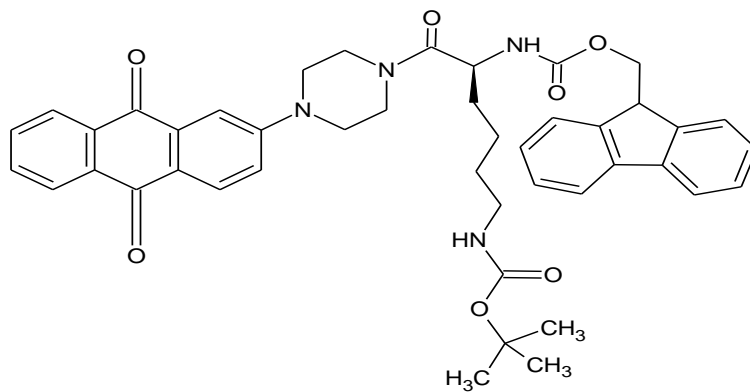
**AQ-PIP-BOC (KA1)**



**AQ-PIP-TFA (KA2)**

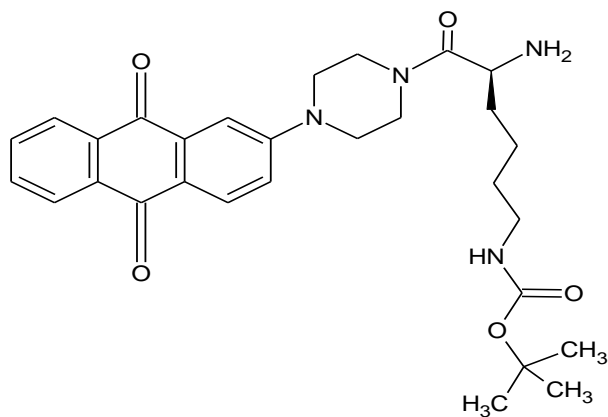


**AQ-PIP-DCA (KA3)**

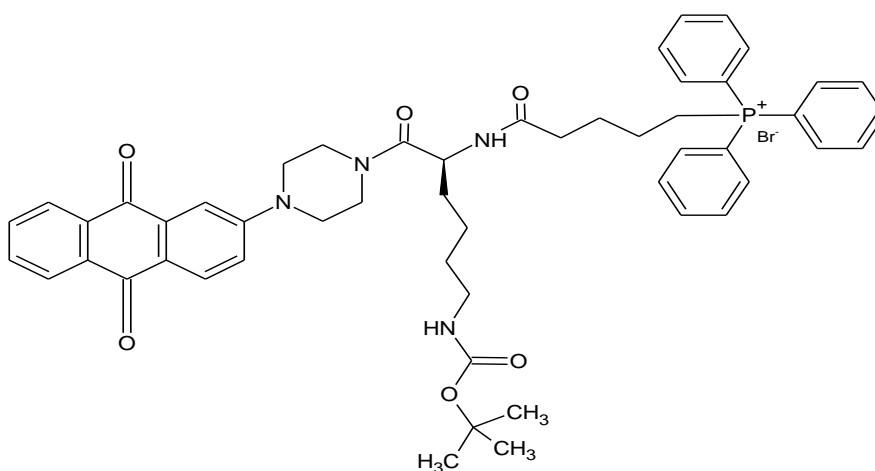


**AQ-PIP-Lys (BOC)-Fmoc (KA4)**

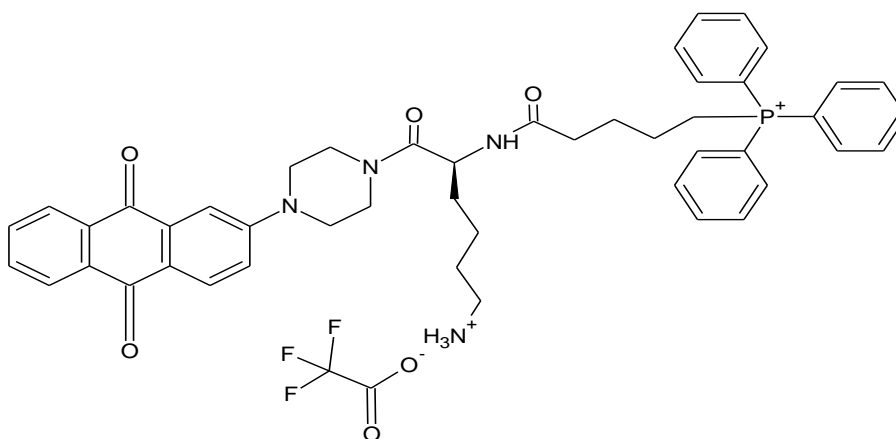




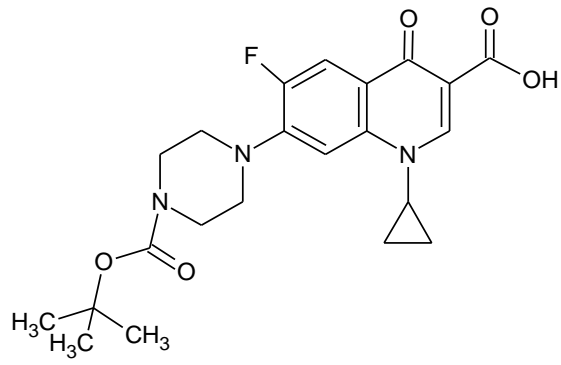
**AQ-PIP-Lys (BOC) (KA5)**



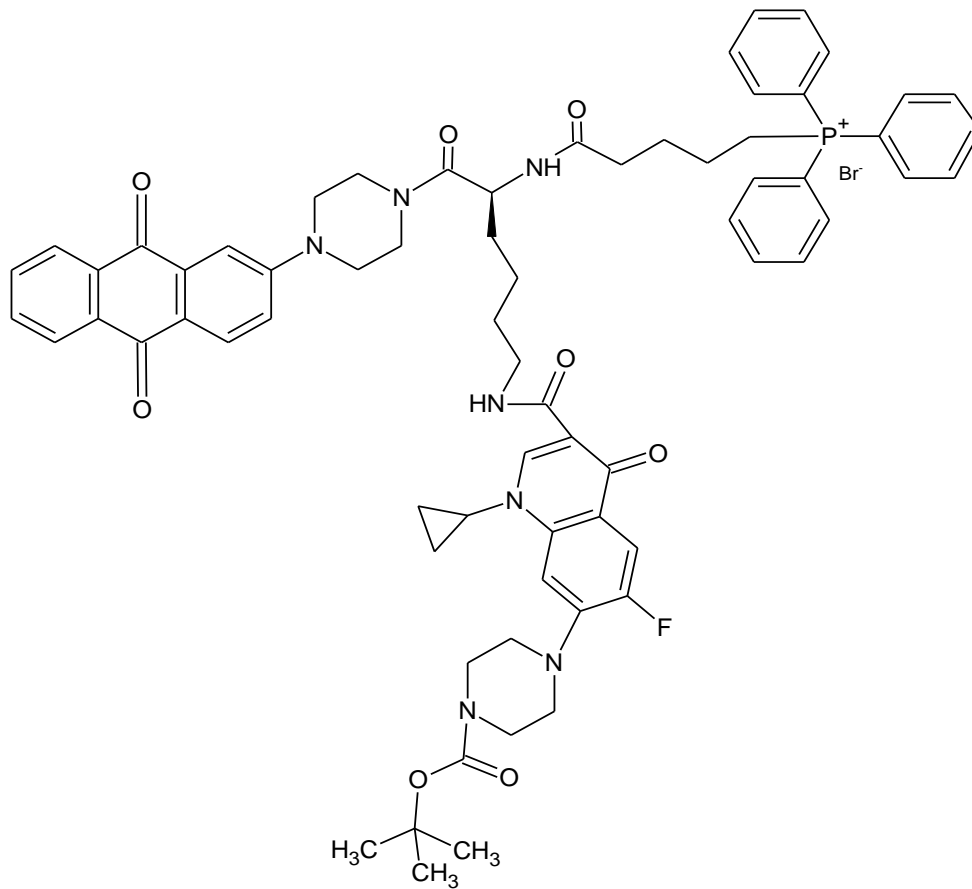
**AQ-PIP-Lys (BOC)-TPP (KA6)**



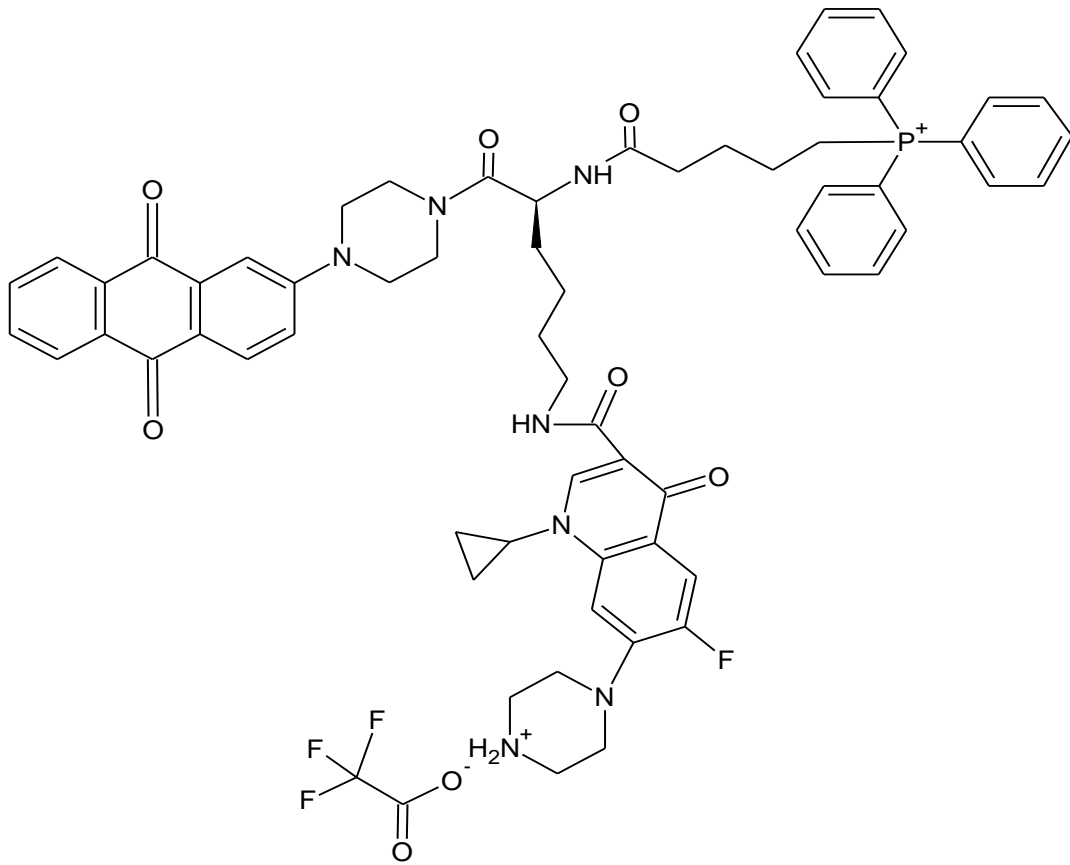
**AQ-PIP-Lys (TFA)-TPP (KA7)**



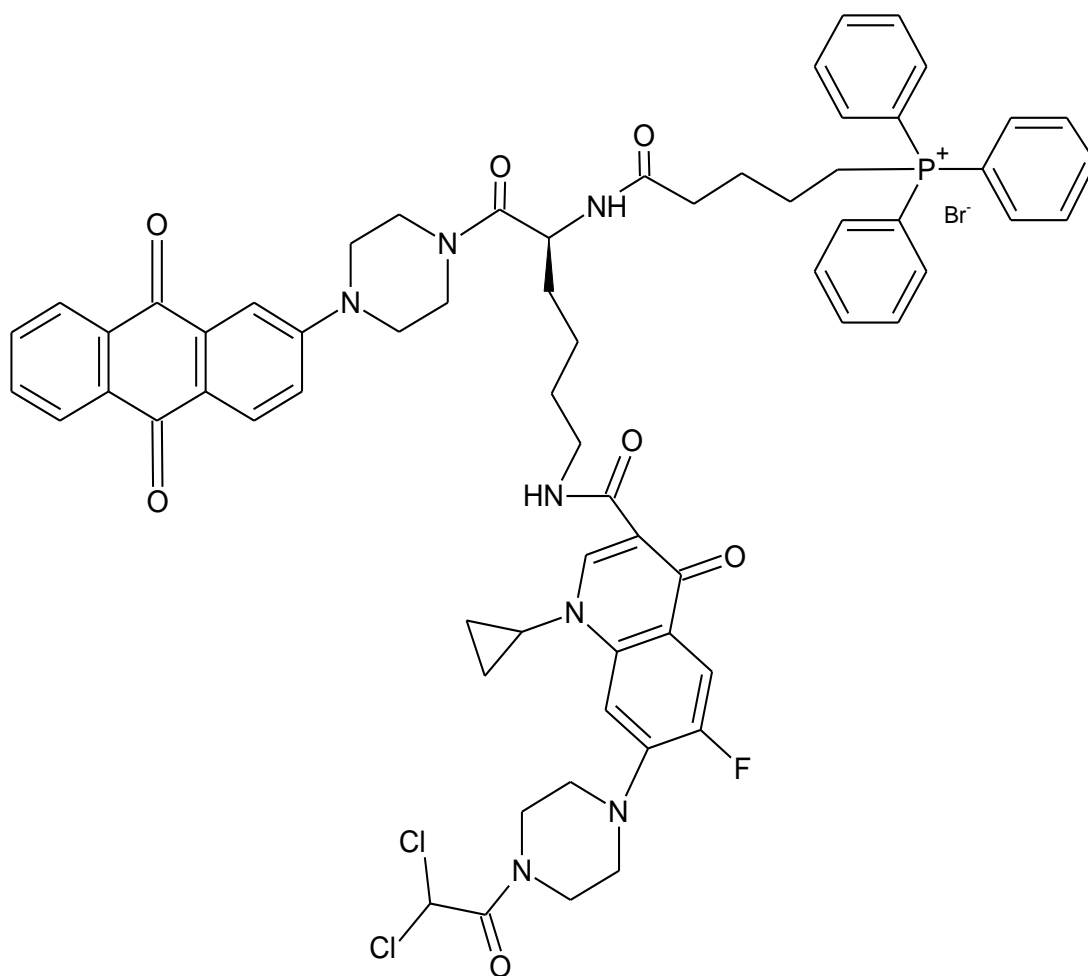
**CIPRO-BOC (KA8)**



**AQ-TPP-CIPRO-BOC (KA9)**



**AQ-TPP-CIPRO-TFA (KA10)**



**AQ-TPP-CIPRO-DCA (KA11)**

## References

**Ahadi**, H., Shokrzadeh, M., Khah, H. Z., Barghi, G. N., Ghasemian, M., Emadi, E., Zargari, M., Asl, R. N., Emami, S. (2020) 'Synthesis and biological assessment of ciprofloxacin-derived 1,3,4-thiadiazoles as anticancer agents', *Bioorganic Chemistry* [Online], **23**, pp. 1-9, Available at: <https://doi.org/10.1016/j.bioorg.2020.104383> [accessed 27 Oct 2021].

**Anderson**, S., Bankier, A. T., Barrell, B. G., de Bruijn, M. H. L., Coulson, A. R., Drouin, J., Eperon, I. C., Nierlich, P. D., Roe, A. B., Sanger, F., Schreier, P. H., Smith, A. J. H., Staden, R., and Young, I. G. (1981) 'Sequence and organization of the human mitochondrial genome', *Nature* [Online], **290(5806)**, pp. 457–465. Available at: <https://doi.org/10.1038/290457a0> [accessed 22 Nov 2022].

**Arora**, P. J., and Jain, R. K. (2012) 'Biotransformation of 4-chloro-2-nitrophenol into 5-chloro-2-methylbenzoxazole by a marine *Bacillus* sp. strain MW-1' *Biodegradation* [Online], **23**, pp. 325-331, Available from: DOI 10.1007/s10532-011-9512-y [accessed 2 Dec 2022].

**Arthur**, J. C., Gharaibeh, R. Z., Uronis, M. J., Chanona, E. P., Sha, W., Tomkovich, S., Muhlbaer, M., Fodor, A. A., and Jobin, C. (2013) 'VSL#3 probiotic modifies mucosal microbial composition but does not reduce colitis-associated colorectal cancer', *Scientific Reports* [Online], **3**, pp. 12–14. Available at: <https://doi.org/10.1038/srep02868> [accessed 9 Sep 2022].

**Azéma**, J., Guidetti, B., Dewelle, J., Calve, L. B., Mijatovic, T., Korolyov, A., Vaysse, J., Martino, M. M., Martino, R., and Kiss, R. (2009) '7-((4-Substituted)piperazin-1-yl) derivatives of ciprofloxacin: Synthesis and in vitro biological evaluation as potential antitumor agents', *Bioorganic and Medicinal Chemistry*. Elsevier Ltd, [Online], **17(15)**, pp. 5396–5407. doi: 10.1016/j.bmc.2009.06.053 [accessed 13 Apr 2022].

**Baker**, S. J., Payne, S. J., Rappuoli, R., Gregorio, E. D. (2018) 'Technologies to address antimicrobial resistance', *Proceedings of the National Academy of Sciences of the United States of America* [Online], **115(51)**, pp. 12887–12895. Available at: <https://doi.org/10.1073/pnas.1717160115> [accessed 29 Aug 2022].

**Baldi**, A., Santini, D., Russo, P., Catricala, C., Amantea, A., Picardo, M., Tatangelo, F., Botti, G., Dragonetti, E., Murace, R., Tonini, G., Natali, P. G., Baldi, F., and Paggi, M. G., (2004) 'Analysis of APAF-1 expression in human cutaneous melanoma progression', *Experimental Dermatology* [Online], **13(2)**, pp. 93–97. Available at: <https://doi.org/10.1111/j.0906-6705.2004.00136.x> [accessed 7 Sep 2022].

**Baltzar**, B. K. and Baltzar, B. K (2017) 'Minimal Inhibitory Concentration (MIC) Prepare medium Prepare the bacterial isolates Prepare the bacterial isolates Prepare the ELISA microplate', (Mic), pp. 10–12 [accessed 15 May 2023].

**Baltzer**, K. B. (2017) 'Minimal Inhibitory Concentration (MIC)', *Department of Biochemistry and Molecular Biology, University of Southern Denmark*, [Online], Available at [dx.doi.org/10.17504/protocols.io.gpwbvpe](https://doi.org/10.17504/protocols.io.gpwbvpe) [accessed 09 Jan 2021].

**Bhasin**, D., Etter, P. J., Chettiar, N. S., Mok, M., and Li, K. P. (2013) 'Antiproliferative activities and SAR studies of substituted anthraquinones and 1,4-naphthoquinones', *Bioorganic and Medicinal Chemistry Letters* [Online], **23(24)**, pp. 6864–6867. Available at: <https://doi.org/10.1016/j.bmcl.2013.09.098> [accessed 4 Dec 2022].

**Berghenegouwen**, V. J., Kraneveld, A. D., Rutten, L., Garssen, J., Arjan, P. V. and Hartog, A. (2016) 'Lipoproteins attenuate TLR2 and TLR4 activation by bacteria and bacterial ligands with differences in affinity and kinetics', *BMC Immunology*. *BMC Immunology*, **17(1)**, pp. 1–10. doi: 10.1186/s12865-016-0180-x [accessed 15 Oct 2022].

**Bock**, D. K., Georgia, M., Schoors, S., Kuchnio, A., Wong, W. B., Cantelmo, R. A., Quaegebeur, A., Ghesquiere, B., Cauwenberghs, S., Eelen, G., Phung, K-L., Betz, I., Tembuysen, B., Brepoels, K., Welti, J., Geudens, L., Segura, I., Cruys, B., Bifari, F.,

Decimo, L., Blanco, R., Wyns, S., Vanginderael, J., Rucha, S., Collins, T. R., Munck, S., Daelemans, D., Imamura, H., Devlieger, R., Rider, M., Veldhoven, V. P. P., Scuit, F., Bartrons, R., Hofkens, J., Fraisl, P., Telang, S., TeBerardinis, J. R., Schoonjans, L., Vinciker, S., Chesney, J., Gerhardt, H., Dewerchin, M., and Carmeliet, P. (2013) 'X-Role of PFKFB3-driven glycolysis in vessel sprouting', *Cell* [Online], **154(3)**, Available at: <https://doi.org/10.1016/j.cell.2013.06.037> [accessed 16 Sep 2022].

**Bonnet**, S., Archer, L. S., Turner, A. J., Haromy, A., Beaulieu, C., Thompson, R., Lee, T. C., Lopaschuk, D. G., Puttagunta, L., Bonnet, S., Harry, G., Hashimoto, K., Porter, J. C., Andrade, A. M., Thebaud, B., and Michelakis, D. E. (2007) 'A Mitochondria-K<sup>+</sup> Channel Axis Is Suppressed in Cancer and Its Normalization Promotes Apoptosis and Inhibits Cancer Growth', *Cancer Cell* [Online], **11(1)**, pp. 37–51. Available at: <https://doi.org/10.1016/j.ccr.2006.10.020> [accessed 25 Apr 2022].

**Chan**, K.Y., Zhang, J. and Chang, C.W.T. (2011) 'Mode of action investigation for the antibacterial cationic anthraquinone analogs', *Bioorganic and Medicinal Chemistry Letters* [Online], **21(21)**, pp. 6353–6356. Available at: <https://doi.org/10.1016/j.bmcl.2011.08.107> [accessed 29 Oct 2022].

**Chen**, G., Wang, F., Trachootham, D., and Huang, P. (2010) 'Preferential killing of cancer cells with mitochondrial dysfunction by natural compounds', *Mitochondrion* [Online], **10(6)**, pp. 614–625. Available at: <https://doi.org/10.1016/j.mito.2010.08.001> [accessed 17 Oct 2022].

**Cheng**, G., Zielonka, J., Ouari, O., Lopez, M., McAllister, D., Boyle, K., Barrios, C. S., Weber, J. J., Johnson, D. W., Hardy, M., Dwinell, B. M., and Kalyanaaraman, B. (2016) 'Mitochondria-targeted analogues of metformin exhibit enhanced antiproliferative and radiosensitizing effects in pancreatic cancer cells', *Cancer Research*, [Online], **76(13)**, pp. 3904–3915. doi: 10.1158/0008-5472.CAN-15-2534 [accessed 21 Jan 2023].

**Chrzanowska**, A., Roszkowski, P., Bielenica, A., Olejarz, W., Stepień, K., and Struga, M. (2020) 'Anticancer and antimicrobial effects of novel ciprofloxacin fatty acids conjugates', *European Journal of Medicinal Chemistry*, [Online], **185**, pp. 1-11, Available at: doi: 10.1016/j.ejmech.2019.111810 [accessed 27 Sep 2021].

**Constance**, E. J. and Lim, S. C. (2012) 'Targeting malignant mitochondria with therapeutic peptides' *Therapeutic Delivery* [Online], **3(8)**, pp. 961-979, Available from: <https://www.ncbi.nlm.nih.gov/pmc/articles/PMC3604891/pdf/nihms-436468.pdf> [accessed 1 Dec 2022].

**Croix**, St. B., Rak, W. J., Kapitain, S., Sheehan, C., Graham, H. C., and Kerbel, R. S. (1996) 'Reversal by hyaluronidase of adhesion-dependent multicellular drug resistance in mammary carcinoma cells', *Journal of the National Cancer Institute* [Online], **88(18)**, pp. 1285–1296. Available at: <https://doi.org/10.1093/jnci/88.18.1285> [accessed 7 Sep 2022].

**DiMasi**, J. A., Hansen, R. W. and Grabowski, H. G. (2003) 'The price of innovation: New estimates of drug development costs', *Journal of Health Economics*, [Online], **22(2)**, pp. 151–185. doi: 10.1016/S0167-6296(02)00126-1 [accessed from 18 Jan 2023].

**Dixon**, S.D., Huynh, M. M., TamilSelvam, B., Spiegelman, M. L., Son, B. S., Eshraghi, A., Blanke, R. S., Bradley, A. K. (2015) 'Distinct roles for CdtA and CdtC during intoxication by cytolethal distending toxins', *PLoS ONE* [Online], **10(11)**, pp. 1–16. Available at: <https://doi.org/10.1371/journal.pone.0143977> [accessed 15 Sep 2022].

**Dong**, L.F., Jameson, V. A. J., Tilly, D., Prochazka, L., Rohlena, J., Valis, K., Truksa, J., Zabalova, R., Mahdavian, E., Kluckova, K., Stantic, M., Stursa, J., Freeman, R., Witting, K. P., Norberg, E., Goodwin, J., Salvatore, A. B., Novotna, J., Turanek, J., Ledvina, M., Hozak, P., Zhivotovsky, B., Coster, J. M., Ralph, J. S., Smith, J. A. R., and Neuzil, J. (2013) 'Erratum: Mitochondrial targeting of  $\alpha$ -tocopheryl succinate enhances its pro-apoptotic efficacy: A new paradigm for effective cancer therapy (Free Radical Biology and Medicine 50 (2011) 1546-1555)', *Free Radical Biology*



*and Medicine* [Online], **65**, pp. 895–896. Available at:  
<https://doi.org/10.1016/j.freeradbiomed.2013.08.164> [accessed 18 Oct 2021].

**Du**, B. H., and Showacre, J. L. (1961) 'Selective localization of tetracycline in mitochondria of living cells', *Science* [Online], **133(3447)**, pp. 196-7, Available from <http://www.ncbi.nlm.nih.gov/pubmed/13724526> 6.- [5<sup>th</sup> Jun 2023].

**El-Gogary**, T. M. (2002) 'Molecular complexes of some anthraquinone anti-cancer drugs: experimental and computational study' *Spectrochimica Acta Part A*, [Online], **59**, pp. 1009-1015, Available at: [www.elsevier.com/locate/saa](http://www.elsevier.com/locate/saa) [accessed 02 Oct 2022].

**Eisenberg-Bord**, M. and Schuldiner, M. (2017) 'Mitochatting – If only we could be a fly on the cell wall', *Biochimica et Biophysica Acta - Molecular Cell Research* [Online], **1864(9)**, pp. 1469–1480. Available at:  
<https://doi.org/10.1016/j.bbamcr.2017.04.012> [accessed 22 Sep 2022].

**Fan**, E., Shi, W. and Lowary, T. L. (2007) 'Synthesis of daunorubicin analogues containing truncated aromatic cores and unnatural monosaccharide residues', *Journal of Organic Chemistry*, [Online], **72(8)**, pp. 2917–2928. doi: 10.1021/jo062542q [accessed 12 Apr 2022].

**Ficker**, M., Paolucci, V. and Christensen, J.B. (2017) 'Improved large-scale synthesis and characterization of small and medium generation PAMAM dendrimers', *Canadian Journal of Chemistry* [Online], **95(9)**, pp. 954–964. Available at: <https://doi.org/10.1139/cjc-2017-0108> [accessed 26 Oct 2022].

**Filipa**, M., Antonio, P., and Isabel, S. (2011). Metalloprobes for functional monitoring of tumour multidrug resistance by nuclear imaging, *Dalton Transactions* [Online], **40(20)**, pp. 5377-5393. Available from [https://www.researchgate.net/publication/50305116\\_Metalloprobes\\_for\\_functional\\_monitoring\\_of\\_tumour\\_multidrug\\_resistance\\_by\\_nuclear\\_imaging](https://www.researchgate.net/publication/50305116_Metalloprobes_for_functional_monitoring_of_tumour_multidrug_resistance_by_nuclear_imaging) [accessed 15 May 2021].

**Fotakis**, G. and Timbrell, J. A. (2006) 'In vitro cytotoxicity assays: Comparison of LDH, neutral red, MTT and protein assay in hepatoma cell lines following exposure to cadmium chloride', *Toxicology Letters*, [Online], **160(2)**, pp. 171–177. doi: 10.1016/j.toxlet.2005.07.001 [accessed 3 Feb 2023].

**France**, L. (2019) 'INTERNATIONAL AGENCY FOR RESEARCH ON CANCER IARC Monographs on the Evaluation of Carcinogenic Risks to Humans Report of the Advisory Group to Recommend Priorities for IARC Monographs during 2015 – 2019', (April 2014) [accessed 15 May 2023]

**Frezza**, C., Cipolat, S. and Scorrano, L. (2007) 'Organelle isolation: Functional mitochondria from mouse liver, muscle and cultured fibroblasts', *Nature Protocols* [Online], **2(2)**, pp. 287–295. Available at: <https://doi.org/10.1038/nprot.2006.478> [accessed 1 Oct 2022].

**Fukuda**, I., Keneko, A., Nishiumi, S., Kawase, M., Nishikiori, R., Fujitake, N., and Ashida, H. (2009) 'Structure-activity relationships of anthraquinones on the suppression of DNA-binding activity of the aryl hydrocarbon receptor induced by 2,3,7,8-tetrachlorodibenzo-p-dioxin', *Journal of Bioscience and Bioengineering* [Online], **107(3)**, pp. 296–300. Available at: <https://doi.org/10.1016/j.jbiosc.2008.10.008> [accessed 24 Jan 2020].

**Fuller**, J. C., Burgoyne, N.J. and Jackson, R.M. (2009) 'Predicting druggable binding sites at the protein-protein interface', *Drug Discovery Today* [Online], **14(3–4)**, pp. 155–161. Available at: <https://doi.org/10.1016/j.drudis.2008.10.009> [accessed 18 Oct 2021].

**Ganushchak**, N. I., Pisko, G. T., Buryak, V. S., Kucher, V. I., Nikolaichuk, N. A., Karinkovskaya, R. B., Nevskaya, T. L., and Zaporozhets, V. I. (1971) 'Synthesis and certain biological properties of arylbutenyl derivatives of piperidine', *Pharm. Chem. J.*, [Online], **5**, pp. 520-522, <https://doi.org/10.1007/BF00771655> [accessed 23 Jan 2023].

**Ge, P.** and Russell, R. A. (1997) 'The synthesis of anthraquinone derivatives as potential anticancer agents', *Tetrahedron* [Online], **53(51)**, pp. 17469–17476. Available at: [https://doi.org/10.1016/S0040-4020\(97\)10195-8](https://doi.org/10.1016/S0040-4020(97)10195-8) [accessed 27 Sep 2021].

**Gellert, M.,** Mizuuchi, K., O'Dea\*, H. M., and Nash, A. H. (1976) 'DNA gyrase: an enzyme that introduces superhelical turns into DNA', *Proceedings of the National Academy of Sciences of the United States of America*, [Online], **73(11)**, pp. 3872–3876. Available at: <https://doi.org/10.1073/pnas.73.11.3872> [accessed 27 Oct 2022].

**Gellert, M.,** Mizuuchi, K., Dea, O. H. M., Itoh, T., and Tomizawa, I. J. (1977) 'Nalidixic acid resistance: A second genetic character involved in DNA gyrase activity', *Proceedings of the National Academy of Sciences of the United States of America* [Online], **74(11)**, pp. 4772–4776. Available at: <https://doi.org/10.1073/pnas.74.11.4772> [accessed 27 Oct 2021].

**Geng, F.,** Zhuang, Y., Lu, Z., Zhuang, S., and Pan, Y. (2020) 'Fusobacterium nucleatum Caused DNA Damage and Promoted Cell Proliferation by the Ku70/p53 Pathway in Oral Cancer Cells', *DNA and Cell Biology* [Online], **39(1)**, pp. 144–151. Available at: <https://doi.org/10.1089/dna.2019.5064> [accessed 29 Sep 2022].

**Gewirtz, D. A.** (1999) 'A critical evaluation of the mechanisms of action proposed for the antitumor effects of the anthracycline antibiotics adriamycin and daunorubicin', *Biochemical Pharmacology* [Online], **57(7)**, pp. 727–741. Available at: [https://doi.org/10.1016/S0006-2952\(98\)00307-4](https://doi.org/10.1016/S0006-2952(98)00307-4) [accessed 7 Sep 2022].

**Giaccone, G.,** Larriba, G. L. J., Oosterom, V. T. A., Alfonso, R., Smit, E. F., Martens, M., Peters, J. G., Van-der-vijgh, F. J. W., Smith, R., Averbuch, S., and Fandi, A. (2004) 'Combination therapy with gefitinib, an epidermal growth factor receptor tyrosine kinase inhibitor, gemcitabine and cisplatin in patients with advanced solid tumors', *Annals of Oncology*, [Online], **15(5)**, pp. 831–838. doi: 10.1093/annonc/mdh188 [accessed from 17 Jan 2023].

**Gootz**, T. D., McGuirk, R. P., Moynihan, S. M., Haskell, L. S. (1994) 'Placement of alkyl substituents on the C-7 piperazine ring of fluoroquinolones: Dramatic differential effects on mammalian topoisomerase II and DNA gyrase', *Antimicrobial Agents and Chemotherapy* [Online], **38(1)**, pp. 130–133. Available at: <https://doi.org/10.1128/AAC.38.1.130> [accessed 12 Aug 2022].

**Grant**, C. D. and Blackmore, A. V. (1994) 'Overexpression of Multidrug resistance-associated protein (MRP) increases resistance to natural product drugs', *Australian Journal of Soil Research* [Online], **32(2)**, pp. 357–358. Available at: <https://www.researchgate.net/publication/14922761> [accessed 17 Jun 2022].

**Guha**, M., Sirinivasan, S., Ruthel, G., Kashina, A. K., Carestens, R. P., Mendoza, A., Khanna, C., Winkle, V. T., and Avadhani, T. (2017) 'Mitochondrial retrograde signaling induces epithelial-mesenchymal transition and generates breast cancer stem cells', *Physiology & behavior*, **176(3)**, pp. 139–148. doi: 10.1053/j.gastro.2016.08.014.CagY [1<sup>st</sup> June 2023].

**Guilhelmelli**, F., Vilela, N., Albuquerque, P., Derengowski, S. D. L., Pereira, S. L., and Kyaw, M. C. (2013) 'Antibiotic development challenges: The various mechanisms of action of antimicrobial peptides and of bacterial resistance', *Frontiers in Microbiology* [Online], **4(DEC)**, pp. 1–12. Available at: <https://doi.org/10.3389/fmicb.2013.00353> [accessed 27 Oct 2022].

**Gürbay**, A., Osman, M., Alain, F., and Hincal, F. (2005) 'Ciprofloxacin-induced cytotoxicity and apoptosis in HeLa cells', *Toxicology Mechanisms and Methods* [Online], **15(5)**, pp. 339–342. Available at: <https://doi.org/10.1080/153765291009877> [accessed 22 Nov 2021].

**Hancock**, J. T., Desikan, R. and Neill, S. J. (2001) 'Role of reactive oxygen species in cell signalling pathways', *Biochemical Society Transactions*. Portland Press Ltd., [Online], **29(2)**, pp. 345–349. doi: 10.1042/bst0290345 [accessed 2 Nov 2022].

**Hara, K., Kasahara, E., Takahashi, N., Konishi, M., Inoue, J., Jikumaru, M., Kubo, S., Okamura, H., Sato, E., and Inoue, M. (2011a)** 'Mitochondria determine the efficacy of anticancer agents that interact with DNA but not the cytoskeleton', *Journal of Pharmacology and Experimental Therapeutics* [Online], **337(3)**, pp. 838–845. Available at: <https://doi.org/10.1124/jpet.111.179473> [accessed 14 Oct 2022].

**Hara, K., Kasahara, E., Takahashi, N., Konishi, M., Inoue, J., Jikumaru, M., Kubo, S., Okamura, H., Sato, E., and Inoue, M. (2011b)** 'Mitochondria determine the efficacy of anticancer agents that interact with DNA but not the cytoskeleton', *Journal of Pharmacology and Experimental Therapeutics* [Online], **337(3)**, pp. 838–845. Available at: <https://doi.org/10.1124/jpet.111.179473> [accessed 16 Oct 2022].

**Heerdt, G. B., Houston, A. M. and Augenlicht, L. H. (2005)** 'The intrinsic mitochondrial membrane potential of colonic carcinoma cells is linked to the probability of tumor progression' *Cancer Research* [Online], **65(21)**, pp. 9861-9867, Available from: [10.1158/0008-5472.CAN-05-2444](https://doi.org/10.1158/0008-5472.CAN-05-2444) [accessed 1 Dec 2022].

**Holland, T., Fowler, V.G. and Shelburne, S.A. (2014)** 'Invasive gram-positive bacterial infection in cancer patients', *Clinical Infectious Diseases* [Online], **59**, pp. S331–S334. Available at: <https://doi.org/10.1093/cid/ciu598> [accessed 11 Jun 2022].

**Hossain, M., Das, S., Das, U., Doroudi, A., Zhu, J., and Dimmock, R. J. (2020)** 'Novel hybrid molecules of 3,5-bis(benzylidene)-4-piperidones and dichloroacetic acid which demonstrate potent tumour-selective cytotoxicity', *Bioorganic and Medicinal Chemistry Letters*. Elsevier, [Online], **30(3)**, p. 126878. doi: [10.1016/j.bmcl.2019.126878](https://doi.org/10.1016/j.bmcl.2019.126878) [accessed 27 Sep 2021].

**Hsu, P.P. and Sabatini, D.M. (2008)** 'Cancer cell metabolism: Warburg and beyond', *Cell* [Online], **134(5)**, pp. 703–707. Available at: <https://doi.org/10.1016/j.cell.2008.08.021> [accessed 15 Oct 2022].

**Hu, X.** and Xuan, Y. (2008) 'Bypassing cancer drug resistance by activating multiple death pathways - A proposal from the study of circumventing cancer drug resistance by induction of necroptosis', *Cancer Letters* [Online], **259(2)**, pp. 127–137. Available at: <https://doi.org/10.1016/j.canlet.2007.11.007> [accessed 7 Jun 2022].

**Hugonnet, S.,** Sax, H., Eggimann, P., Chevrolet, C. J., and Pittet, D. (2004) 'Nosocomial Bloodstream Infection and Clinical Sepsis', *Emerging Infectious Diseases* [Online], **10(1)**, pp. 76–81. Available at: <https://doi.org/10.3201/eid1001.030407> [accessed 15 Sep 2022].

**Irrazabal, T.,** Thakur, K. B., Kang, M., Malaise, Y., Streutker, C., Wong, Y. O. E., Copeland, J., Gryfe, R., Guttman, S. D., Navarre, W. W., and Martin, A. (2020) 'Limiting oxidative DNA damage reduces microbe-induced colitis-associated colorectal cancer', *Nature Communications* [Online], **11(1)**, Available at: <https://doi.org/10.1038/s41467-020-15549-6> [accessed 15 Sep 2022].

**Jean, S. R.,** Tulumello, V. D., Wisnovsky, P. S., Lei, E. K., Pereira, P. M., Kelley, S. O. (2014) 'Molecular vehicles for mitochondrial chemical biology and drug delivery' *ACS Chemical Biology* [Online], **9(2)**, pp. 323-333, Available from: [dx.doi.org/10.1021/cb400821p](https://doi.org/10.1021/cb400821p) [accessed 28 Mar 2021].

**Jones, R. J.,** Matsui, W.H. and Smith, B.D. (2004) 'Cancer stem cells: Are we missing the target?', *Journal of the National Cancer Institute* [Online], **96(8)**, pp. 583–585. Available at: <https://doi.org/10.1093/jnci/djh095> [accessed 10 Sep 2021].

**Jonnalagadda, S. K.,** Wielenberg, K., Ronayne, T. C., Jonnalagadda, S., Kiprof, P., Jonnalagadda, C. S., and Mereddy, R. V. (2020) 'Synthesis and biological evaluation of arylphosphonium-benzoxaborole conjugates as novel anticancer agents', *Bioorganic and Medicinal Chemistry Letters* [Online], **30(14)**, p. 127259. Available at: <https://doi.org/10.1016/j.bmcl.2020.127259> [accessed 11 Oct 2021].

**Kang, S.**, Sunwoo, K., Jung, Y., Hur, K. J., Park, H. K., Kim, S. J., and Kim, D. (2020) 'Membrane-targeting triphenylphosphonium functionalized ciprofloxacin for methicillin-resistant staphylococcus aureus (Mrsa)', *Antibiotics*, [Online], **9(11)**, pp. 1–16. doi: 10.3390/antibiotics9110758 [accessed 13 Apr 2022].

**Kassab, A. E.** and Gedawy, E. M. (2018) 'Novel ciprofloxacin hybrids using biology oriented drug synthesis (BIODS) approach: Anticancer activity, effects on cell cycle profile, caspase-3 mediated apoptosis, topoisomerase II inhibition, and antibacterial activity', *European Journal of Medicinal Chemistry*. Elsevier Masson SAS, [Online], **150**, pp. 403–418. doi: 10.1016/j.ejmech.2018.03.026 [accessed 27 Sep 2022].

**Kelso, G. F.**, Poteous, M. C., Coulter, V. C., Hughes, G., Porteous, K. W., Ledgerwood, C. E., Smith, J. A. R., and Murphy, P. M. (2001) 'Selective Targeting of a Redox-active Ubiquinone to Mitochondria within Cells', *The Journal of Biological Chemistry*. © 2001 ASBMB. Currently published by Elsevier Inc; originally published by American Society for Biochemistry and Molecular Biology., [Online], **276(7)**, pp. 4588–4596. doi: 10.1074/jbc.M009093200 [30 Jan 2023].

**Khutornenko, A. A.**, Roudko, V. V., Chernyak, B. V., Vartapetian, B. A., Chumakov, M. P., and Evstafieva, G. A. (2010) 'Pyrimidine biosynthesis links mitochondrial respiration to the p53 pathway', *Proceedings of the National Academy of Sciences of the United States of America* [Online], **107(29)**, pp. 12828–12833. Available at: <https://doi.org/10.1073/pnas.0910885107> [accessed 1 Oct 2022].

**Kloskowski, T.**, Gurtowska, N., Olkowska, J., Nowak, M. J., Adamowicz, J., Tworkiewicz, J., Debski, R., Grazanka, A., and Drewa, T. (2012) 'Ciprofloxacin is a potential topoisomerase II inhibitor for the treatment of NSCLC', *International Journal of Oncology* [Online], **41(6)**, pp. 1943–1949. Available at: <https://doi.org/10.3892/ijo.2012.1653> [accessed 17 Oct 2021].

**Koga**, H., Itoh, A., Murayama, S., Suzue, S., and Irikura, T. (1980) 'Structure-Activity Relationships Of Antibacterial 6, 7-and 7, 8-Disubstituted 1-Alkyl-1, 4-Dihydro-4-Oxoquinoline-3-Carboxylic Acids', *Journal of Medicinal Chemistry*, [Online], **23(12)**, pp. 1358–1363. doi: 10.1021/jm00186a014 [accessed 27 Oct 2022].

**Korniluk**, A., Koper, O., Kemon, H., and Piekarska, D. V. (2017) 'From inflammation to cancer', *Irish Journal of Medical Science* [Online], **186(1)**, pp. 57–62. Available at: <https://doi.org/10.1007/s11845-016-1464-0> [accessed 15 Sep 2022].

**Kou**, J. F., J. F., Qian, C., Wang, Q. J., Chen, X., Wang, L. L., Chao, H., and Ji, N. L. (2012) 'Chiral ruthenium(II) anthraquinone complexes as dual inhibitors of topoisomerases I and II', *Journal of Biological Inorganic Chemistry*, [Online], **17(1)**, pp. 81–96. doi: 10.1007/s00775-011-0831-6 [accessed 2<sup>nd</sup> Nov 2022].

**Lant**, B., and Derry, B. W. (2013) 'Methods for detection and analysis of apoptosis signaling in the *C. elegans* germline' *Methods*, **61**, pp. 174-182, Available from <http://dx.doi.org/10.1016/j.ymeth.2013.04.022> [accessed 10 Nov 2022].

**Larkin**, S. and Aukim-Hastie, C. (2011) *Proteomic evaluation of cancer cells: Identification of cell surface proteins*, *Methods in Molecular Biology*. [Online], doi: 10.1007/978-1-61779-80-5\_32 [accessed 3<sup>rd</sup> Feb 2023].

**Lehmann**, M. W. and Evans, D. H. (2001) 'Mechanism of the electrochemical reduction of 3,5-di-tert-butyl-1,2-benzoquinone. Evidence for a concerted electron and proton transfer reaction involving a hydrogen-bonded complex as reactant', *Journal of Physical Chemistry B*, [Online], **105(37)**, pp. 8877–8884. doi: 10.1021/jp0109269 [accessed 19 Jan 2023].

**Lehouritis**, P., Cummins, J., Stanton, M., Murohy, T. C., McCarthy, O. F., Reid, G., Urbaniak, C., Byrne, L. W., and Tangney, M. (2015) 'Local bacteria affect the efficacy of chemotherapeutic drugs', *Scientific Reports*. Nature Publishing Group, [Online], **5**. doi: 10.1038/srep14554 [accessed 12 Feb 2022].



Li, X., Lewis, T. M., Gutierrez, C., Osborne, K. C., Wu, F. M., Hilsenbeck, S. G., Pavlick, A., Zhang, X., Chamness, G. C., Wong, H., Rosen, J., and Chang, J. C. (2008) 'Intrinsic resistance of tumorigenic breast cancer cells to chemotherapy', *Journal of the National Cancer Institute* [Online], **100(9)**, pp. 672–679. Available from: <https://doi.org/10.1093/jnci/djn123> [accessed 10 Sep 2021].

Li, C. H., Cheng, Y. W., Liao, P. L., Yang, Y. T. and Kang, J. J. (2010) 'Chloramphenicol Causes Mitochondrial Stress, Decreases ATP Biosynthesis, Induces Matrix Metalloproteinase-13 Expression, and Solid-Tumor Cell Invasion', *Toxicological Sciences*, **116(1)**, pp. 140–150, Available from doi:10.1093/toxsci/kfq085 [accessed 5<sup>th</sup> Jun 2023].

Li, T., Kon, N., Jiang, L., Tan, M., Ludwig, T., Zhao, Y., Baer, R., and Gu, W. (2012) 'Tumor suppression in the absence of p53-mediated cell-cycle arrest, apoptosis, and senescence', *Cell* [Online], **149(6)**, pp. 1269–1283. Available at: <https://doi.org/10.1016/j.cell.2012.04.026> [accessed 17 Oct 2012].

Li, Q., Ma, L., Shen, S., Guo, Y., Cao, Q., Cai, X., Feng, J., Yan, Y., Hu, T., Lu, S., Zhou, L., Peng, B., Yang, Z., and Hua, Y. (2019) 'Intestinal dysbacteriosis-induced IL-25 promotes development of HCC via alternative activation of macrophages in tumor microenvironment', *Journal of Experimental and Clinical Cancer Research* [Online], **38(1)**, pp. 1–13. Available at: <https://doi.org/10.1186/s13046-019-1271-3> [accessed 29 Sep 2022].

Li, M., Li, M., Liu, S., Wang, M., Hu, H., Yin, J., Liu, C., and Huang, Y. (2020) 'Gut Microbiota Dysbiosis Associated with Bile Acid Metabolism in Neonatal Cholestasis Disease', *Scientific Reports* [Online], **10(1)**, pp. 1–10. Available at: <https://doi.org/10.1038/s41598-020-64728-4> [accessed 15 Oct 2022].

Liang, D., Su, Z., Tian, W., Li, Z., Wang, C., Li, D., and Hou, H. (2020) 'Synthesis and screening of novel anthraquinone-quinazoline multitarget hybrids as promising anticancer candidates', *Future Medicinal Chemistry*, [Online], **12(2)**, pp. 111–126. doi: 10.4155/fmc-2019-0230 [accessed from 19 Jan 2023].

**Lien, J. C., Huang, J. L., Wang, P. J., Tang, M. C., Lee, H. K., and Kuo, C. S. (1997)** 'Synthesis and antiplatelet, antiinflammatory, and antiallergic activities of 2-substituted 3-chloro-1,4-naphthoquinone derivatives', *Bioorganic and Medicinal Chemistry*, [Online], **5(12)**, pp. 2111–2120. doi: 10.1016/S0968-0896(97)00133-8 [accessed 21 Jan 2023].

**Liu, X., Jiang, J., Xu, Y., Hou, S., Sun, L., Ye, Q., and Lou, L. (2015)** 'Chronic inflammation-related HPV: A driving force speeds oropharyngeal carcinogenesis', *PLoS ONE* [Online], **10(7)**, pp. 1–14. Available at: <https://doi.org/10.1371/journal.pone.0133681> [accessed 27 Sep 2021].

**Lu, W., Ogasawara, M.A. and Huang, P. (2008)** 'Models of reactive oxygen species in cancer', *Cancer* [Online], **4(2)**, pp. 67–73. Available at: <https://doi.org/10.1016/j.ddmod.2007.10.005> [accessed 16 Oct 2022].

**Mashayekhi, V., Eskandari, R. M., Kobarfard, F., Khajeamiri, and A., Hosseini, M. J. (2014)** 'Induction of mitochondrial permeability transition (MPT) pore opening and ROS formation as a mechanism for methamphetamine-induced mitochondrial toxicity', *Naunyn-Schmiedeberg's Archives of Pharmacology* [Online], **387(1)**, pp. 47–58. Available at: <https://doi.org/10.1007/s00210-013-0919-3> [accessed 14 Oct 2022].

**Millard, M., Pathania, D., Shabaik, Y., Taheri, L., Deng, J., and Neamati, N. (2010)** 'Preclinical evaluation of novel triphenylphosphonium salts with broad-spectrum activity' *PLoS ONE* [Online], **5(10)**, pp. 1-18, Available from: [10.1371/journal.pone.0013131](https://doi.org/10.1371/journal.pone.0013131) [accessed 15 Nov 2022].

**Mikulska, M., Viscoli, C., Orasch, C., Livermore, D. M., Averbuch, D., Cordonnier, C., Akova, M., (2014)** 'Aetiology and resistance in bacteraemias among adult and paediatric haematology and cancer patients', *Journal of Infection* [Online], **68(4)**, pp. 321–331. Available at: <https://doi.org/10.1016/j.jinf.2013.12.006> [accessed 6 Sep 2022].

**Mohammed**, O., Hussain, S., Mincher, D., and Turnbull, A. (2016) 'Design, synthesis and evaluation of novel and clinically used anti-cancer agents targeted to mitochondria', *European Journal of Cancer*, **61**, p. S126. doi: 10.1016/s0959-8049(16)61446-6 [accessed 5<sup>th</sup> Jun 2023].

**Mohammed**, O. (2021) 'Design, synthesis and evaluation of novel and clinically used anticancer agents targeted intracellularly', *Edinburgh Napier Research Repository*

[Online], Available from:

[https://napier.primo.exlibrisgroup.com/discovery/fulldisplay?docid=alma9923774061402111&context=L&vid=44NAP\\_INST:44NAP\\_ALMA\\_VU1&lang=en&search\\_scope=MyInst\\_and\\_CI&adaptor=Local%20Search%20Engine&isFrbr=true&tab=Everything&query=any,contains,SH1&sortby=date\\_d&facet=frbrgroupid,include,52637928875625572&offset=0](https://napier.primo.exlibrisgroup.com/discovery/fulldisplay?docid=alma9923774061402111&context=L&vid=44NAP_INST:44NAP_ALMA_VU1&lang=en&search_scope=MyInst_and_CI&adaptor=Local%20Search%20Engine&isFrbr=true&tab=Everything&query=any,contains,SH1&sortby=date_d&facet=frbrgroupid,include,52637928875625572&offset=0) [accessed 27 Sep 2021].

**Morais**, R., Zinkewich-peotti, K., Parent, M., Wang, H., Babai, F. and Zollinger, Ms. (1994) 'Tumor-forming Ability in Athymic Nude Mice of Human Cell Lines Devoid of Mitochondrial DNA', *Cancer Research* [Online], **54(14)**, pp. 3889–3896, Available from: <https://www.researchgate.net/publication/15166359> Tumor-forming [accessed 1 Oct 2022].

**Morrison**, L. and Zembower, T. R. (2020) 'Antimicrobial Resistance', *Gastrointestinal Endoscopy Clinics of North America*, **30(4)**, pp. 619–635. doi: 10.1016/j.giec.2020.06.004 [accessed 11 May 2023].

**Moergel**, M., Kammerer, P., Kasaj, A., Armouti, E., Alshihri, A., Weyer, V., Al-Nawas, B. (2013) 'Chronic periodontitis and its possible association with oral squamous cell carcinoma-a retrospective case control study', *Head and Face Medicine* [Online], **9(39)**, pp. 2–7, Available from: <http://www.head-face-med.com/content/9/1/39> [accessed 14 Oct 2022].

**Mosmann**, T. (1983) 'Rapid colorimetric assay for cellular growth and survival: Application to proliferation and cytotoxicity assays. *Journal of Immunological Methods* [Online], **65**, pp. 55-63. Available at doi:10.1016/0022-1759(83)90303-4

[accessed 23 Dec 2022].

**Niedziałkowski**, P., Czaczyk, E., Jarosz, J., Wcislo, A., Bialobrzaska, W., Wietrzyk, J., and Ossowski, T. (2019) 'Synthesis and electrochemical, spectral, and biological evaluation of novel 9,10-anthraquinone derivatives containing piperidine unit as potent antiproliferative agents', *Journal of Molecular Structure*, [Online], **1175**, pp. 488–495. doi: 10.1016/j.molstruc.2018.07.070 [accessed 23 OCT 2022].

**Nicolas**, I., Bordeau, V., Bondon, A., Baudy-Flouc'h, M., and Fleden, B. (2019) 'Novel antibiotics effective against gram-positive and -negative multi-resistant bacteria with limited resistance', *PLoS Biology*, [Online], **17(7)**, pp. 1–23. Available at: <https://doi.org/10.1371/journal.pbio.3000337> [accessed 28 Aug 2022].

**Patel**, H., Wu, X. Z., Chen, Y., Bo, L., Chen, S. Z. (2021) 'Drug resistance: from bacteria to cancer', *Molecular Biomedicine*. *Molecular Biomedicine*, **2(1)**, doi: 10.1186/s43556-021-00041-4.

**Park**, B.W., Zhuang, J., Yasa, O and Sitti, M. (2017) 'Multifunctional Bacteria-Driven Microswimmers for Targeted Active Drug Delivery', *ACS Nano* [Online], **11(9)**, pp. 8910–8923. Available at: <https://doi.org/10.1021/acsnano.7b03207> [accessed 29 Sep 2022].

**Papandreou**, I., Goliassova, T. and Denko, N.C. (2011) 'Anticancer drugs that target metabolism: Is dichloroacetate the new paradigm?', *International Journal of Cancer* [Online], **128(5)**, pp. 1001–1008. Available at: <https://doi.org/10.1002/ijc.25728> [accessed 5th Oct 2021].

**Pathak**, R.K., Marrache, S., Harn, A. D., (2014) 'Mito-DCA: A mitochondria targeted molecular scaffold for efficacious delivery of metabolic modulator dichloroacetate', *ACS Chemical Biology* [Online], **9(5)**, pp. 1178–1187. Available at: <https://doi.org/10.1021/cb400944y> [28 Mar 2021].

**Pavlova**, N. N., and Thompson, C. B. (2016) 'The Emerging Hallmarks of Cancer Metabolism' *Cell Metabolism* [Online], **23(1)**, pp. 27-47, Available from: <http://dx.doi.org/10.1016/j.cmet.2015.12.006> [accessed 11 Oct 2022].

**Payne**, R. J., Nowak, M. A., and Blumberg, B. S. (1992) 'Analysis of a cellular model to account for the natural history of infection by the hepatitis B virus and its role in the development of primary hepatocellular carcinoma'. *J Theor Biol*, **159**, pp. 215-240, Available from DOI: 10.1016/s0022-5193(05)80703-9 [accessed from 19 May 2023].

**Perez**, F., Adachi, J. and Bonomo, R.A. (2014) 'Antibiotic-resistant gram-negative bacterial infections in patients with cancer', *Clinical Infectious Diseases* [Online], **59(Suppl 5)**, pp. S335–S339. Available at: <https://doi.org/10.1093/cid/ciu612> [accessed 6 Sep 2022].

**Piplani**, M., Rajak, H. and Sharma, P. C. (2017) 'Synthesis and characterization of N-Mannich based prodrugs of ciprofloxacin and norfloxacin: In vitro anthelmintic and cytotoxic evaluation', *Journal of Advanced Research*. Cairo University, [Online], **8(4)**, pp. 463–470. doi: 10.1016/j.jare.2017.06.003 [accessed 5 Oct 2021].

**Pluen**, A., Boucher, Y., Ramanujan, S., Mckee, T. D., Gohongi, T., Tomaso, D. E., Brown, B. E., Izumi, Y., Campbell, B. R., Berk, D. A. and Jain, R. K. (2001) 'Role of tumor-host interactions in interstitial diffusion of macromolecules: Cranial vs. subcutaneous tumors', *Proceedings of the National Academy of Sciences of the United States of America* [Online], **98(8)**, pp. 4628–4633. Available at: <https://doi.org/10.1073/pnas.081626898> [accessed 7 Sep 2022].

**Reily**, C., Mitchell, T., Chacko, K. B., Benavides, A. G., Murphy, P. M., and Usmar, D. M. R. (2013) 'Mitochondrially targeted compounds and their impact on cellular bioenergetics', *Redox Biology*. Elsevier, [Oline], **1(1)**, pp. 86–93. doi: 10.1016/j.redox.2012.11.009 [accessed 28 Mar 2021].

**Reuveni, D.**, Halperin, D., Shalit, I., Priel, E., and Fabian, I. (2008) 'Quinolones as enhancers of camptothecin-induced cytotoxic and anti-topoisomerase I effects', *Biochemical Pharmacology* [Online], **75(6)**, pp. 1272–1281. Available at: <https://doi.org/10.1016/j.bcp.2007.11.014> [accessed 22 Nov 2021].

**Rudin, D.**, Li, L., Niu, N., Kalari, R. K., Gillbert, A. J., Ames, M. M., and Wang, L. (2011) 'Gemcitabine Cytotoxicity: Interaction of Efflux and Deamination', *Journal of Drug Metabolism & Toxicology* [Online], **02(01)**, Available at: <https://doi.org/10.4172/2157-7609.1000107> [accessed 21 Nov 2022].

**Ruggieri, V.**, Agriesti, F., Scrima, R., Laurenzana, I., Perrone, D., Tataranni, T., Mazzoccoli, C., Muzio, L. L., Capitanio, N., Piccoli, C. (2015) 'Dichloroacetate, a selective mitochondria-targeting drug for oral squamous cell carcinoma: A metabolic perspective of treatment', *Oncotarget* [Online], **6(2)**, pp. 1217–1230. Available at: <https://doi.org/10.18632/oncotarget.2721> [accessed 17 Oct 2021].

**Safdar, A.** and Armstrong, D. (2011) 'Infections in patients with hematologic neoplasms and hematopoietic stem cell transplantation: Neutropenia, humoral, and splenic defects', *Clinical Infectious Diseases* [Online], **53(8)**, pp. 798–806. Available at: <https://doi.org/10.1093/cid/cir492> [accessed 6 Sep 2022].

**Sagan, L.** (1967) 'On the origin of mitosing cells', *J Theor Biol*, **14**, pp. 225–274, doi: [https://doi.org/10.1016/0022-5193\(67\)90079-3](https://doi.org/10.1016/0022-5193(67)90079-3) [accessed 2 Jun 2023].

**Samir, M.**, ramadan, M., Abdelrahman, H. M., Abdelbaset, S. M., Abourehab, A. S. M., Aziz, A. M., Rahma, A. A. D. G. (2021) '3,7-bis-benzylidene hydrazide ciprofloxacin derivatives as promising antiproliferative dual TOP I & TOP II isomerases inhibitors', *Bioorganic Chemistry*. Elsevier Inc., **110(November 2020)**, p. 104698. doi: [10.1016/j.bioorg.2021.104698](https://doi.org/10.1016/j.bioorg.2021.104698) [accessed 27 Sep 2021].

**Schmidt, M., Teitge, M., Castillo, E. M., Brandt, T., Dobner, B., and Langner, A.** (2008) 'Synthesis and biochemical characterization of new phenothiazines and related drugs as MDR reversal agents', *Archiv der Pharmazie* [Online], **341(10)**, pp. 624–638. Available from: <https://doi.org/10.1002/ardp.200800115> [accessed 11 April 2021].

**Schimpff, S., Satterlee, W., Young, V. M., and Serpick, A.** (1971) 'Empiric therapy with carbenicillin and gentamicin for febrile patients with cancer and granulocytopenia' *The New England Journal of Medicine* [Online]. **284**, pp. 1061-1065, Available from: DOI: 10.1056/NEJM197105132841904 [accessed 27 Sep 2021].

**Schneeweiss, A., Mobus, V., Tesch, H., Hanusch, C., Denkert, C., Lubbe, K., Untch, M., Kast, K., Jackisch, C., Thomalla, J., Heppner, I, B., Blohmer, U. J., Rezai, M., Frank, M., Engels, K., Rhiem, K., Fasching, P. A., Nekljudova, V., Minckwitz, V. G., and Loibl, S.** (2019) 'Intense dose-dense epirubicin, paclitaxel, cyclophosphamide versus weekly paclitaxel, liposomal doxorubicin (plus carboplatin in triple-negative breast cancer) for neoadjuvant treatment of high-risk early breast cancer (GeparOcto—GBG 84): A randomised pha', *European Journal of Cancer*, [Online], **106**, pp. 181–192. doi: 10.1016/j.ejca.2018.10.015 [accessed 19 Jan 2023].

**Schwarz, M. A. and Firkin, B. G.** (1976) 'Chloramphenicol-a possible role in the treatment of leukaemia?', *Med J Aust.* [Online], **1**, pp. 687–690, Available from <https://pubmed.ncbi.nlm.nih.gov/1065792/> [accessed 15 May 2023].

**Seliem, A. I., Panda, S. S., Girgis, S. A., Nagy, I. Y., George, F. R., Fayad, W., Fawzy, G. N., Ibrahim, S. T., Al-Mahmoudy, M. M. A., Sakhuja, R., Abdel-samii, M. K. Z.,** (2019). 'Design, synthesis, antimicrobial, and DNA gyrase inhibitory properties of fluoroquinolones-dichloroacetic acid hybrids' *Chemical Biology & Drug Design* [Online], **95**, pp. 248-259, Available from: doi: 10.1111/cbdd.13638 [accessed 27 Sep 2021].

**Sharma**, A., Lee, G. M., Shi, H., Won, M., Arambula, J. F., Sessler, J. L., Lee, J. Y., Chi, G. S., and Kim, S. J. (2018) 'Overcoming Drug Resistance by Targeting Cancer Bioenergetics with an Activatable Prodrug', *Chem. Elsevier Inc.*, [Online], **4(10)**, pp. 2370–2383. doi: 10.1016/j.chempr.2018.08.002 [accessed 22 Jan 2021].

**Shchekotikhin**, A. E., Dezhenkova, G. L., Tsvetkov, B. V., Luzikov, N. Y., Volodina, L. Y., Tatarskiy, V. V., Kalinina, A. A., Treshalin, I. M., Treshalina, M. H., Romanenko, I. V., Kaluzhny, N. D., Kubbutat, M., Schols, D., Pommier, Y., Shtil, A. A., and Probrzhenskaya, N. M. (2016) 'Discovery of antitumor anthra[2,3-b]furan-3-carboxamides: Optimization of synthesis and evaluation of antitumor properties', *European Journal of Medicinal Chemistry*. Elsevier Masson SAS, [Online], **112**, pp. 114–129. doi: 10.1016/j.ejmech.2016.01.050 [accessed 20 Jan 2023].

**Škrtić**, M., Sriskanthadevan, S., Jhas, B., Gebbia, M., Wang, X., Wang, Z., Hurren, R., Jitkova, Y., Gronda, M., Maclean, N., Lai, C. K., Eberhard, Y., Bartoszko, J., Spagnuolo, P., Rutledge, A. C., Datti, A., Ketela, T., Moffat, J., Robinson, B. H., Cameron, J. H., Wrana, J., Eaves, C. J., Minden, D. M., Wang, J. C. Y., Dick, J. E., Humphries, K., Nislow, C., Giaever, G., and Schimmer, A. D. (2012) 'Inhibition of mitochondrial translation as a therapeutic strategy for human acute myeloid leukemia', *Cancer Cell*. [Online], **20(5)**, pp. 674–688, Available from doi:10.1016/j.ccr.2011.10.015.

**Shindikar**, A. A., and Viswanathan, C. L. (2005) 'Novel fluoroquinolones: Design, synthesis, and in vivo activity in mice against Mycobacterium tuberculosis H37Rv' *Bioorganic and Medicinal Chemistry Letters* [Online], **15(7)**, pp. 1803-1806, Available from: 10.1016/j.bmcl.2005.02.037 [accessed 11 Aug 2022].

**Singh**, H., Sareen, D., George, M. J., Bhardwaj, J., Rha, S., Lee, J. S., Sharma, S., Sharma, A., and Kim, S. J. (2022) 'Mitochondria targeted fluorogenic theranostic agents for cancer therapy', *Coordination Chemistry Reviews*. Elsevier B.V., [Online], **452**, p. 214283. doi: 10.1016/j.ccr.2021.214283 [accessed 13 Nov 2022].

**Sivagnanam**, V., Zhu, X. and Schlichter, L.C. (2010) 'Dominance of E. coli phagocytosis over LPS in the inflammatory response of microglia', *Journal of*



*Neuroimmunology* [Online], **227(1–2)**, pp. 111–119. Available at:  
<https://doi.org/10.1016/j.jneuroim.2010.06.021> [accessed 15 Sep 2022].

**Smart**, D. J., Halicka, D. H., Traganos, F., Darzynkiewicz, Z and Williams, G. M. (2008) 'Ciprofloxacin-induced G2 arrest and apoptosis in TK6 lymphoblastoid cells is not dependent on DNA double-strand break formation', *Cancer Biology & Therapy* [Online], **7**, pp. 113-119, DOI: 10.4161/cbt.7.1.5136 [12 Sep 2022].

**Smith**, R. A. J., Porteous, M. C., Coulter, V. C., and Murphy, P. M. (1999) 'Selective targeting of an antioxidant to mitochondria', *European Journal of Biochemistry*, [Online], **263(3)**, pp. 709–716. doi: 10.1046/j.1432-1327.1999.00543.x [accessed 12 Oct 2022].

**Solankee**, A., Kapadia, K, Ciric, A., Sokovic, M., Dovtchinova, I., and Geronikaki, A. (2010) 'Synthesis of some new S-triazine based chalcones and their derivatives as potent antimicrobial agents', *European Journal of Medicinal Chemistry*, [Online], **45(2)**, pp. 510–518. doi: 10.1016/j.ejmech.2009.10.037 [accessed 30 Jan 2023].

**Stacpoole**, P.W., Henderson, N. G., Yan, Z., James, O. M. (1998) 'Clinical pharmacology and toxicology of dichloroacetate', *Environmental Health Perspectives* [Online], **106(SUPPL. 4)**, pp. 989–994. Available at:  
<https://doi.org/10.1289/ehp.98106s4989> [accessed 22 Nov 2021].

**Stander**, X. X., Stander, B. A., and Joubert, A. M. (2015) ' Synergistic Anticancer Potential of Dichloroacetate and Estradiol Analogue Exerting their Effect via ROS-JNK-Bcl-2- Mediated Signalling Pathways', *Cell Physiol Biochem* [Online], **35**, pp. 1499-1526 Available from DOI: 10.1159/000369710.

**Stein**, W. D. (1967). The movement of molecules across cell membranes. *New York: Academic Press* [online], Available from:  
[https://books.google.co.uk/books/about/The\\_Movement\\_Of\\_Molecules\\_Across\\_Cell\\_Me.html?id=Ncs0DzQjwPEC&redir\\_esc=y](https://books.google.co.uk/books/about/The_Movement_Of_Molecules_Across_Cell_Me.html?id=Ncs0DzQjwPEC&redir_esc=y) [accessed 4 April 2022].

**Stockwin**, L. H., Yu, X. S., Borgel, S., Hancock, C., Wolfe, L. T., Phillips, R. L., Hollingshead, G. M., and Newton, L. D. (2010) 'Sodium dichloroacetate selectively targets cells with defects in the mitochondrial ETC', *International Journal of Cancer* [Online], **127(11)**, pp. 2510–2519. Available at: <https://doi.org/10.1002/ijc.25499> [accessed 16 Aug 2022].

**Sullivan**, L.B., Gracia, M. E., Nguyen, H., Mullen, R. A., Dufour, E., Sudrashan, S., Licht, D. J., Deberaridins, J. R., and Chandel, S., N. (2013) 'The Proto-oncometabolite Fumarate Binds Glutathione to Amplify ROS-dependent signaling', *Molecular Cell* [Online], **51(2)**, pp. 236–248. Available at: <https://doi.org/10.1016/j.molcel.2013.05.003> [accessed 1 Oct 2022].

**Sullivan**, L. B. and Chandel, N. S. (2014) 'Mitochondrial reactive oxygen species and cancer', *Cancer Metabolism*, **2**, pp. 1-12. doi: 10.1186/2049-3002-2-17 [accessed from 1<sup>st</sup> Jun 2023].

**Sun**, R. C., Fadia, M., Dahlstrom, E. J., Parish, R. C., Board, G. P., and Blackburn, C. A. (2010) 'Reversal of the glycolytic phenotype by dichloroacetate inhibits metastatic breast cancer cell growth in vitro and in vivo', *Breast Cancer Research and Treatment* [Online], **120(1)**, pp. 253–260. Available at: <https://doi.org/10.1007/s10549-009-0435-9> [accessed 22 Nov 2021].

**Sutendra**, G., Dromparis, P., Wright, P., Bonnet, S., Haromy, A., Hao, Z., McMurtry, M., Michalak, M., Vance, J. E., Sessa, C. W., and Michelakis, D. E. (2011) 'The role of nogo and the mitochondria-endoplasmic reticulum unit in pulmonary hypertension', *Science Translational Medicine*, **3(88)**. doi: 10.1126/scitranslmed.3002194 [accessed 29 Aug 2022].

**Sutendra**, G., Dormapris, P., Kinnaird, A., Stenson, T. H., Harmony, A., Parker, J. M. R., McMurtry, M. S., and Michelakis, E. D. (2013) 'Mitochondrial activation by inhibition of PDKII suppresses HIF1a signaling and angiogenesis in cancer', *Oncogene*, **32(13)**, pp. 1638–1650. Available at: <https://doi.org/10.1038/onc.2012.198> [accessed 22 Nov 2021].

**Tegos**, G. P., Masago. K., Aziz, F., Higginbotham, A., Stermitz, R. F., and Hamblin, R. M. (2008) 'Inhibitors of bacterial multidrug efflux pumps potentiate antimicrobial photoinactivation', *Antimicrobial Agents and Chemotherapy* [Online], **52(9)**, pp. 3202–3209. Available at: <https://doi.org/10.1128/AAC.00006-08> [accessed 24 Oct 2022].

**Tillotson**, G. S. (1996) 'Quinolones: Structure-activity relationships and future predictions', *Journal of Medical Microbiology*, **44(5)**, [Online], pp. 320–324. doi: 10.1099/00222615-44-5-320 [accessed 27 Sep 2021].

**Trachootham**, D., Zhang, H., Zhang, W., Feng, L., Du, M., Zhou, Y., Chen, Z., Pelicano, H., Plunkett, W., Wierda, W. G., Keating, J. M., and Huang, P. (2008) 'Effective elimination of fludarabine-resistant CLL cells by PEITC through a redox-mediated mechanism', *Blood* [Online], **112(5)**, pp. 1912–1922. Available at: <https://doi.org/10.1182/blood-2008-04-149815> [accessed from 14 Oct 2022].

**Triller**, N., Korosec, P., Kern, I., Kosnik, M., and Debeljak, A. (2006) 'Multidrug resistance in small cell lung cancer: Expression of P-glycoprotein, multidrug resistance protein 1 and lung resistance protein in chemo-naive patients and in relapsed disease', *Lung Cancer* [Online] **54(2)**, pp. 235–240. Available at: <https://doi.org/10.1016/j.lungcan.2006.06.019> [accessed 6 Oct 2022].

**Tripathi**, A. N., Chauhan, L., Thankachan, P. P., and Barthwal, R. (2001) 'Quantum chemical and nuclear magnetic resonance spectral studies on molecular properties and electronic structure of berberine and berberrubine', *Journal of Medicinal and Pharmaceutical Chemistry*, **2(1)**, pp. 1941–1944. doi: 10.1002/mrc [accessed 21 Jan 2023].

**Valero**, A., Merino, F., Wolbers, F., Luttege, R., Vermes, I., Andersson, H., and Berg, D. V. G. A. (2005) 'Apoptotic cell death dynamics of HL60 cells studied using a microfluidic cell trap device', *Lab on a Chip* [Online], **5(1)**, pp. 49–55. Available at: <https://doi.org/10.1039/b415813j> [accessed 22 Nov 2022].

**Van Meerloo**, J., Kaspers, G. J. L. and Cloos, J. (2011) 'Cell sensitivity assays: The MTT assay', *Methods in Molecular Biology*, **731(March)**, pp. 237–245. doi: 10.1007/978-1-61779-80-5\_20 [accessed 15 May 2023].

**Vogelstein**, B. and Kinzler, K. W. (2004) 'Cancer genes and the pathways they control', *Nature Medicine* [Online], **10(8)**, pp. 789–799. Available at: <https://doi.org/10.1038/nm1087> [accessed 6 Sep 2022].

**Wagai**, N., Tawara, K. (1991) 'Quinolone antibacterial-agent-induced cutaneous phototoxicity: ear swelling reactions in BALB/c mice. *Toxicol. Lett.* 58, pp. 215–223. [https://doi.org/10.1016/0378-4274\(91\)90176-7](https://doi.org/10.1016/0378-4274(91)90176-7) [accessed 30 Jan 2023].

Warburg, O. (1956) 'On the origin of cancer cells', *Science* [Online], **123(3191)**, pp. 309–314. Available at: <https://doi.org/10.1126/science.123.3191.309> [accessed 15 Oct 2022].

**Ward**, P. S., and Thompson, C. B. (2012) 'Metabolic Reprogramming: A Cancer Hallmark Even Warburg Did Not Anticipate', *Cancer Cell* [Online], **21(3)**, pp. 297–308. Available at: <https://doi.org/10.1016/j.ccr.2012.02.014> [accessed 16 Aug 2022].

Wcisło, A. *et al.* (2019) 'Unusual behavior in di-substituted piperidine and piperazine anthraquinones upon protonation – Spectral, electrochemical, and quantum chemical studies', *Journal of Molecular Liquids*, **279**, pp. 154–163. doi: 10.1016/j.molliq.2019.01.115 [16 Oct 2022].

**Weyler**, L., Engelbrecht, M., Forseberg, M. M., Brehwens, K., Vare, D., Vielfort, K., Wojcik, A., and Aro, H. (2014) 'Restriction endonucleases from invasive *Neisseria gonorrhoeae* cause double-strand breaks and distort mitosis in epithelial cells during infection', *PLoS ONE* [Online], **9(12)**, pp. 1–23. Available at: <https://doi.org/10.1371/journal.pone.0114208> [accessed 15 Sep 2022].

**Wen**, S., Zhu, D. and Huang, P. (2013) 'Targeting cancer cell mitochondria as a therapeutic approach', *Future Medicinal Chemistry* [Online], **5(1)**, pp. 53–67. Available at: <https://doi.org/10.4155/fmc.12.190> [accessed 14 Nov 2021].

**Williamott**, C. J. R., Critchlow, E. S., Eperon, I. C., and Maxwell, A. (1994) 'The Complex of DNA Gyrase and Quinolone Drugs with DNA Forms a Barrier to Transcription by RNA Polymerase' *Academic Press Limited* [Online], **242**, pp. 351–363. Available at: <https://reader.elsevier.com/reader/sd/pii/S0022283684715865?token=3C6BF754BE909454C395950FCE8E0E33F8C8655CF41C30967C473B831329E293582332124456A27292E1A9A7B6F722CF&originRegion=eu-west-1&originCreation=20221116113856> [Accessed 16 Nov 2022].

**Wu**, T., Chen, Z., To, K. W. K., Fang, X., Wang, F., Cheng, B., and Fu, L. (2017) 'Effect of abemaciclib (LY2835219) on enhancement of chemotherapeutic agents in ABCB1 and ABCG2 overexpressing cells in vitro and in vivo', *Biochemical Pharmacology. Elsevier Inc.*, **124**, pp. 29–42. doi: 10.1016/j.bcp.2016.10.015 [accessed from 29 Aug 2022].

**Xi**, J., Wang, Y., Gao, X., Huang, Y., Chen, J., Chen, Y., Fan, L., and Gao, L. (2022) 'Reverse intratumor bacteria-induced gemcitabine resistance with carbon nanozymes for enhanced tumor catalytic-chemo therapy', *Nano Today. Elsevier B.V.*, [Online], **43**, Available at: doi: 10.1016/j.nantod.2022.101395 [accessed 13 Oct 2022].

**Yadav**, V., Varshney, P., Sultana, S., Yadav, J., and Siani, N. (2015) 'Moxifloxacin and ciprofloxacin induces S-phase arrest and augments apoptotic effects of cisplatin in human pancreatic cancer cells via ERK activation', *BMC Cancer* [Online], **15(1)**, pp. 1–15. Available at: <https://doi.org/10.1186/s12885-015-1560-y> [accessed 28 Mar 2021].

**Yang**, D., Oyaizu, H., Oyaizu, H., Olsen, J. G., and Woese, C. R. (1985) 'Mitochondrial origins', *Proceedings of the National Academy of Sciences of the United States of America* [Online], **82(13)**, pp. 4443–4447. Available at: <https://doi.org/10.1073/pnas.82.13.4443> accessed 22 Oct 2022].

**Yang, Y.**, Shang, P., Cheng, C., Wang, D., Yang, P., Zhang, F., Li, T., Lu, A., and Zhao, Y. (2010) 'Novel N-phenyl dichloroacetamide derivatives as anticancer reagents: Design, synthesis and biological evaluation', *European Journal of Medicinal Chemistry* [Online], **45(9)**, pp. 4300–4306. Available at: <https://doi.org/10.1016/j.ejmech.2010.06.032> [accessed 12 Oct 2021].

**Yang, D.** and Kim, J. (2019) 'Mitochondrial retrograde signalling and metabolic alterations in the tumour microenvironment', *Cells*, **8(3)**, pp. 1–19. doi: 10.3390/cells8030275 [accessed from 1 Jun 2023].

**Ye, M.**, Gu, X., Han, Y., Jin, M., Ren, T. (2016) 'Gram-negative bacteria facilitate tumor outgrowth and metastasis by promoting lipid synthesis in lung cancer patients', *Journal of Thoracic Disease* [Online], **8(8)**, pp. 1943–1955. Available at: <https://doi.org/10.21037/jtd.2016.06.47> [accessed 15 Sep 2022].

**Yu, M.**, Li, R., and Zhang, J. (2016), 'Repositioning of antibiotic levofloxacin as a mitochondrial biogenesis inhibitor to target breast cancer', *Biochemical and Biophysical Research Communications* [Online], **471**, pp. 639-645, Available from <http://dx.doi.org/10.1016/j.bbrc.2016.02.072> [accessed 12 May 2023].

**Yu, L.**, Lu, M., Jia, D., Ma, J., Jacob, B. E., Levine, H., Kaiparettu, A. B., and Onuchic, N. J. (2017) 'Modeling the genetic regulation of cancer metabolism: Interplay between glycolysis and oxidative phosphorylation', *Cancer Research*, [Online], **77(7)**, pp. 1564–1574. Available at: <https://doi.org/10.1158/0008-5472.CAN-16-2074> [accessed 17 Oct 2022].

**Zhang, Y.**, Ji, W., He, L., Chen, Y., D., X., Sun, Y., Hu, S., Yang, H., Huang, W., Zhang, Y., Liu, F., and Xia, L. (2018) 'E. coli Nissle 1917-derived minicells for targeted delivery of chemotherapeutic drug to hypoxic regions for cancer therapy', *Theranostics* [Online] **8(6)**, pp. 1690–1705. Available at: <https://doi.org/10.7150/thno.21575> [accessed 28 Aug 2022].

**Zhang**, X., Chen, X., Guo, Y., Gao, G., Wang, D., Wu, Y., Liu, J., Liang, G., Zhao, Y., and Wu, F. G. (2021) 'Dual Gate-Controlled Therapeutics for Overcoming Bacterium-Induced Drug Resistance and Potentiating Cancer Immunotherapy', *Angewandte Chemie - International Edition* [Online], **60(25)**, pp. 14013–14021. Available at: <https://doi.org/10.1002/anie.202102059> [accessed 8 Jun 2022].

**Zhou**, X., Chen, C., Zhong, N. Y. A., Zhao, F., Hao, Z., Xu, Y., Lai, R., Shen, G., Yin, X. (2020) 'Effect and mechanism of vitamin D on the development of colorectal cancer based on intestinal flora disorder', *Journal of Gastroenterology and Hepatology (Australia)* [Online], **35(6)**, pp. 1023–1031. Available at: <https://doi.org/10.1111/jgh.14949> [accessed 15 Oct 2022].

**Zielonka**, J., Joseph, J., Sikora, A., Hardy, M., Ouari, M., Vivar, V. J., Cheng, G., Lopez, M., and Kalyanaraman, B. (2017) 'Mitochondria-Targeted Triphenylphosphonium-Based Compounds: Syntheses, Mechanisms of Action, and Therapeutic and Diagnostic Applications', *Chemical Reviews*, [Online], **117(15)**, pp. 10043–10120. doi: 10.1021/acs.chemrev.7b00042 [accessed 4 Jan 2021].

